SIAM J. Applied Dynamical Systems
Vol. 10, No. 2, pp. 744–787

Nonlinear Analysis of Breathing Pulses in a Synaptically Coupled Neural Network*

Stefanos E. Folias†

Abstract. We analyze the weakly nonlinear stability of a stationary pulse undergoing a Hopf bifurcation in a neural field model with an excitatory or Mexican hat synaptic weight function and Heaviside firing rate nonlinearity. The presence of a spatially localized input inhomogeneity $I(x)$ precludes the 0 eigenvalue related to translation invariance of the pulse. Consequently, in the spectral analysis of the linearization about the stationary pulse $\mathcal{U}(x)$, there are two spatial modes, either of which can undergo a Hopf bifurcation in the Mexican hat network to produce a periodic orbit that either expands/contracts (*breather*) or moves side-to-side (*slosher*). We derive the normal form for each mode becoming critical in the Hopf bifurcation by (i) the method of *amplitude equations* and (ii) *center manifold reduction*, which are shown to agree. Importantly, the critical third order coefficient of the normal form is found to be in strong agreement with numerical simulations of the full model, particularly when the bifurcation switches from *super-* to *subcritical*. The motivation of this work is to establish the framework for a perturbative analysis of the breather in a neighborhood of the Hopf bifurcation point to study weakly interacting breathers analytically.

Key words. breathers, stationary pulse, Hopf bifurcation, weakly nonlinear stability, firing rate neural network, Wilson–Cowan equations, amplitude equations, center manifold reduction

AMS subject classifications. 92B20, 37L10, 34E10, 45K05

DOI. 10.1137/100815852

1. Introduction.

The study of spatiotemporal dynamics in synaptically coupled neuronal firing rate models is a growing field of research that continues to establish an understanding of the basic patterns of activity arising from synaptic interactions within large, spatially distributed populations of neurons [71, 25, 28, 51, 55, 57, 13, 56, 32, 96, 98, 84, 31, 30, 58, 50, 95, 75, 102, 97, 20, 64, 74, 5, 4, 35, 9, 10, 39, 40, 87, 19, 18, 7, 34, 63, 81, 89, 33, 12, 22, 17, 8, 11, 104, 24, 65, 66, 49, 103, 67, 88, 79, 80, 100, 93, 41, 15, 78, 77, 76, 27, 52, 26, 59, 1]. First introduced by Wilson and Cowan [101], these neural field models are systems of nonlocal integrodifferential equations that treat the neural tissue as a continuum and describe the activity of the populations in terms of mean neuronal firing rates. Though such models ignore the intricate dynamics captured in neuronal spiking models, it is believed that neural field models can provide a foundation for studying large populations of interacting neurons that facilitates analytic tractability and is numerically less intensive. Already some models have been shown to relate to propagating waves generated in in vitro slice preparations [85, 82, 48, 79].

Given the ubiquity of intrinsic and stimulus-evoked oscillations in the brain, this paper concerns the study of localized patterns of oscillatory activity induced by localized stimulus

*Received by the editors November 23, 2010; accepted for publication (in revised form) by J. Keener February 2, 2011; published electronically June 23, 2011. This work was supported by Burroughs Welcome Fund award 1001749 and US National Science Foundation (NSF) award EMSW21-RTG 0739261.
http://www.siam.org/journals/siads/10-2/81585.html
†Department of Mathematics & Statistics and Center for Biodynamics, Boston University, Boston, MA, and Department of Mathematics, University of Pittsburgh, Pittsburgh, PA (sf@math.bu.edu, stefanos@pitt.edu).

inputs or regions of increased excitability. In previous work [33, 11], we considered the existence and linear stability of a stationary pulse induced by a spatially localized input in the excitatory firing rate neuronal network model introduced by Pinto and Ermentrout [79, 78] to study disinhibited ($w(x) > 0$) cortical tissue:

$$\begin{aligned} \tau \frac{\partial u}{\partial t}(x,t) &= -u(x,t) - \rho n(x,t) + \int_{\mathbb{R}} w(x-y)\, f\big(u(y,t)\big)\, dy + I(x), \\ \frac{1}{\nu}\frac{\partial n}{\partial t}(x,t) &= +u(x,t) - n(x,t). \end{aligned} \tag{1.1}$$

We concentrated on the response of system (1.1) to a time-independent, excitatory input, localized in space, by taking advantage of the analytically tractable simplification introduced by Amari [1], wherein the sigmoidal neuronal *firing rate function* f is taken to be a Heaviside function with firing threshold κ so that $f(u) = H(u - \kappa)$. Our analysis showed that, for sufficiently strong adaptation ρ and sufficiently strong input amplitude $I_\circ$, the system is attracted to a stationary pulse solution which can undergo a Hopf bifurcation leading to stable periodic oscillations if the input amplitude $I_\circ$ is decreased. The periodic oscillations took the shape of an expanding/contracting or *breathing* pulse, and, although there is no synaptic inhibition, local negative feedback mediated by n is capable of balancing the recurrent excitatory synaptic feedback.

Breathing pulses were initially found in one-dimensional reaction-diffusion systems by Koga and Kuramoto [60], in which a stationary localized pattern destabilized in a Hopf bifurcation leading to a "breathing motion." Hopf bifurcation was first described in the Hodgkin–Huxley equations by Gurel [38] and analyzed for the space-clamped axon (spatially uniform) by Troy [94] (see also [42]). The bifurcation to periodic orbits was studied in the context of *spatially nonuniform* solutions induced by a time-independent, δ-function input in the spatially extended FitzHugh–Nagumo equations (as a reduction of the Hodgkin–Huxley equations) to represent the axon of a neuron being stimulated by an electrode [86]. In this case, a Hopf bifurcation of a spatially attenuated equilibrium solution gave rise to both nonpropagating localized oscillations as well as outward propagating periodic impulses. More recently, in a variety of neural networks of nonlocal integrodifferential equations, stationary and traveling pulses have been shown to bifurcate into periodic breathing pulses or other types of periodic solutions when the network is driven by a time-independent input [11, 33, 34, 87, 35, 70, 51] as well as in the absence of any input [77, 103, 19, 7, 16, 64, 55, 57], and in some cases periodic wave emission is also exhibited [33, 34, 57, 56].

In this work, we extend the linear analysis in [33, 11] for the neural field (1.1) with Heaviside firing rate by developing the weakly nonlinear stability analysis of a stationary pulse solution in the vicinity of a Hopf bifurcation. While the linear analysis correctly describes the stability of stationary pulses (equilibria), nonlinear analysis is necessary to describe the stability and characteristic dynamics of the periodic orbit that emerges in the Hopf bifurcation. The motivation for this analysis is to develop the perturbative framework for the analysis of weakly interacting breathers. The local linear feedback mechanism and the solitary nonlocal term perhaps make (1.1) the simplest neural field of Wilson–Cowan type to develop this analysis, and, furthermore, it may naturally be adapted to other neural field models that similarly use a Heaviside firing rate and include analogous spatial integrals. Depending on the

specific interpretation of the neural field variables, a breather can be interpreted abstractly as an oscillation in the average activity of a local population of neurons.

We begin by reviewing and extending the existence and linear stability analysis of stationary pulses in [33, 11] to the case of the Mexican hat synaptic weight function (local excitation/lateral inhibition). Mexican hat networks have been used as effective representations of excitatory-inhibitory networks in equilibrium, but, with regard to the temporal dynamics, one underlying assumption that can be used to justify the use of the Mexican hat weight function is that the temporal dynamics of the inhibitory population are in a quasi-steady state with respect to all other variables [36]. However, whether this assumption accurately reflects the dynamics in real neural tissue remains to be seen. Our use of the Mexican hat weight function, instead, is to demonstrate that it is possible to generate a different type of periodic orbit that arises from a Hopf bifurcation in (1.1) and, in particular, one that is found to occur in more complicated neural field models whose weight functions do *not* change sign [36]. This further supports our notion that (1.1) serves as the simplest neural field for this nonlinear analysis as it captures the two basic types of periodic orbits that emerge in the two-variable neural fields. The periodic orbits arise from the destabilization of one of two spatial eigenmodes of the linearized system, and, in the Mexican hat network, either mode is capable of destabilizing the stationary pulse, with the Hopf bifurcation giving rise to a time-periodic modulation of the pulse that, in one case, expands and contracts (*breathers*) while, in the new case, moves side-to-side (*sloshers*) as a consequence of broken translation invariance due to the input. This is analogous to (1.1) with Heaviside firing rate on a two-dimensional domain wherein the Mexican hat weight function is capable of destabilizing nonradially symmetric modes [35].

An alternative approach to studying linear stability of a stationary pulse was introduced by Amari [1] and considers the perturbative dynamics of the threshold boundaries of the pulse as an ODE-reduction for the spatial model. Blomquist, Wyller, and Einevoll [7] attempted to extend the Amari ODE-reduction to a two-variable excitatory-inhibitory neural field model but found a mismatch with the linear stability analysis of the full model. We investigated a similar ODE-reduction (results not included) for (1.1) and found that the conditions for linear stability agree identically with those for the point spectrum in the full model. The deficiency in the analysis of [7] is not due to the Amari ODE-reduction but is instead due to their restriction that the dynamics of two threshold boundaries evolve with even symmetry rather than independently. The same conclusion was reached independently by Venkov [98]. Although the ODE-reduction would considerably simplify the nonlinear analysis of breathing pulses in the full model (1.1), an inherent difficulty is that the higher order terms in the expansion of the spatial gradient $\partial_x u(x,t)$ are not evident a priori. Blomquist and coauthors carried out such an analysis, ignoring these higher order terms in their ODE-reduction, and found it to match the numerics of the full model in *some* cases but not all cases [7]. After a thorough investigation, we have found that ignoring the higher order terms produces a normal form which is in utter disagreement with numerical simulations of the full model (1.1) regarding whether the bifurcation is sub/supercritical and, in particular, where the switch occurs. We conjecture that any Amari ODE-reduction that does *not* extend the expansion of $\partial_x u(x,t)$ past lowest order will be mismatched with the full model. Hence, we develop the nonlinear analysis in the full model and examine the ODE-reduction in a subsequent paper with the analysis herein serving for comparison.

In section 3, we pursue the nonlinear analysis for the Hopf bifurcation by two different approaches: (i) *amplitude equations* and (ii) *center manifold reduction*. The approach using amplitude equations originated with the ideas of Landau [68, 69] and the work of Stuart [92] and Watson [99]. The center manifold approach is rooted in the ideas of Poincaré [83] and the work of Andronov [2] and Hopf [45, 46] as well as many others. We follow the approach described in [43], which uses projections to obtain the dynamics on the center manifold. (For some additional references regarding higher order analysis for a Hopf bifurcation, see [53, 61, 47, 44, 91, 37, 21, 62, 23, 72, 14, 6].) Due to the prevalence of each approach within different research areas, we present both approaches to make the results more widely accessible. In this treatment, both methods rely on the same set of operators and core calculations, allowing for a direct comparison of the approach and the results of each without considerable additional work (see Appendices A–E). Moreover, the comparison serves as a check on the resulting bifurcation formulae since the results of the two approaches should be related. Finally, the critical coefficient, at third order of the normal form, that determines whether the bifurcation is supercritical or subcritical, is shown to be in strong agreement with numerical simulations of (1.1).

2. Existence and linear stability of a stationary pulse $\mathcal{U}_{\bar{a}}$.

The basic mechanism for the generation of a stimulus-induced breathing pulse is through a Hopf bifurcation of a stationary pulse [11, 33]. In sections 2.1 and 2.2 we begin by briefly reviewing and expanding our previous analysis of this mechanism by considering the additional case of a Mexican hat weight function which has an important implication for the destabilization of a stationary pulse induced by a localized input.

2.1. Existence of a stationary bump.

Consider the neural field equation (1.1), where $u(x,t)$ is a neural field that represents the local activity of a population of neurons at position $x \in \mathbb{R}$, while $n(x,t)$ represents a local negative feedback mechanism, such as spike frequency adaptation or synaptic depression, with ρ, ν determining the relative strength and rate of feedback, respectively. τ denotes the membrane time constant, and f denotes a neuronal output *firing rate function*. Following Amari [1], we consider $f(u) = H(u-\kappa)$, where H denotes the Heaviside function and κ the threshold for firing. And, without loss of generality, we take $\tau = 1$. We have additionally included in (1.1) an excitatory current *input inhomogeneity* $I(x) = I_\circ G(x)$ with amplitude $I_\circ > 0$ and an even-symmetric, Gaussian-like spatial profile $G(x) > 0$ that satisfies $G(x) \to 0$ monotonically as $x \to \pm\infty$.

The *synaptic weight function* $w(x-y)$ defines the strength of the synaptic connections in terms of the distance between neurons at x and y; the integral term effectively sums over the inputs to x from all neurons connected to it, weighting them by w. We assume that $w \in C^\infty(\mathbb{R},\mathbb{R})$ is even-symmetric with a bounded integral over $\mathbb{R}$ and satisfies $w(0) > w(x)$ for all $x \neq 0$ with $w(x) \to 0$ as $x \to \pm\infty$. The weight functions are either *excitatory* ($w(x) > 0$) or have *Mexican hat* form (locally positive, laterally negative), e.g., by taking $\sigma_i > \sigma_e$ and $\bar{w}_i < \bar{w}_e$ for w in (2.1). In general, we take $w, I \in C^\infty(\mathbb{R},\mathbb{R})$, and, for numerical calculations, we take w and I to be of the form

$$w(x) = \frac{\bar{w}_e}{\sqrt{\pi}\sigma_e} \mathrm{e}^{-(x/\sigma_e)^2} - \frac{\bar{w}_i}{\sqrt{\pi}\sigma_i} \mathrm{e}^{-(x/\sigma_i)^2}, \qquad I(x) = I_\circ \, \mathrm{e}^{-(x/\sigma)^2}. \tag{2.1}$$

An even-symmetric, stationary pulse solution centered about $x = 0$ and having a stationary pulse *half-width* $\bar{a} > 0$ satisfies $u(x,t) = n(x,t) = \mathcal{U}(x)$, where

$$\begin{aligned} &\mathcal{U}(x) > \kappa, \qquad x \in (-\bar{a}, \bar{a}), && \mathcal{U}(\pm\bar{a}) = \kappa, \\ &\mathcal{U}(x) < \kappa, \qquad x \in (-\infty, -\bar{a}) \cup (\bar{a}, \infty), && \mathcal{U}(\pm\infty) = 0. \end{aligned}$$

Under the above assumptions and defining $W(x) = \int_0^x w(y)\,dy$, (1.1) becomes

$$\mathcal{U}_{\bar{a}}(x) = \frac{1}{1+\rho}\Big(W(x+\bar{a}) - W(x-\bar{a}) + I(x)\Big), \tag{2.2}$$

where the profile $\mathcal{U}_{\bar{a}}(x)$ of the stationary pulse is parameterized by the *half-width* $\bar{a}$ which is determined by imposing the self-consistency condition $\mathcal{U}_{\bar{a}}(\bar{a}) = \kappa$, i.e.,

$$\big(1+\rho\big)\kappa \;=\; W\big(2\bar{a}\big) + I\big(\bar{a}\big) \;\equiv\; N\big(\bar{a}\big). \tag{2.3}$$

This guarantees the existence of a stationary pulse $\mathcal{U}_{\bar{a}}(x)$ provided it crosses threshold κ exactly once. Importantly, it determines the nonlinear dependence of the half-width $\bar{a}$ on all other parameters, particularly the input strength $I_\circ$.

In the case of zero input ($I_\circ = 0$), Amari [1] showed that a network with a Mexican hat weight function can support a stable/unstable pair of bumps over a range of thresholds κ. However, the network here is contrasted with that of Amari in that stability of the stationary pulse additionally depends upon the dynamics of the adaptation variable n. In particular, as we shall show, if $\nu < \rho$ with $I_\circ = 0$, all stationary pulses are unstable. Stable stationary pulses in the scalar model of Amari extend to this model only in the case that $\nu > \rho$, which does not produce Hopf bifurcations. Therefore, we assume that the network operates in the $\nu < \rho$ regime, and, consequently, in the absence of any input, there are no stable stationary bumps.

Figure 1 illustrates typical existence curves for stimulus-induced ($I_\circ > 0$) bumps in the case of the Mexican hat weight function (2.1) relating the half-width $\bar{a}$ to $I_\circ$ using (2.3). Reflecting the graph in Figure 1(b) across the line $a = I_\circ$ produces Figure 1(c), which alternatively illustrates the dependence of $I_\circ$ on the half-width $\bar{a}$, a relationship we denote by $I_\circ(\bar{a})$. This alternative perspective turns out to be useful in both the linear and nonlinear analyses of the Hopf bifurcation.

We now determine an important relationship to aid the stability analysis in section 2.2. Consider $I_\circ$ to be dependent on $\bar{a}$ as in Figure 1(c), and differentiate (2.3) with respect to $\bar{a}$ to obtain

$$0 \;= \frac{d}{d\bar{a}}\Big[W\big(2\bar{a}\big) + I\big(\bar{a}\big)\Big] = \;\; 2w(2\bar{a}) \;+ I_\circ(\bar{a})\,G'(\bar{a}) \;+\; I_\circ'(\bar{a})\,G(\bar{a}).$$

This implies that

$$I_\circ'(\bar{a}) \;=\; -\,\frac{N'(\bar{a})}{G(\bar{a})}, \qquad \text{where} \quad N'(\bar{a}) = 2w(2\bar{a}) \;+ \overbrace{I_\circ(\bar{a})\,G'(\bar{a})}^{I'(\bar{a})}. \tag{2.4}$$

Since $G(\bar{a}) > 0$, then $I_\circ'(\bar{a}) > 0$ implies that $N'(\bar{a}) < 0$ (and vice-versa), which allows us to relate the geometry of the curves in Figures 1(c) to stability condition (2.14).

Note that, to avoid confusion with notation, we equate $I'(x) \equiv I_\circ G'(x) \equiv I_\circ(\bar{a})G'(x)$.

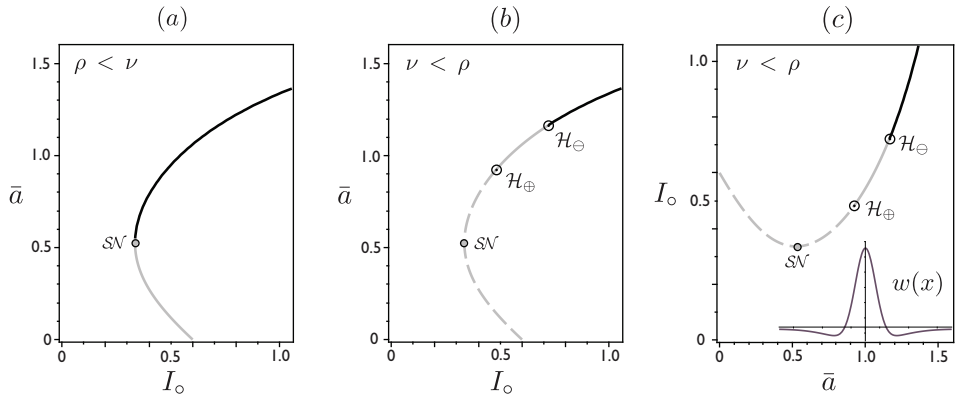

Figure 1. *Bifurcation curves for the Mexican hat weight function illustrating the dependence of the stationary pulse half-width $\bar{a}$ on $I_\circ$ in* (a) *for $\rho < \nu$ and in* (b) *for $\nu < \rho$. Black (gray) denote stability (instability) of the stationary pulse. $\mathcal{SN}$ denotes a saddle-node bifurcation, and $\mathcal{H}_\oplus$ and $\mathcal{H}_\ominus$ denote Hopf bifurcations with respect to the sum and difference modes, respectively. The graph in* (c) *is that of* (b) *reflected across the line $I_\circ = \bar{a}$. The Mexican hat weight function $w(x)$, inset in* (c), *is given by $a_e = 1$, $\sigma_e = 1$, $a_i = 0.4$, $s_i = 2$. Other parameters are $\kappa = 0.3$, $\rho = 1$, $\nu = 0.025$, $\sigma = 1.2$.*

2.2. The linearized operator $\mathcal{M}_{\bar{a}}$ and its spectrum. The linear stability of a stationary pulse $\mathcal{U}_{\bar{a}}(x)$ with half-width $\bar{a}$ is studied by expressing $u(x,t) = \mathcal{U}_{\bar{a}}(x) + \hat{\varphi}(x,t)$ and $n(x,t) = \mathcal{U}_{\bar{a}}(x) + \hat{\psi}(x,t)$, where $(\hat{\varphi}, \hat{\psi})$ represents a small arbitrary perturbation to the pulse. Expanding (1.1) to first order in $(\hat{\varphi}, \hat{\psi})^{\mathrm{T}}$ leads to the formal linearization

$$\begin{aligned} \frac{\partial \hat{\varphi}}{\partial t}(x,t) &= -\hat{\varphi}(x,t) - \rho\hat{\psi}(x,t) \; + \; \int_{-\infty}^{\infty} w(x-y)\, H'\big(\mathcal{U}_{\bar{a}}(y) - \kappa\big)\, \hat{\varphi}(y,t)\, dy, \\ \frac{1}{\nu}\frac{\partial \hat{\psi}}{\partial t}(x,t) &= -\hat{\psi}(x,t) + \hat{\varphi}(x,t). \end{aligned} \tag{2.5}$$

Accordingly, we consider solutions of the form $\hat{\varphi}(x,t) = \mathrm{e}^{\lambda t}\varphi(x)$ and $\hat{\psi}(x,t) = \mathrm{e}^{\lambda t}\psi(x)$, with $(\varphi,\psi)^{\mathrm{T}} \in \mathscr{H} \oplus i\mathscr{H}$, where the Hilbert space $\mathscr{H} = \mathscr{L}^2(\mathbb{R},\mathbb{R}^2)$, which denotes the set of Lebesgue square integrable functions $f : \mathbb{R} \longrightarrow \mathbb{R}^2$. The integral is reexpressed using

$$\left(\frac{dH}{d\mathcal{U}_{\bar{a}}}\big(\mathcal{U}_{\bar{a}} - \kappa\big)\right)(x) \; = \; \frac{\delta(x-\bar{a})}{|\mathcal{U}'_{\bar{a}}(\bar{a})|} + \frac{\delta(x+\bar{a})}{|\mathcal{U}'_{\bar{a}}(-\bar{a})|}, \tag{2.6}$$

leading from (2.5) to the spectral problem

$$\mathcal{M}_{\bar{a}}\boldsymbol{\phi} = \lambda\boldsymbol{\phi}, \qquad \mathcal{M}_{\bar{a}}\boldsymbol{\phi} \; = \; \begin{bmatrix} -1 & -\rho \\ \nu & -\nu \end{bmatrix} \begin{pmatrix} \varphi \\ \psi \end{pmatrix} + \begin{pmatrix} \mathcal{N}_{\bar{a}}\,\varphi \\ 0 \end{pmatrix},$$

where $\boldsymbol{\phi} = (\varphi,\psi)^{\mathrm{T}}$ and $\mathcal{N}_{\bar{a}}$ is a nonlocal spatial operator defined by

$$\big(\mathcal{N}_{\bar{a}}\,\varphi\big)(x) \; = \; \int_{\mathbb{R}} \left(\frac{\delta(y-\bar{a})}{|\mathcal{U}'_{\bar{a}}(\bar{a})|} + \frac{\delta(y+\bar{a})}{|\mathcal{U}'_{\bar{a}}(-\bar{a})|}\right) w(x-y)\,\varphi(y)dy.$$

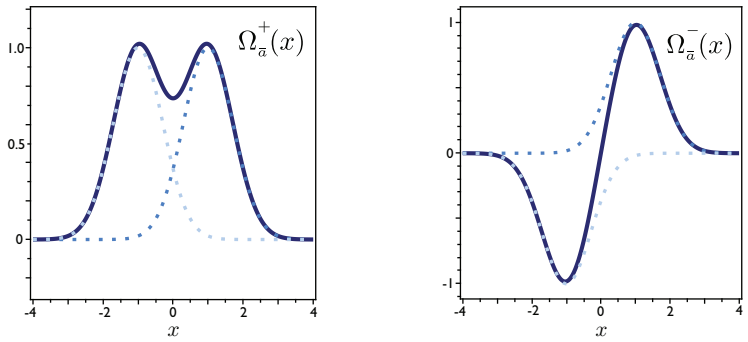

(a) sum mode $\Omega_{\bar{a}}^{+}(x)$ (b) difference mode $\Omega_{\bar{a}}^{-}(x)$

Figure 2. *Spatial modes* $\Omega_{\bar{a}}^{\pm}$ *(solid curves) for the linearized system* (2.5) *with profiles* $\Omega_{\bar{a}}^{\pm}(x)$ *given by* (2.11)–(2.13). *Dotted graphs indicate the components* $w(x \pm \bar{a})$ *with* $\bar{a} = 1$.

We write the subscript in $\mathcal{M}_{\bar{a}}$ to express its dependence on the pulse *half-width* $\bar{a}$ which is important in the analysis of the bifurcation. Since $\psi(x) = \left(\frac{\nu}{\lambda+\nu}\right)\varphi(x)$, the spectrum is then determined by solutions (λ, φ) of the equation

$$\left(\lambda + 1 + \frac{\nu\rho}{\lambda+\nu}\right)\varphi(x) \;=\; \frac{w\big(x-\bar{a}\big)}{\big|\mathcal{U}_{\bar{a}}'(\bar{a})\big|}\,\varphi(\bar{a}) \;+\; \frac{w\big(x+\bar{a}\big)}{\big|\mathcal{U}_{\bar{a}}'(-\bar{a})\big|}\,\varphi(-\bar{a}), \tag{2.7}$$

where $\mathcal{U}_{\bar{a}}'(-\bar{a}) = -\mathcal{U}_{\bar{a}}'(\bar{a}) > 0$. From (2.2) the spatial derivative $\mathcal{U}_{\bar{a}}'(\bar{a})$ is given by

$$\mathcal{U}_{\bar{a}}'(\bar{a}) = \tfrac{1}{1+\rho}\Big(I'(\bar{a}) - w(0) + w(2\bar{a})\Big) < 0. \tag{2.8}$$

Essential spectrum. The essential spectrum is composed of $\lambda = \lambda_{\pm}^{\circ}$, where

$$\lambda_{\pm}^{\circ} = -\tfrac{1}{2}\big(1+\nu\big) \pm \tfrac{1}{2}\sqrt{\big(1+\nu\big)^2 - 4\nu\big(1+\rho\big)}. \tag{2.9}$$

Associated with it is the infinite set of functions $\boldsymbol{\phi}(x) = \boldsymbol{v}_{\pm}^{\circ}\,\varphi^{\circ}(x)$ which are constructed as products of any scalar function $\varphi^{\circ}(x) \in \mathscr{L}^2(\mathbb{R}, \mathbb{R})$ that vanishes at $x = \pm\,\bar{a}$, with either of the eigenvectors $\boldsymbol{v}_{\pm}^{\circ}$ of the matrix $\mathcal{M}_{\circ}$, where

$$\mathcal{M}_{\circ} \;=\; \begin{bmatrix} -1 & -\rho \\ \nu & -\nu \end{bmatrix}.$$

Since $\mathcal{M}_{\bar{a}}$ is a closed operator and $\lambda_{\pm}^{\circ}$ are isolated points of the spectrum with infinite geometric multiplicity, it follows that $\lambda_{\pm}^{\circ}$ belong to the essential spectrum of $\mathcal{M}_{\bar{a}}$ [54]. Moreover, the essential spectrum plays no role in instability since $\mathcal{R}e\big\{\lambda_{\pm}^{\circ}\big\} < 0$.

The point spectrum and the spatial modes $\Omega_{\bar{a}}^{\pm}$. Comprising the point spectrum are two pairs of eigenvalues $\lambda_{\pm}^{+}, \lambda_{\pm}^{-}$, each corresponding to one of the two spatial eigenmodes $\Omega_{\bar{a}}^{\pm} \in \mathscr{L}^2(\mathbb{R}, \mathbb{R})$ of the linearization about the stationary pulse which are illustrated in Figure 2.

- The *sum mode* $\Omega_{\bar{a}}^{+}$ has eigenvalues $\lambda = \lambda_{\pm}^{+}$ which are given by

$$\lambda_{\pm}^{+}(\bar{a}) = \frac{-\Theta_{+} \pm \sqrt{\Theta_{+}^{2} - 4\,\Upsilon_{+}}}{2}, \tag{2.10}$$

$$\begin{aligned} \Theta_{+}(\bar{a}) &= (1+\nu) - (1+\rho)\,\Gamma_{+}(\bar{a}), \\ \Upsilon_{+}(\bar{a}) &= \nu\,(1+\rho)\,\big(1 - \Gamma_{+}(\bar{a})\big), \\ \Gamma_{+}(\bar{a}) &= \frac{\Omega_{\bar{a}}^{+}(\bar{a})}{w(0) - w(2\bar{a}) + \big|I'(\bar{a})\big|} \end{aligned}$$

and correspond to the eigenfunctions $\boldsymbol{\phi} = \boldsymbol{v}_{\pm}^{+}(x)$, where $\boldsymbol{v}_{\pm}^{+}(x) = \Omega_{\bar{a}}^{+}(x)\,\mathring{\boldsymbol{v}}_{\pm}^{+}$ and

$$\Omega_{\bar{a}}^{+}(x) = w(x-\bar{a}) + w(x+\bar{a}), \qquad \mathring{\boldsymbol{v}}_{\pm}^{+} = \begin{pmatrix} 1 & \dfrac{\nu}{\lambda_{\pm}^{+} + \nu} \end{pmatrix}^{\mathrm{T}}. \tag{2.11}$$

- The *difference mode* $\Omega_{\bar{a}}^{-}$ has eigenvalues $\lambda = \lambda_{\pm}^{-}$ which are given by

$$\lambda_{\pm}^{-}(\bar{a}) = \frac{-\Theta_{-} \pm \sqrt{\Theta_{-}^{2} - 4\,\Upsilon_{-}}}{2}, \tag{2.12}$$

$$\begin{aligned} \Theta_{-}(\bar{a}) &= (1+\nu) - (1+\rho)\,\Gamma_{-}(\bar{a}), \\ \Upsilon_{-}(\bar{a}) &= \nu\,(1+\rho)\,\big(1 - \Gamma_{-}(\bar{a})\big), \\ \Gamma_{-}(\bar{a}) &= \frac{\Omega_{\bar{a}}^{-}(\bar{a})}{w(0) - w(2\bar{a}) + \big|I'(\bar{a})\big|} \end{aligned}$$

and correspond to the eigenfunctions $\boldsymbol{\phi} = \boldsymbol{v}_{\pm}^{-}(x)$, where $\boldsymbol{v}_{\pm}^{-}(x) = \Omega_{\bar{a}}^{-}(x)\,\mathring{\boldsymbol{v}}_{\pm}^{-}$ and

$$\Omega_{\bar{a}}^{-}(x) = w(x-\bar{a}) - w(x+\bar{a}), \qquad \mathring{\boldsymbol{v}}_{\pm}^{-} = \begin{pmatrix} 1 & \dfrac{\nu}{\lambda_{\pm}^{-} + \nu} \end{pmatrix}^{\mathrm{T}}. \tag{2.13}$$

Note that $\Omega_{\bar{a}}^{+}(x)$ is an *even* function and $\Omega_{\bar{a}}^{-}(x)$ is an *odd* function since $w(x)$ is even.

No input ($I_\circ = 0$). The *difference mode* $\Omega_{\bar{a}}^{-}$ has eigenvalue $\lambda_{+}^{-} = 0$, as a result of $\Gamma_{-} = 1$, reflecting the translation invariance of the system. The other eigenvalue for the difference mode is positive for $\rho > \nu$ and negative for $\rho < \nu$. A stationary pulse is therefore always linearly unstable in the case $\rho > \nu$. For $\rho < \nu$, a stationary pulse, with half-width $\bar{a}$, can be linearly stable only if $w(2\bar{a}) < 0$ which occurs only in the case of the Mexican hat weight function ($w(2\bar{a}) < 0 \;\Rightarrow\; \Gamma_{+} < 1$). Also, since $\rho < \nu$, it is not possible for a stable stationary pulse to undergo a Hopf bifurcation.

Excitatory inputs ($I_\circ > 0$). The input $I(x)$ can stabilize a stationary pulse by moving all eigenvalues into the left half-plane. A stationary pulse is linearly stable when $\lambda_{\pm}^{+}, \lambda_{\pm}^{-} < 0$, which occurs when $\Gamma_{+}, \Gamma_{-} < 1$ and $\Theta_{+}, \Theta_{-} > 0$. Since $\Gamma_{-} < 1$ is automatically satisfied, and $\Theta_{+}, \Theta_{-} > 0$ are equivalent to $\Gamma_{+}, \Gamma_{-} < (1+\nu)/(1+\rho)$, linear stability of the stationary pulse reduces to the conditions

$$\Gamma_{+} < 1 \quad \text{if } \nu > \rho \qquad \text{and} \qquad \Gamma_{+}, \Gamma_{-} < \frac{1+\nu}{1+\rho} \quad \text{if } \nu < \rho.$$

These conditions translate in terms of the gradient $|I'(\bar{a})|$ to

$$\nu > \rho: \quad \big|I'(\bar{a})\big| > D_{\mathcal{SN}}(\bar{a}) = 2\,w(2\bar{a}) \iff N'(\bar{a}) < 0, \tag{2.14}$$

$$\nu < \rho: \quad \big|I'(\bar{a})\big| > D_{\mathcal{H}}(\bar{a}) = \begin{cases} \left(\frac{\rho-\nu}{1+\nu}\right)\Omega_{\bar{a}}^{+}(\bar{a}) + 2w(2\bar{a}), & w(2\bar{a}) > 0, \\ \left(\frac{\rho-\nu}{1+\nu}\right)\Omega_{\bar{a}}^{-}(\bar{a}), & w(2\bar{a}) < 0, \end{cases} \tag{2.15}$$

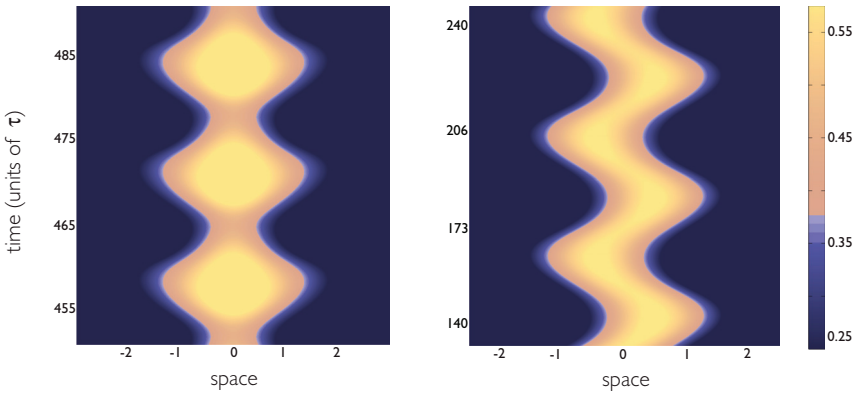

Figure 3. *Breathing and sloshing pulses arising from destabilization of different spatial modes in a Hopf bifurcation of a stationary pulse solution as the input amplitude $I_\circ$ is decreased.* (a) *even-symmetric breather arising from the destabilization of the sum mode $\Omega_{\bar{a}}^+(x)$ for the parameters $I_\circ = 1.9$, $\bar{w}_i = 0.0$, $\rho = 2.75$, $\nu = 0.1$, $\kappa = 0.375$.* (b) *Asymmetric breather, or slosher, arising from destabilization of the difference mode $\Omega_{\bar{a}}^-(x)$ for the parameters $I_\circ = 1.5$, $\bar{w}_i = 0.4$, $\sigma_i = 2$, $\rho = 2.6$, $\nu = 0.01$, $\kappa = 0.35$. Parameters common to both cases are $\sigma = 1.2, \bar{w}_e = 1$, $\sigma_e = 1, \tau = 1$. Yellow indicates superthreshold activity; light blue denotes the firing threshold κ.*

where $N'(\bar{a})$ is given in (2.4). We no longer necessarily have a 0 eigenvalue due to the loss of translation invariance of the stationary pulse. A pair of complex eigenvalues crosses into the right half-plane when $\left|I'(\bar{a})\right| = D_{\mathcal{H}}(\bar{a})$, which determines the Hopf bifurcation point $(\bar{a}, I_\circ(\bar{a})) = (\bar{a}_{\mathcal{H}}, I_\circ^{\mathcal{H}})$. In contrast to [33, 11], when w is a Mexican hat, the fact that $w(2\bar{a}) < 0$ introduces a new case in (2.15) wherein it is additionally possible for the *difference mode* $\Omega_{\bar{a}}^-$ to lose stability in a Hopf bifurcation of a stationary pulse $\mathcal{U}_{\bar{a}}$. In particular, at the bifurcation point $\bar{a} = \bar{a}_{\mathcal{H}}$, the sum mode $\Omega_{\bar{a}}^+$ destabilizes if $w(2\bar{a}_{\mathcal{H}}) > 0$, while the difference mode $\Omega_{\bar{a}}^-$ destabilizes if $w(2\bar{a}_{\mathcal{H}}) < 0$. A loss of stability of the *sum mode* $\Omega_{\bar{a}}^+$ gives rise to the expanding-contracting type of breather which commonly occurs in this model [33, 11]. Interestingly, destabilization of the difference mode $\Omega_{\bar{a}}^+$ can give rise to a different type of stable periodic solution which oscillates with a time-periodic side-to-side motion. We refer to such localized periodic solutions as *side-to-side* breathers or *sloshers* due to their motion which is illustrated in Figure 3(b).

Finally, we show how the geometry of the solution branches in Figure 1 relates to stability condition (2.14) using the relationship identified in (2.4).

Case A ($\nu > \rho$). From (2.14), a stationary pulse $\mathcal{U}_{\bar{a}}$ is stable when $N'(\bar{a}) < 0$ and unstable when $N'(\bar{a}) > 0$. Equation (2.4) then implies that stable pulses occur on branches along which $I_\circ'(\bar{a}) > 0$, while unstable pulses lie along branches where $I_\circ'(\bar{a}) < 0$. (We mention that, although no stability results are affected, there is a minor error in the analysis of [33] that is corrected by this analysis. The difference is in the derivatives $I_\circ'(\bar{a})$ and $I'(\bar{a})$.) Recall that Figure 1(c) graphs the existence condition from the alternative perspective of the dependence of $I_\circ$ on the half-width $\bar{a}$. Stability of the branches is determined by the slope of the tangent at each point. A saddle-node bifurcation occurs at $\bar{a} = \bar{a}_{\mathcal{SN}}$ when $I_\circ'(\bar{a}) = 0$, i.e., when $|I'(\bar{a})| \equiv |I_\circ(\bar{a})G'(\bar{a})|$ passes through $D_{\mathcal{SN}}(\bar{a})$, with the vanishing of the real eigenvalue λ^+.

(Note that $w(2\bar{a}_{SN}) > 0$ for $N'(\bar{a}_{SN}) = 0$.) Hence, if $\nu > \rho$, then the right branch in Figure 1(c) is stable and the left branch is unstable for all $\bar{a}$.

Case B ($\nu < \rho$). At $\rho = \nu$, a pair of zero eigenvalues suggests a codimension 2 Bogdanov–Takens bifurcation. As ν decreases from ρ, a Hopf bifurcation point emerges from the saddle-node point and traverses along the branch that is stable for $\rho < \nu$, destabilizing the segment from the saddle-node to the Hopf bifurcation points.

3. Nonlinear analysis of the Hopf bifurcation. We analyze the nonlinear stability of a stationary pulse in (1.1) near a Hopf bifurcation by two approaches: in section 3.3 by the method of *multiple scales* and *amplitude equations* and in section 3.4 by projection onto the *center manifold* which is approximated to second order. This provides the framework for studying the dynamics of the periodic solution bifurcating from a stationary pulse in a neighborhood of the Hopf bifurcation point. As the two approaches use a related set of operators arising in the expansion of the dynamical system about the stationary pulse $\mathcal{U}_{\bar{a}}(x)$, we begin by collecting a variety of results in sections 3.1 and 3.2 that are used throughout sections 3.3 and 3.4 to calculate the normal form coefficients and bifurcation formulae for the Hopf bifurcation. To streamline the exposition, the core calculations are collected separately in Appendices A–E. The analytical results are then compared with numerical simulations in section 3.5 demonstrating strong agreement regarding the direction of bifurcation and whether the bifurcation is sub/supercritical.

3.1. Preliminaries. We consider the firing rate model (1.1) in the presence of a localized, excitatory input inhomogeneity $I(x)$, which we reexpress as

$$\begin{aligned} \frac{\partial u}{\partial t}(x,t) &= -u(x,t) - \rho\, n(x,t) + \big(F(u)\big)(x,t) + I(x), \\ \frac{1}{\nu}\frac{\partial n}{\partial t}(x,t) &= u(x,t) - n(x,t), \end{aligned} \tag{3.1}$$

where the nonlinearity $F(u)$ is given by

$$\big(F(u)\big)(x,t) = \Big(w * H(u-\kappa)\Big)(x,t) \equiv \int_{\mathbb{R}} w(x-y) H\big(u(y,t)-\kappa\big)\, dy.$$

We assume the parameters of the system are such that (3.1) supports a stable stationary pulse $\big(\mathcal{U}_{\bar{a}}(x), \mathcal{U}_{\bar{a}}(x)\big)$ with $\mathcal{U}_{\bar{a}}(x)$ as given in (2.2). In particular, we consider the bifurcation parameter $I_\circ$ in a small neighborhood of a Hopf bifurcation point, which is taken to occur at $(\bar{a}, I_\circ) = (\bar{a}_{\mathcal{H}}, I_\circ^{\mathcal{H}})$, and consider the evolution of an arbitrary, small perturbation $\boldsymbol{\phi} = (\varphi, \psi)^T$ to the stationary pulse $\big(\mathcal{U}_{\bar{a}}, \mathcal{U}_{\bar{a}}\big)^T$ by setting

$$\begin{pmatrix} u(x,t) \\ n(x,t) \end{pmatrix} = \begin{pmatrix} 1 \\ 1 \end{pmatrix} \mathcal{U}_{\bar{a}}(x) + \boldsymbol{\phi}(x,t). \tag{3.2}$$

Since Taylor expansion extends, in the sense of distributions, to the Heaviside function and the δ-function [29], we may formally express the nonlinearity $F(u)$ in terms of a Taylor expansion for small φ about the equilibrium $u(x,t) = \mathcal{U}_{\bar{a}}(x)$, i.e.,

$$\begin{aligned} F(u) = {} & w * H(\mathcal{U}_{\bar{a}} - \kappa) + w * \big[\, \delta(\mathcal{U}_{\bar{a}} - \kappa)\varphi \,\big] \\ & + \tfrac{1}{2!}\, w * \big[\, \delta'(\mathcal{U}_{\bar{a}} - \kappa)\varphi^2 \,\big] + \tfrac{1}{3!}\, w * \big[\, \delta''(\mathcal{U}_{\bar{a}} - \kappa)\varphi^3 \,\big] \;+\; \mathcal{O}(\varphi^4). \end{aligned}$$

Consequently, the perturbation $\boldsymbol{\phi}$ evolves according to

$$\frac{\partial \boldsymbol{\phi}}{\partial t} = \mathcal{M}_{\bar{a}}\boldsymbol{\phi} + \tfrac{1}{2!}\,\mathrm{B}_{\bar{a}}(\boldsymbol{\phi},\boldsymbol{\phi}) + \tfrac{1}{3!}\,\mathrm{C}_{\bar{a}}(\boldsymbol{\phi},\boldsymbol{\phi},\boldsymbol{\phi}) + \mathcal{O}\big(\|\boldsymbol{\phi}\|^4\big), \tag{3.3}$$

where the first order term is given by the linear operator $\mathcal{M}_{\bar{a}}$,

$$\mathcal{M}_{\bar{a}}\,\boldsymbol{\phi} \;=\; \begin{bmatrix} -1 & -\rho \\ \nu & -\nu \end{bmatrix} \begin{pmatrix} \varphi \\ \psi \end{pmatrix} + \begin{pmatrix} w * \big[\delta(\mathcal{U}_{\bar{a}} - \kappa)\,\varphi\big] \\ 0 \end{pmatrix},$$

and the second and third order terms are given by the multilinear operators

$$\mathrm{B}_{\bar{a}}(\boldsymbol{\phi},\boldsymbol{\phi}) = \begin{pmatrix} w * [\,\delta'(\mathcal{U}_{\bar{a}} - \kappa)\,\varphi^2\,] \\ 0 \end{pmatrix}, \qquad \mathrm{C}_{\bar{a}}(\boldsymbol{\phi},\boldsymbol{\phi},\boldsymbol{\phi}) = \begin{pmatrix} w * [\,\delta''(\mathcal{U}_{\bar{a}} - \kappa)\,\varphi^3\,] \\ 0 \end{pmatrix}.$$

While in (3.3) we treat the *input amplitude* $I_\circ$ as the bifurcation parameter for fixed $\nu, \rho, \kappa, \sigma$, it is directly related to the *stationary pulse half-width* $\bar{a}$, through condition (2.3), and therefore both parameters, simultaneously, control the bifurcation. However, since $\bar{a}$ is explicitly present throughout the equations, it is more mathematically convenient to treat the bifurcation as being controlled solely by the pulse half-width $\bar{a}$ and, instead, to view the input amplitude $I_\circ$ as being dependent upon $\bar{a}$, thereby recognizing a single bifurcation parameter for the higher order analysis. This is appropriate in the neighborhood of a Hopf bifurcation point $(\bar{a}, I_\circ) = (\bar{a}_\mathcal{H}, I_\circ^\mathcal{H})$ that is sufficiently far from any other bifurcation point, as the relationship between the two parameters can be expressed as one-to-one. The relationship between $I_\circ$ and $\bar{a}$ in the vicinity of the Hopf bifurcation point is approximated in Appendix A, and we occasionally write $I_\circ(\bar{a})$ to express this dependence.

3.2. Operators $\mathcal{M}_\mathcal{H}, \mathrm{B}_\mathcal{H}, \mathrm{C}_\mathcal{H}$, and $\mathcal{U}'_\mathcal{H}$ at criticality ($\bar{a} = \bar{a}_\mathcal{H}$). In this section, we collect the expressions and properties for the stationary pulse $\mathcal{U}_{\bar{a}}(x)$ and the operators $\mathcal{M}_{\bar{a}}, \mathrm{B}_{\bar{a}}, \mathrm{C}_{\bar{a}}$ evaluated at the critical point $\bar{a} = \bar{a}_\mathcal{H}$. These are the primary operators common to both the amplitude equation and center manifold reduction. Important results for inner products involving these operators are also summarized. As the calculations are rather involved, the details are collected in Appendices A–E.

Derivatives of the stationary pulse $\mathcal{U}_{\bar{a}}$. The spatial derivative $\mathcal{U}'_{\bar{a}}(x)$ of the stationary pulse at the critical point $(\bar{a}, I_\circ) = (\bar{a}_\mathcal{H}, I_\circ^\mathcal{H})$ of the Hopf bifurcation appears ubiquitously in the various operators and is given by

$$\mathcal{U}'_\mathcal{H}(x) \;\equiv\; \tfrac{d}{dx}\mathcal{U}_{\bar{a}_\mathcal{H}}(x) \;=\; \frac{1}{1+\rho}\Big(w(x+\bar{a}_\mathcal{H}) - w(x-\bar{a}_\mathcal{H}) + I_\circ^\mathcal{H}\,G'(x)\Big). \tag{3.4}$$

The pulse profile $\mathcal{U}_{\bar{a}}(x)$ is even in x, and we define the symbol $|\mathcal{U}'_\mathcal{H}|$, where

$$|\mathcal{U}'_\mathcal{H}| \;=\; -\tfrac{d}{dx}\mathcal{U}_{\bar{a}_\mathcal{H}}(x)\Big|_{x=\bar{a}_\mathcal{H}} \;=\; \tfrac{d}{dx}\mathcal{U}_{\bar{a}_\mathcal{H}}(x)\Big|_{x=-\bar{a}_\mathcal{H}} = |-\mathcal{U}'_\mathcal{H}|$$

since $|\mathcal{U}'_{\bar{a}_\mathcal{H}}(\pm\bar{a}_\mathcal{H})|$ appears frequently throughout the analysis. Higher order derivatives of the stationary pulse are defined and collected in Appendix A.

Linearized operator $\mathcal{M}_{\mathcal{H}}$ and the critical spatial eigenmode Ω. The linear operator $\mathcal{M}_{\bar{a}}$ at the critical point $\bar{a} = \bar{a}_{\mathcal{H}}$ is denoted by

$$\mathcal{M}_{\mathcal{H}}\boldsymbol{\phi} \equiv \mathcal{M}_{\bar{a}_{\mathcal{H}}}\boldsymbol{\phi} = \begin{bmatrix} -1 & -\rho \\ \nu & -\nu \end{bmatrix} \begin{pmatrix} \varphi \\ \psi \end{pmatrix} + \begin{pmatrix} \mathcal{N}_{\mathcal{H}}\,\varphi \\ 0 \end{pmatrix},$$

where the nonlocal spatial operator $\mathcal{N}_{\mathcal{H}}$ is expressed as

$$\Big(\mathcal{N}_{\mathcal{H}}\,\varphi\Big)(x) = \int_{\mathbb{R}} \left(\frac{\delta(y-\bar{a}_{\mathcal{H}})}{|u'_{\mathcal{H}}|} + \frac{\delta(y+\bar{a}_{\mathcal{H}})}{|-u'_{\mathcal{H}}|} \right) w(x-y)\,\varphi(y)dy.$$

The operator $\mathcal{M}_{\mathcal{H}}$ has a pair of imaginary eigenvalues $\lambda, \bar{\lambda}$, where $\lambda = i\omega_\circ$, with their respective eigenvectors $\boldsymbol{v}(x), \bar{\boldsymbol{v}}(x) \in \mathscr{H} \oplus i\mathscr{H} \equiv \mathscr{L}^2(\mathbb{R}, \mathbb{C}^2)$ given by

$$\mathcal{M}_{\mathcal{H}}\boldsymbol{v} = i\omega_\circ\,\boldsymbol{v}, \qquad \boldsymbol{v}(x) = \begin{pmatrix} 1 \\ \frac{\nu}{\rho} - i\frac{\omega_\circ}{\rho} \end{pmatrix} \Omega(x), \tag{3.5}$$

where $\nu < \rho$ and the *Hopf frequency* $\omega_\circ$ is

$$\omega_\circ = \sqrt{\nu(\rho-\nu)}.$$

Ω denotes the *critical spatial mode* for the Hopf bifurcation which satisfies

$$\mathcal{N}_{\mathcal{H}}\Omega(x) = (1+\nu)\,\Omega(x).$$

From (2.11)–(2.13), there are only two spatial modes, and we introduce the notation

$$\Omega_\pm(x) \equiv \Omega^\pm_{\bar{a}}(x)\Big|_{\bar{a}=\bar{a}_{\mathcal{H}}}.$$

In the case that the *sum mode* $\Omega = \Omega_+$ becomes critical in the Hopf bifurcation,

$$\Omega_+\big(x\big) = w\big(x-\bar{a}_{\mathcal{H}}\big) + w\big(x+\bar{a}_{\mathcal{H}}\big), \qquad \text{(SUM MODE)} \tag{3.6}$$

whereas if the *difference mode* $\Omega = \Omega_-$ becomes critical,

$$\Omega_-\big(x\big) = w\big(x-\bar{a}_{\mathcal{H}}\big) - w\big(x+\bar{a}_{\mathcal{H}}\big), \qquad \text{(DIFFERENCE MODE)} \tag{3.7}$$

and, whichever mode Ω becomes critical in the bifurcation, it satisfies

$$\Omega\big(\bar{a}_{\mathcal{H}}\big) = (1+\nu)|u'_{\mathcal{H}}|. \tag{3.8}$$

We reiterate that destabilizing the *sum* mode Ω_+ leads to the *expanding-contracting* breather, whereas the *difference* mode Ω_- leads to the side-to-side or *sloshing* breather in a Hopf bifurcation of a stationary pulse. Note that the $\pm$ notation for denoting the dependence of expressions on spatial modes $\Omega_\pm$ is often suppressed to Ω in equations until it becomes relevant to distinguish.

Adjoint operator $\mathcal{M}^*_{\mathcal{H}}$. Defining the usual inner product on $\mathscr{H} \oplus i\mathscr{H}$ as

$$\langle \boldsymbol{q}, \boldsymbol{p} \rangle = \sum_{i=1}^{2} \int_{\mathbb{R}} \bar{q}_i(x)\, p_i(x)\, dx,$$

where $\boldsymbol{p} = (p_1, p_2)^T$, $\boldsymbol{q} = (q_1, q_2)^T$, we proceed to calculate the adjoint operator $\mathcal{M}^*_{\mathcal{H}}$. The adjoint operator $\mathcal{M}^*_{\mathcal{H}}$ satisfies $\langle \boldsymbol{q}, \mathcal{M}_{\mathcal{H}} \boldsymbol{p} \rangle = \langle \mathcal{M}^*_{\mathcal{H}} \boldsymbol{q}, \boldsymbol{p} \rangle$ and is given by

$$\mathcal{M}^*_{\mathcal{H}} \boldsymbol{\phi} = \begin{bmatrix} -1 & \nu \\ -\rho & -\nu \end{bmatrix} \begin{pmatrix} \varphi \\ \psi \end{pmatrix} + \begin{pmatrix} \mathcal{N}^*_{\mathcal{H}}\, \varphi \\ 0 \end{pmatrix}, \tag{3.9}$$

where

$$\mathcal{N}^*_{\mathcal{H}}\, \varphi(x) \;=\; \left(\frac{\delta(x - \bar{a}_{\mathcal{H}})}{|u'_{\mathcal{H}}|} + \frac{\delta(x + \bar{a}_{\mathcal{H}})}{|-u'_{\mathcal{H}}|} \right) \int_{\mathbb{R}} w(x - y)\, \varphi(y)\, dy. \tag{3.10}$$

The operator $\mathcal{N}^*_{\mathcal{H}}$ is formally defined in the sense of distributions and arises as follows:

$$\begin{aligned} \left\langle \boldsymbol{q}, \begin{pmatrix} \mathcal{N}_{\mathcal{H}}\, p_1 \\ 0 \end{pmatrix} \right\rangle &= \int_{\mathbb{R}} \overline{q}_1(x) \left[\int_{\mathbb{R}} \left(\frac{\delta(y - \bar{a}_{\mathcal{H}})}{|u'_{\mathcal{H}}|} + \frac{\delta(y + \bar{a}_{\mathcal{H}})}{|-u'_{\mathcal{H}}|} \right) w(x - y)\, p_1(y)\, dy \right] dx \\ &= \int_{\mathbb{R}} \left[\left(\frac{\delta(y - \bar{a}_{\mathcal{H}})}{|u'_{\mathcal{H}}|} + \frac{\delta(y + \bar{a}_{\mathcal{H}})}{|-u'_{\mathcal{H}}|} \right) \int_{\mathbb{R}} w(y - x)\, \overline{q}_1(x)\, dx \right] p_1(y)\, dy \\ &= \left\langle \begin{pmatrix} \mathcal{N}^*_{\mathcal{H}}\, q_1 \\ 0 \end{pmatrix}, \boldsymbol{p} \right\rangle, \end{aligned}$$

where the even symmetry of w is used. Since $w \in C^\infty(\mathbb{R}, \mathbb{R})$ and the δ-functions have compact support, the exchange of the order of integration is permissible [73].

Nullspace of the operator $\mathcal{M}^*_{\mathcal{H}} + i\omega_\circ \mathrm{I}$. The two approaches in sections 3.3 and 3.4 involve the adjoint eigenvectors $\boldsymbol{y}$, $\bar{\boldsymbol{y}}$, associated with the adjoint operator $\mathcal{M}^*_{\mathcal{H}}$, where

$$\mathcal{M}^*_{\mathcal{H}}\, \boldsymbol{y} = -\, i\omega_\circ\, \boldsymbol{y}. \tag{3.11}$$

Due to the appearance of the δ-function outside of the integral in (3.9)–(3.10), we consider the solution $\boldsymbol{y}(x)$ in a *weak* formulation of (3.11) given by

$$\left\langle \boldsymbol{y}, (\mathcal{M}^*_{\mathcal{H}} - i\omega_\circ \mathrm{I})^* \boldsymbol{u} \right\rangle = 0 \qquad \text{for each } \boldsymbol{u} \in \mathcal{D}(\mathbb{R}) \equiv \mathcal{C}^\infty_0(\mathbb{R}, \mathbb{C}^2). \tag{3.12}$$

Depending on which of the two spatial modes $\Omega(x) = \Omega_\pm(x)$ becomes critical in the Hopf bifurcation and using $\omega_\circ^2 = \nu(\rho - \nu)$, solutions of (3.11) are of the form

$$\boldsymbol{y}(x) = \zeta \begin{pmatrix} 1 \\ -\big(1 + i\frac{\omega_\circ}{\nu}\big) \end{pmatrix} \Delta(x), \qquad \zeta \;=\; \frac{1}{4\,\Omega(\bar{a}_{\mathcal{H}})} \left(1 - i\frac{\omega_\circ}{\rho - \nu} \right). \tag{3.13}$$

ζ is a constant chosen so that $\langle \boldsymbol{y}, \boldsymbol{v} \rangle = 1$, and the function $\Delta(x)$ satisfies the equation

$$(1+\nu)\,\Delta(x) \;=\; \mathcal{N}^*_{\mathcal{H}}\Delta(x). \tag{3.14}$$

There are various ways to solve (3.14), and, in Appendix D, we demonstrate one such method, applying Fourier transforms to construct the solution. The solutions of (3.14) depend on which eigenmode $\Omega_\pm$ goes critical in the Hopf bifurcation.

In the case that the *sum mode* Ω_+ goes critical,

$$\Delta_+(x) \;=\; \delta(x-\bar{a}_{\mathcal{H}}) + \delta(x+\bar{a}_{\mathcal{H}}), \qquad \text{(SUM MODE)}$$

whereas in the case that the *difference mode* Ω_- goes critical,

$$\Delta_-(x) \;=\; \delta(x-\bar{a}_{\mathcal{H}}) - \delta(x+\bar{a}_{\mathcal{H}}). \qquad \text{(DIFFERENCE MODE)}$$

Also, it is straightforward to show by substitution that the above solutions $\Delta_\pm$ satisfy the weak formulation of (3.14).

Higher order terms $\mathrm{B}_{\mathcal{H}}$ and $\mathrm{C}_{\mathcal{H}}$ at criticality. The methods in sections 3.3 and 3.4 involve the operators $\mathrm{B}_{\bar{a}}, \mathrm{C}_{\bar{a}}$ at the critical point $\bar{a} = \bar{a}_{\mathcal{H}}$ which we denote $\mathrm{B}_{\mathcal{H}}, \mathrm{C}_{\mathcal{H}}$. The subscripts $\pm$ correspond to the spatial mode $\Omega_\pm$ that becomes critical in the Hopf bifurcation, with $+$ and $-$ denoting the *sum* and *difference modes*, respectively.

The *bilinear operator* $\mathrm{B}_{\bar{a}_{\mathcal{H}}}$ for $\boldsymbol{\phi} = (\varphi, \psi)^{\mathrm{T}} \in \mathscr{H}$ was calculated using (E.1) to be

$$\begin{aligned}
\mathrm{B}_{\mathcal{H}}(\boldsymbol{\phi},\boldsymbol{\phi})(x) \equiv \Big(\mathrm{B}_{\bar{a}_{\mathcal{H}}}(\boldsymbol{\phi},\boldsymbol{\phi})\Big)(x) &= \begin{pmatrix} \big(w * [\delta'(\mathcal{U}_{\mathcal{H}} - \kappa)\varphi^2]\big)(x) \\ 0 \end{pmatrix} \\
&= \begin{pmatrix} 1 \\ 0 \end{pmatrix} \int_{\mathbb{R}} \delta'\Big(\mathcal{U}_{\mathcal{H}}(y) - \kappa\Big)\, w(x-y)\, \varphi^2(y)\, dy \\
&= \begin{pmatrix} 1 \\ 0 \end{pmatrix} \int_{\mathbb{R}} \left[\frac{\delta(y-\bar{a}_{\mathcal{H}})}{|\mathcal{U}'_{\mathcal{H}}|} + \frac{\delta(y+\bar{a}_{\mathcal{H}})}{|-\mathcal{U}'_{\mathcal{H}}|}\right] \cdot \frac{\partial}{\partial y}\left[-\frac{w(x-y)}{\mathcal{U}'_{\mathcal{H}}(y)}\,\varphi^2(y)\right] dy.
\end{aligned} \tag{3.15}$$

The *trilinear operator* $\mathrm{C}_{\bar{a}_{\mathcal{H}}}$ for $\boldsymbol{\phi} = (\varphi, \psi)^{\mathrm{T}} \in \mathscr{H}$ was calculated using (E.2) to be

(3.16)

$$\begin{aligned}
\mathrm{C}_{\mathcal{H}}(\boldsymbol{\phi},\boldsymbol{\phi},\boldsymbol{\phi})(x) \equiv \Big(\mathrm{C}_{\bar{a}_{\mathcal{H}}}(\boldsymbol{\phi},\boldsymbol{\phi},\boldsymbol{\phi})\Big)(x) &= \begin{pmatrix} \big(w * [\delta''(\mathcal{U}_{\mathcal{H}} - \kappa)\varphi^3]\big)(x) \\ 0 \end{pmatrix} \\
&= \begin{pmatrix} 1 \\ 0 \end{pmatrix} \int_{\mathbb{R}} \delta''\Big(\mathcal{U}_{\mathcal{H}}(y) - \kappa\Big)\, w(x-y)\, \varphi^3(y)\, dy \\
&= \begin{pmatrix} 1 \\ 0 \end{pmatrix} \int_{\mathbb{R}} \left[\frac{\delta(y-\bar{a}_{\mathcal{H}})}{|\mathcal{U}'_{\mathcal{H}}|} + \frac{\delta(y+\bar{a}_{\mathcal{H}})}{|-\mathcal{U}'_{\mathcal{H}}|}\right] \cdot \frac{d}{dy}\left[\frac{1}{\mathcal{U}'_{\mathcal{H}}(y)}\frac{d}{dy}\left[\frac{w(x-y)\,\varphi^3(y)}{\mathcal{U}'_{\mathcal{H}}(y)}\right]\right] dy.
\end{aligned}$$

For either eigenvector $\boldsymbol{v}(x), \bar{\boldsymbol{v}}(x)$ of $\mathcal{M}_{\mathcal{H}}$, where $\boldsymbol{v} = (v_1, v_2)^{\mathrm{T}}$, we have $v_1 = \bar{v}_1 = \Omega(x)$. Consequently, for different permutations of $\boldsymbol{\phi} = \boldsymbol{v}, \bar{\boldsymbol{v}}$, it follows that

$$\mathrm{B}_{\mathcal{H}}(\boldsymbol{v},\boldsymbol{v}) \;=\; \mathrm{B}_{\mathcal{H}}(\boldsymbol{v},\bar{\boldsymbol{v}}) \;=\; \mathrm{B}_{\mathcal{H}}(\bar{\boldsymbol{v}},\boldsymbol{v}) \;=\; \mathrm{B}_{\mathcal{H}}(\bar{\boldsymbol{v}},\bar{\boldsymbol{v}}) \;=\; \begin{pmatrix} 1 \\ 0 \end{pmatrix} \Sigma_{\pm}(x),$$

where $\Sigma_\pm(x)$ is even for either mode $\Omega = \Omega_\pm$ and is given in (B.1) in Appendix B. The relevant inner products involving $\mathrm{B}_\mathcal{H}$ with $\boldsymbol{v}, \bar{\boldsymbol{v}}$ and adjoint eigenvectors $\boldsymbol{y}, \bar{\boldsymbol{y}}$ are

$$\begin{aligned}
\big\langle \boldsymbol{y}, \mathrm{B}_\mathcal{H}(\boldsymbol{v},\boldsymbol{v})\big\rangle = \big\langle \boldsymbol{y}, \mathrm{B}_\mathcal{H}(\boldsymbol{v},\bar{\boldsymbol{v}})\big\rangle = \big\langle \boldsymbol{y}, \mathrm{B}_\mathcal{H}(\bar{\boldsymbol{v}},\bar{\boldsymbol{v}})\big\rangle &= \zeta \int_\mathbb{R} \Delta_\pm(x)\,\Sigma_\pm(x)\,dx,\\
\big\langle \bar{\boldsymbol{y}}, \mathrm{B}_\mathcal{H}(\boldsymbol{v},\boldsymbol{v})\big\rangle = \big\langle \bar{\boldsymbol{y}}, \mathrm{B}_\mathcal{H}(\boldsymbol{v},\bar{\boldsymbol{v}})\big\rangle = \big\langle \bar{\boldsymbol{y}}, \mathrm{B}_\mathcal{H}(\bar{\boldsymbol{v}},\bar{\boldsymbol{v}})\big\rangle &= \bar{\zeta} \int_\mathbb{R} \Delta_\pm(x)\,\Sigma_\pm(x)\,dx,\\
\int_\mathbb{R} \Delta_\pm(x)\,\Sigma_\pm(x)\,dx &= \begin{cases} 2\,\Sigma_+(\bar{a}_\mathcal{H}), & \text{(SUM MODE)}\\ 0, & \text{(DIFFERENCE MODE)}\end{cases}
\end{aligned}$$

where $\Sigma_+(\bar{a}_\mathcal{H})$ is given in (B.2) in Appendix B and $\boldsymbol{y} = (y_1, y_2)^\mathrm{T}$ with $y_1 = \zeta\,\Delta_\pm(x)$.

We express $\mathrm{C}_\mathcal{H}\big(\boldsymbol{v},\boldsymbol{v},\bar{\boldsymbol{v}}\big)$ in terms of $\Lambda(x)$, which is given in (B.5) in Appendix B:

$$\mathrm{C}_\mathcal{H}\big(\boldsymbol{v},\boldsymbol{v},\bar{\boldsymbol{v}}\big)(x) = \begin{pmatrix}1\\0\end{pmatrix}\Lambda_\pm(x).$$

$\Lambda_+(x)$ is an *even* function in the case of the *sum mode* Ω_+; conversely, $\Lambda_-(x)$ contains both *even* $\Lambda^e_-(x)$ and *odd* $\Lambda^o_-(x)$ components in the case of the *difference mode* Ω_-.

$$\big\langle \boldsymbol{y},\, \mathrm{C}_\mathcal{H}\big(\boldsymbol{v},\boldsymbol{v},\bar{\boldsymbol{v}}\big)\big\rangle = \zeta \int_\mathbb{R} \Delta_\pm(x)\,\Lambda_\pm(x)\,dx = \begin{cases} 2\zeta\,\Lambda_+(\bar{a}_\mathcal{H}), & \text{(SUM MODE)}\\ 2\zeta\,\Lambda^\mathrm{o}_-(\bar{a}_\mathcal{H}). & \text{(DIFFERENCE MODE)}\end{cases}$$

3.3. Amplitude equation for the breather. We start by repeating (3.3) for the evolution of the perturbations $\boldsymbol{\phi}(t) \in \mathscr{H}$ about the stationary pulse $\mathcal{U}_{\bar{a}}$:

$$\tfrac{\partial}{\partial t}\boldsymbol{\phi} = \mathcal{M}_{\bar{a}}\boldsymbol{\phi} + \tfrac{1}{2!}\mathrm{B}_{\bar{a}}\big(\boldsymbol{\phi},\boldsymbol{\phi}\big) + \tfrac{1}{3!}\mathrm{C}_{\bar{a}}\big(\boldsymbol{\phi},\boldsymbol{\phi},\boldsymbol{\phi}\big) + \mathcal{O}\left(\|\boldsymbol{\phi}\|^4\right). \tag{3.17}$$

Let $\lambda_\pm(\bar{a})$ be the pair of complex eigenvalues becoming critical with all other eigenvalues lying in the left half-plane. The bifurcation parameter $I_\circ$ is directly related to the stationary pulse half-width $\bar{a}$, and, if the Hopf bifurcation point lies sufficiently far from the saddle-node bifurcation point, a restriction can be used locally in which $\bar{a}$ and $I_\circ$ are in one-to-one dependence. We then express deviations of $(\bar{a}, I_\circ)$ from the bifurcation point $(\bar{a}_\mathcal{H}, I^\mathcal{H}_\circ)$ in terms of the small parameter ϵ^2 as

$$\bar{a} = \bar{a}_\mathcal{H} + \alpha\epsilon^2, \qquad I_\circ(\bar{a}) = I^\mathcal{H}_\circ + \alpha\epsilon^2\, I'_\circ(\bar{a}_\mathcal{H}) + \mathcal{O}(\epsilon^4),$$

where $I'_\circ(\bar{a}_\mathcal{H})$ is calculated in Appendix A. The constant $\alpha = \pm 1$ is introduced to allow for the limit cycle to appear on either side of the bifurcation point and remains undetermined at this point. Note that this expansion is done a priori in the case of a Hopf bifurcation since inclusion of the odd powers of ϵ in the expansion typically results in the condition that the corresponding coefficients must vanish according to the Fredholm alternative. However, in some cases odd powers may be present [43].

Accordingly, we expand the operators $\mathcal{M}_{\bar{a}}$, $\mathrm{B}_{\bar{a}}$, and $\mathrm{C}_{\bar{a}}$ to relevant order as

$$\mathcal{M}_{\bar{a}} = \mathcal{M}_\mathcal{H} + \alpha\epsilon^2\,\mathcal{M}_1 + \mathcal{O}(\epsilon^4), \qquad \mathrm{B}_{\bar{a}} = \mathrm{B}_\mathcal{H} + \mathcal{O}(\epsilon^2), \qquad \mathrm{C}_{\bar{a}} = \mathrm{C}_\mathcal{H} + \mathcal{O}(\epsilon^2),$$

with $\lambda(a) = i\omega_\circ + \alpha\epsilon^2\lambda_1 + \mathcal{O}(\epsilon^2)$, where $\mathcal{M}_\mathcal{H}$, $\mathrm{B}_\mathcal{H}$, $\mathrm{C}_\mathcal{H}$ are defined in (3.5), (3.15), (3.16). $\mathcal{M}_1$ and λ_1 are calculated in Appendix A. The standard approach for computing the amplitude equation for a Hopf bifurcation uses two-timing effectively to separate out the dynamics on the center manifold which are taken to evolve on an independent, slow time scale $\tau = \epsilon^2 t$ that is introduced. This results in the operator $\partial_t \mapsto \partial_t + \epsilon^2\,\partial_\tau$. Finally, we expand $\boldsymbol{\phi} = (\varphi, \psi)^{\mathrm{T}}$ in orders of ϵ and include its dependence on τ:

$$\boldsymbol{\phi}(x,t,\tau) \;=\; \boldsymbol{\phi}_1(x,t,\tau)\,\epsilon \;+\; \boldsymbol{\phi}_2(x,t,\tau)\,\epsilon^2 \;+\; \boldsymbol{\phi}_3(x,t,\tau)\,\epsilon^3 \;+\; \mathcal{O}\big(\epsilon^4\big).$$

Under these expansions the system (3.17) becomes

$$\begin{aligned}\left(\frac{\partial}{\partial t} + \epsilon^2\frac{\partial}{\partial \tau}\right)&\left(\boldsymbol{\phi}_1\epsilon + \boldsymbol{\phi}_2\epsilon^2 + \boldsymbol{\phi}_3\epsilon^3 + \cdots\right)\\ &= \left(\mathcal{M}_\mathcal{H} + \alpha\epsilon^2\,\mathcal{M}_1 + \cdots\right)\left(\boldsymbol{\phi}_1\epsilon + \boldsymbol{\phi}_2\epsilon^2 + \boldsymbol{\phi}_3\epsilon^3 + \cdots\right)\\ &\quad + \epsilon^2\left[\tfrac{1}{2!}\mathrm{B}_\mathcal{H}(\boldsymbol{\phi}_1,\boldsymbol{\phi}_1)\right] + \epsilon^3\Big[\mathrm{B}_\mathcal{H}(\boldsymbol{\phi}_1,\boldsymbol{\phi}_2) + \tfrac{1}{3!}\mathrm{C}_\mathcal{H}(\boldsymbol{\phi}_1,\boldsymbol{\phi}_1,\boldsymbol{\phi}_1)\Big] + \mathcal{O}\big(\epsilon^4\big).\end{aligned}$$

Defining the nonlocal, linear spatiotemporal operator $L_\mathcal{H}\boldsymbol{\phi} = \left(\frac{\partial}{\partial t} - \mathcal{M}_\mathcal{H}\right)\boldsymbol{\phi}$, we express the hierarchy of equations according to the order of ϵ as

$$\mathcal{O}(\epsilon) \;:\quad L_\mathcal{H}\boldsymbol{\phi}_1 = 0, \tag{3.18}$$

$$\mathcal{O}(\epsilon^2) \;:\quad L_\mathcal{H}\boldsymbol{\phi}_2 = \tfrac{1}{2!}\,\mathrm{B}_\mathcal{H}\big(\boldsymbol{\phi}_1,\boldsymbol{\phi}_1\big), \tag{3.19}$$

$$\mathcal{O}(\epsilon^3) \;:\quad L_\mathcal{H}\boldsymbol{\phi}_3 = \mathrm{B}_\mathcal{H}\big(\boldsymbol{\phi}_1,\boldsymbol{\phi}_2\big) + \tfrac{1}{3!}\mathrm{C}_\mathcal{H}\big(\boldsymbol{\phi}_1,\boldsymbol{\phi}_1,\boldsymbol{\phi}_1\big) - \frac{\partial\boldsymbol{\phi}_1}{\partial\tau} + \alpha\mathcal{M}_1\boldsymbol{\phi}_1. \tag{3.20}$$

By separation of variables, the nondecaying solution to the $\mathcal{O}(\epsilon)$ equation is given by

$$\boldsymbol{\phi}_1(x,t,\tau) \;=\; z(\tau)\,\boldsymbol{v}(x)\,e^{i\omega_\circ t} + \bar{z}(\tau)\,\bar{\boldsymbol{v}}(x)\,e^{-i\omega_\circ t},$$

where $\boldsymbol{v}(x)$ is given in (3.5), and the *complex amplitude* $z(\tau)$ of the oscillation is ultimately determined by the $\mathcal{O}(\epsilon^3)$ equation.

Continuing to solve the equation hierarchy requires applying the Fredholm alternative to ensure solvability of the equations. We define the following inner product for time $\frac{2\pi}{\omega_\circ}$-periodic functions $\boldsymbol{q}, \boldsymbol{p} \in \mathscr{L}^2\big([0, \frac{2\pi}{\omega_\circ}] \times \mathbb{R},\, \mathbb{C}^2\big)$:

$$\big\langle \boldsymbol{q}, \boldsymbol{p}\big\rangle_{2\pi} = \sum_{i=1}^{2}\frac{\omega_\circ}{2\pi}\int_0^{\frac{2\pi}{\omega_\circ}}\int_{\mathbb{R}} \bar{q}_i(x,t)\,p_i(x,t)\,dx\,dt.$$

Note that the slow time τ is not included in the inner product. The adjoint operator $L_\mathcal{H}^*$ is found using the relation $\big\langle L_\mathcal{H}^*\boldsymbol{q}, \boldsymbol{p}\big\rangle_{2\pi} = \big\langle \boldsymbol{q}, L_\mathcal{H}\,\boldsymbol{p}\big\rangle_{2\pi}$ and is given by

$$L_\mathcal{H}^*\boldsymbol{\phi} \;=\; -\frac{\partial}{\partial t}\boldsymbol{\phi} - \mathcal{M}_\mathcal{H}^*\boldsymbol{\phi},$$

with $\mathcal{M}_\mathcal{H}^*$ defined in (3.9). The null space of $L_\mathcal{H}^*$ is spanned by $\boldsymbol{\mathcal{Y}}, \bar{\boldsymbol{\mathcal{Y}}}$, where

$$\boldsymbol{\mathcal{Y}}(x,t) = \boldsymbol{y}(x)\,e^{i\omega_\circ t}, \qquad\qquad \bar{\boldsymbol{\mathcal{Y}}}(x,t) = \bar{\boldsymbol{y}}(x)\,e^{-i\omega_\circ t}$$

with $\boldsymbol{y}$ given in (3.13) for the sum and difference modes. At $\mathcal{O}(\epsilon^2)$, the Fredholm alternative guarantees solutions to equation (3.19) if

$$\Big\langle \boldsymbol{\mathcal{Y}},\, \mathrm{B}_{\mathcal{H}}(\boldsymbol{\phi}_1, \boldsymbol{\phi}_1) \Big\rangle_{2\pi} = 0,$$

which is naturally satisfied as $\mathrm{B}_{\mathcal{H}}(\boldsymbol{\phi}_1, \boldsymbol{\phi}_1)$ produces only terms with $e^{\pm i2\omega_\circ t}$ and e^0:

$$\mathrm{B}_{\mathcal{H}}(\boldsymbol{\phi}_1, \boldsymbol{\phi}_1) = \tfrac{1}{2} z^2\, e^{i2\omega_\circ t} \mathrm{B}_{\mathcal{H}}(\boldsymbol{v}, \boldsymbol{v}) \,+\, z\bar{z}\, \mathrm{B}_{\mathcal{H}}(\boldsymbol{v}, \bar{\boldsymbol{v}}) \,+\, \tfrac{1}{2}\bar{z}^2\, e^{-i2\omega_\circ t} \mathrm{B}_{\mathcal{H}}(\bar{\boldsymbol{v}}, \bar{\boldsymbol{v}}).$$

Consequently, we expect solutions to the $\mathcal{O}(\epsilon^2)$ equation (3.19) to be of the form

$$\boldsymbol{\phi}_2(x,t,\tau) \,=\, \tfrac{1}{2} z^2\, e^{i2\omega_\circ t} \boldsymbol{h}_{20}(x) \,+\, z\bar{z}\, \boldsymbol{h}_{11}(x) \,+\, \tfrac{1}{2}\bar{z}^2\, e^{-i2\omega_\circ t} \boldsymbol{h}_{02}(x) + \vartheta \boldsymbol{\phi}_1(x,t,\tau),$$

which, when substituted into (3.19), results in the $\mathcal{O}(\epsilon^2)$ equations for $\boldsymbol{h}_{11}, \boldsymbol{h}_{20} = \bar{\boldsymbol{h}}_{02}$,

$$\begin{aligned} \Big(2\omega_\circ i\, \mathrm{I} - \mathcal{M}_{\mathcal{H}}\Big)\, \boldsymbol{h}_{20}(x) &= \mathrm{B}_{\mathcal{H}}(\boldsymbol{v}, \boldsymbol{v})(x), \\ -\mathcal{M}_{\mathcal{H}}\ \boldsymbol{h}_{11}(x) &= \mathrm{B}_{\mathcal{H}}(\boldsymbol{v}, \bar{\boldsymbol{v}})(x), \\ \Big(-2\omega_\circ i\, \mathrm{I} - \mathcal{M}_{\mathcal{H}}\Big)\, \boldsymbol{h}_{02}(x) &= \mathrm{B}_{\mathcal{H}}(\bar{\boldsymbol{v}}, \bar{\boldsymbol{v}})(x), \end{aligned} \tag{3.21}$$

by the linear independence of $e^{\pm i2\omega_\circ t}$, e^0. The *upright* I denotes the identity operator. In Appendix C we solve (3.21) for this specific case and for a general right-hand side. This determines the solution $\boldsymbol{\phi}_2(x,t)$ at $\mathcal{O}(\epsilon^2)$, which is present in terms at $\mathcal{O}(\epsilon^3)$. Note that the coefficient ϑ, which is undetermined at this order, does not contribute to the amplitude equation. Equations (3.21) may be compared with (3.32) in section 3.4 which arises in the center manifold reduction of the dynamical system (3.3). As we show in Appendix C.3, the additional terms present in (3.32) ultimately do not contribute to the coefficient $c_1(0)$ at third order in the Poincaré normal form.

At $\mathcal{O}(\epsilon^3)$, the amplitude equation arises from the *solvability condition* for (3.20) whereby the Fredholm alternative requires

$$\Big\langle \boldsymbol{\mathcal{Y}},\, \big[\mathrm{B}_{\mathcal{H}}(\boldsymbol{\phi}_1, \boldsymbol{\phi}_2) + \tfrac{1}{3!}\mathrm{C}_{\mathcal{H}}(\boldsymbol{\phi}_1, \boldsymbol{\phi}_1, \boldsymbol{\phi}_1) - \tfrac{\partial}{\partial\tau}\boldsymbol{\phi}_1 + \alpha \mathcal{M}_1 \boldsymbol{\phi}_1\big] \Big\rangle_{2\pi} \,=\, 0. \tag{3.22}$$

These terms may be expressed in terms of the following *spatial* inner products $\langle \cdot, \cdot \rangle$ which do not vanish automatically under the inner product:

$$\begin{aligned} \Big\langle \boldsymbol{\mathcal{Y}},\, \mathrm{B}_{\mathcal{H}}(\boldsymbol{\phi}_1, \boldsymbol{\phi}_2) \Big\rangle_{2\pi} &= \, z|z|^2 \Big\langle \boldsymbol{y},\, \mathrm{B}_{\mathcal{H}}(\boldsymbol{v}, \boldsymbol{h}_{11}) + \tfrac{1}{2}\mathrm{B}_{\mathcal{H}}(\bar{\boldsymbol{v}}, \boldsymbol{h}_{20}) \Big\rangle, \\ \Big\langle \boldsymbol{\mathcal{Y}},\, \tfrac{1}{3!}\mathrm{C}_{\mathcal{H}}(\boldsymbol{\phi}_1, \boldsymbol{\phi}_1, \boldsymbol{\phi}_1) \Big\rangle_{2\pi} &= \, z|z|^2 \Big\langle \boldsymbol{y},\, \tfrac{1}{2}\mathrm{C}_{\mathcal{H}}(\boldsymbol{v}, \boldsymbol{v}, \bar{\boldsymbol{v}}) \Big\rangle, \\ \Big\langle \boldsymbol{\mathcal{Y}},\, \big[-\tfrac{\partial}{\partial\tau}\boldsymbol{\phi}_1 + \alpha \mathcal{M}_1 \boldsymbol{\phi}_1\big] \Big\rangle_{2\pi} &= \, -\langle \boldsymbol{y}, \boldsymbol{v} \rangle \tfrac{dz}{d\tau} + \alpha \Big\langle \boldsymbol{y},\, \mathcal{M}_1 \boldsymbol{v} \Big\rangle z \;=\; -\tfrac{dz}{d\tau} + \alpha\lambda_1 z. \end{aligned}$$

The solvability condition (3.22) results in the *complex amplitude equation*

$$\frac{dz}{d\tau} \,=\, \alpha\, \lambda_1\, z \,+\, \mathcal{X}\, z|z|^2, \tag{3.23}$$

commonly known as the Stuart–Landau equation, and $\mathcal{X}$ the second Landau constant. The calculation of $\lambda_1 \equiv \varrho_1 + i\omega_1 = \langle \boldsymbol{y}, \mathcal{M}_1 \boldsymbol{v} \rangle$ is collected in Appendix A, and the coefficient $\mathcal{X}$ is expressed as

$$\mathcal{X} = \left\langle \boldsymbol{y},\ \tfrac{1}{2}\mathrm{C}_{\mathcal{H}}(\boldsymbol{v},\boldsymbol{v},\bar{\boldsymbol{v}}) + \mathrm{B}_{\mathcal{H}}(\boldsymbol{v},\boldsymbol{h}_{11}) + \tfrac{1}{2}\mathrm{B}_{\mathcal{H}}(\bar{\boldsymbol{v}},\boldsymbol{h}_{20}) \right\rangle \tag{3.24}$$

$$= \zeta \left[\ \Lambda_{\pm}(\bar{a}_{\mathcal{H}}) \ + 2\,\Xi^{c}_{\pm}(\bar{a}_{\mathcal{H}}) \ + \ \Xi^{d}_{\pm}(\bar{a}_{\mathcal{H}}) \ \right]. \tag{3.25}$$

$\Lambda_{\pm}(\bar{a}_{\mathcal{H}})$ is calculated in Appendix B, and $\Xi^{c}{}_{\pm}(\bar{a}_{\mathcal{H}}), \Xi^{d}{}_{\pm}(\bar{a}_{\mathcal{H}})$, which depend on $\Sigma_{\pm}(\bar{a}_{\mathcal{H}})$, are calculated in Appendix C.2. Additionally, the coefficient $\mathcal{X}$ identically matches the related coefficient $c_1(0)$ in the Poincaré normal form in (3.36).

Taking $z = re^{i\theta}$ and decomposing $\mathcal{X} = \mathcal{X}_{\mathcal{R}\mathsf{e}} + i\,\mathcal{X}_{\mathsf{Im}}$, (3.23) can be expressed as the pair of real equations

$$\dot{r} \ = \ \alpha\varrho_1 r \ + \ \mathcal{X}_{\mathcal{R}\mathsf{e}}\, r^3, \qquad\qquad \dot{\theta} \ = \ \alpha\omega_1 \ + \ \mathcal{X}_{\mathsf{Im}}\, r^2$$

which admits the periodic solution $(r,\theta) = \big(r_\circ, \theta_\circ(\tau)\big)$, with arbitrary phase ϕ, where

$$r_\circ = \sqrt{\frac{\varrho_1}{|\mathcal{X}_{\mathcal{R}\mathsf{e}}|}}, \qquad\qquad \theta_\circ = \breve{\omega}_1\tau + \phi, \qquad\qquad \breve{\omega}_1 = \alpha\omega_1 + \mathcal{X}_{\mathsf{Im}}\, r_\circ^2.$$

The limit cycle appears for $\operatorname{sgn}(\alpha\varrho_1) = -\operatorname{sgn}(\mathcal{X}_{\mathcal{R}\mathsf{e}})$ implying that $\alpha = -\operatorname{sgn}(\mathcal{X}_{\mathcal{R}\mathsf{e}}/\varrho_1)$. The bifurcation is *supercritical* producing *stable* periodic orbits if $\mathcal{R}\mathsf{e}\,\mathcal{X} < 0$ and is *subcritical* producing *unstable* periodic orbits if $\mathcal{R}\mathsf{e}\,\mathcal{X} > 0$, where

$$\mathcal{X}_{\mathcal{R}\mathsf{e}} \ \equiv \ \mathcal{R}\mathsf{e}\,\mathcal{X} \ = \ \frac{\Lambda_{\pm}(\bar{a}_{\mathcal{H}}) + 2\Xi^{c}_{\pm}(\bar{a}_{\mathcal{H}}) + \mathcal{R}\mathsf{e}\left\{\left(1 - \sqrt{\frac{\nu}{\rho-\nu}}\,i\right)\Xi^{d}_{\pm}(\bar{a}_{\mathcal{H}})\right\}}{4\,\Omega_{\pm}(\bar{a}_{\mathcal{H}})},$$

$\mathcal{R}\mathsf{e}\,\zeta = (4\Omega_{\pm}(\bar{a}_{\mathcal{H}}))^{-1}$, both $\Lambda_{\pm}(\bar{a}_{\mathcal{H}})$ and $\Xi^{c}_{\pm}(\bar{a}_{\mathcal{H}})$ are real, and $\Xi^{d}_{\pm}(\bar{a}_{\mathcal{H}})$ is complex. "Supercritical" is taken to mean that the bifurcation transfers stability from an equilibrium to the bifurcating limit cycle. The sign of α determines on which side of the bifurcation point the periodic orbit appears. Note that in section 2 it was found that the stationary pulse loses stability as $\bar{a}$ (and $I_\circ$) is *decreased* through the Hopf bifurcation point, implying that $\varrho_1 < 0$. If the bifurcation is supercritical ($\mathcal{R}\mathsf{e}\,\mathcal{X} < 0$), then $\alpha = -\operatorname{sgn}(\mathcal{X}_{\mathcal{R}\mathsf{e}}/\varrho_1) < 0$, indicating that the stable periodic orbit appears for $\bar{a} < \bar{a}_{\mathcal{H}}$.

Finally, the small amplitude periodic orbit can be expressed to $\mathcal{O}(\epsilon)$ as

$$\begin{pmatrix} u(x,t) \\ n(x,t) \end{pmatrix} \ \approx \ \begin{pmatrix} 1 \\ 1 \end{pmatrix} \mathcal{U}_{\mathcal{H}}(x) + \epsilon \left(r_\circ \boldsymbol{v}(x)\, e^{i\left(\omega_\circ + \epsilon^2\breve{\omega}_1\right)t} \ + \ r_\circ \bar{\boldsymbol{v}}(x)\, e^{-i\left(\omega_\circ + \epsilon^2\breve{\omega}_1\right)t} \right)$$

from $\boldsymbol{\phi} \approx \boldsymbol{\phi}_1$ in (3.2) with $z(\tau) = r_\circ\, e^{\breve{\omega}_1\tau}$ and $\tau = \epsilon^2 t$. Expressions for $\omega_\circ$, $\boldsymbol{v}, \bar{\boldsymbol{v}}$ are given in (3.5), and $\mathcal{U}_{\mathcal{H}}(x)$ is calculated from (2.2) with $\bar{a} = \bar{a}_{\mathcal{H}}$. From the expression for $\boldsymbol{v}$, the periodic orbit, to lowest order, can be seen as a time-periodic modulation of the profile of the spatial mode $\Omega_{\pm}(x)$ about the stationary pulse, naturally reflecting the geometry of the breathers and sloshers exhibited in the numerical simulations.

3.4. Center manifold reduction. We study the evolution of perturbations $\boldsymbol{\phi} = (\varphi, \psi)^{\mathrm{T}}$ about the stationary pulse $\mathcal{U}_{\bar{a}}$ in (3.3), where $\boldsymbol{\phi}(t) \in \mathscr{H} \equiv \mathscr{L}^2(\mathbb{R}, \mathbb{R}^2)$. We consider initial conditions and orbits belonging to $\mathscr{H} \cap C^n(\mathbb{R}, \mathbb{R}^2)$ for $t > 0$ as classical solutions of (3.3). We shall proceed by assuming that there is a center manifold theorem for this infinite-dimensional dynamical system, which perhaps could be demonstrated through an extension of [90]. In particular, we shall assume there exists a local, two-dimensional invariant manifold $\mathcal{W}^c_{\bar{a}} \subset \mathscr{H} \cap C^n(\mathbb{R}, \mathbb{R}^2)$ for (3.3) that depends on the parameter $\bar{a}$, is locally attracting, and is tangent at the bifurcation point $\bar{a} = \bar{a}_{\mathcal{H}}$ to the critical real eigenspace $\mathcal{T}^c$ of the equilibrium. The flow restricted to this locally-defined manifold $\mathcal{W}^c_{\bar{a}}$ is described by a pair of ODEs which exhibit a Hopf bifurcation, with a unique limit cycle appearing on one side of the bifurcation point. In particular, it is assumed that the linear operator $\mathcal{M}_{\bar{a}}$ has a pair of complex eigenvalues $\lambda, \bar{\lambda}$, where $\lambda(0) = i\omega_\circ$ and $\frac{d}{d\bar{a}} \mathcal{R}\mathsf{e}\, \lambda(\bar{a} - \bar{a}_{\mathcal{H}})\,|_{\bar{a}=\bar{a}_{\mathcal{H}}} \neq 0$. Ordinarily, the periodic orbit may appear by either increasing or decreasing $\bar{a}$ through the bifurcation point $\bar{a}_{\mathcal{H}}$, and this is determined by the expansion for $\bar{a}$ in (3.38).

There are two spatial modes $\Omega_\pm$ (described in sections 2.2 and 3.2), either of which may form the two-dimensional critical eigenspace for the Hopf bifurcation, and we assume throughout that, for a sufficiently large neighborhood of the bifurcation point $\bar{a}_{\mathcal{H}}$, only one eigenmode becomes critical with all other eigenvalues in the left half-plane. The critical eigenvectors $\boldsymbol{v}, \bar{\boldsymbol{v}} \in \mathscr{H} \oplus i\mathscr{H}$ of the linear operator $\mathcal{M}_{\mathcal{H}}$ determine the critical *real* eigenspace $\mathcal{T}_c = \{z\boldsymbol{v} + \bar{z}\bar{\boldsymbol{v}} : z \in \mathbb{C}\} = \mathrm{span}\{\mathcal{R}\mathsf{e}\ \boldsymbol{v}, \mathsf{Im}\ \boldsymbol{v}\}$. Importantly, the direction of bifurcation is governed at the *critical point* $\bar{a} = \bar{a}_{\mathcal{H}}$ by the third order coefficient $c_1(0)$ in the Poincaré normal form for the expansion of (3.3) about the stationary pulse (related to the first Lyapunov coefficient $\ell_1(0)$). Since we need only to calculate the *critical* center manifold $\mathcal{W}^c_{\mathcal{H}} \equiv \mathcal{W}^c_{\bar{a}_{\mathcal{H}}}$, we consider (3.3) at $\bar{a} = \bar{a}_{\mathcal{H}}$, where $\boldsymbol{\phi} = (\varphi, \psi)^T$ and the operators $\mathcal{M}_{\mathcal{H}}, \mathrm{B}_{\mathcal{H}}, \mathrm{C}_{\mathcal{H}}$ were introduced in section 3.2, to obtain

$$\frac{\partial \boldsymbol{\phi}}{\partial t} = \mathcal{M}_{\mathcal{H}}\boldsymbol{\phi} + \mathrm{B}_{\mathcal{H}}(\boldsymbol{\phi}, \boldsymbol{\phi}) + \mathrm{C}_{\mathcal{H}}(\boldsymbol{\phi}, \boldsymbol{\phi}, \boldsymbol{\phi}) + \mathcal{O}(\|\boldsymbol{\phi}\|^4). \tag{3.26}$$

$\mathcal{M}_{\mathcal{H}}$ is not self-adjoint. $(\mathcal{M}_{\mathcal{H}} - i\omega_\circ \mathrm{I})$ and $(\mathcal{M}^*_{\mathcal{H}} + i\omega_\circ \mathrm{I})$ have one-dimensional nullspaces and are Fredholm operators with index 0. Consequently, we have the orthogonal direct sum decomposition

$$\mathscr{H} \oplus i\mathscr{H} = \mathcal{R}\mathsf{an}(\mathcal{M}_{\mathcal{H}} - i\omega_\circ \mathrm{I}) \oplus \mathcal{N}\mathsf{ul}(\mathcal{M}^*_{\mathcal{H}} + i\omega_\circ \mathrm{I}),$$

where $\mathcal{N}\mathsf{ul}(\mathcal{M}^*_{\mathcal{H}} + i\omega_\circ \mathrm{I})$ is spanned by the adjoint eigenvector $\boldsymbol{y}$ defined above in (3.13). We use this decomposition and follow the approach of [43] to project the system, at the bifurcation point $\bar{a} = \bar{a}_{\mathcal{H}}$, onto the critical center manifold $\mathcal{W}^c_{\mathcal{H}}$.

Since $\mathcal{W}^c_{\mathcal{H}}$ is tangent to $\mathcal{T}_c$, we define the real subspace $\mathcal{T}_s$, where

$$\mathcal{T}_s = \{\boldsymbol{\phi} \in \mathscr{H} : \langle \boldsymbol{y}, \boldsymbol{\phi} \rangle = 0\} \subset \mathcal{R}\mathsf{an}(\mathcal{M}_{\mathcal{H}} - i\omega_\circ \mathrm{I}),$$

and express the center manifold $\mathcal{W}^c_{\mathcal{H}}$ as the graph of a function $\boldsymbol{m} : \mathcal{T}_c \cong \mathbb{C} \longrightarrow \mathcal{T}_s$:

$$\boldsymbol{m}(z, \bar{z}) = \tfrac{1}{2}\boldsymbol{w}_{20} z^2 + 2\boldsymbol{w}_{11} z\bar{z} + \tfrac{1}{2}\boldsymbol{w}_{02}\bar{z}^2 + \mathcal{O}(|z|^3). \tag{3.27}$$

The point $z\boldsymbol{v} + \bar{z}\bar{\boldsymbol{v}}$ in $\mathcal{T}_c$ identifies with the point $\boldsymbol{m}(z, \bar{z})$ on the center manifold, where the second order coefficients $\boldsymbol{w}_{20}$, $\boldsymbol{w}_{11}$, $\boldsymbol{w}_{02} \in \mathcal{T}_s$ are yet to be determined. Next, we define the

projections $\mathcal{P}_s$ and $\mathcal{P}_c$ on the real space $\mathscr{H}$ by

$$\begin{aligned}\mathcal{P}_s\,\boldsymbol{\phi} &= \big(\mathrm{I} - \mathcal{P}_c\big)\,\boldsymbol{\phi},\\ \mathcal{P}_c\,\boldsymbol{\phi} &= \big\langle \boldsymbol{y},\boldsymbol{\phi}\big\rangle\,\boldsymbol{v} + \big\langle \bar{\boldsymbol{y}},\boldsymbol{\phi}\big\rangle\,\bar{\boldsymbol{v}} \;=\; 2\,\mathcal{R}\mathsf{e}\,\big\{\big\langle \boldsymbol{y},\boldsymbol{\phi}\big\rangle\,\boldsymbol{v}\big\}\end{aligned}$$

to put (3.26) into a form typically assumed for center manifold theorems. The critical center manifold $\mathcal{W}^c_{\mathcal{H}}$ lies in $\mathcal{T}_s$ and the projection $\mathcal{P}_s$ leaves $\mathcal{T}_s$ invariant; the projection $\mathcal{P}_c$ maps $\mathcal{T}_s^{\perp}$ into the critical eigenspace $\mathcal{T}_c$ defining new coordinates. Although $\mathcal{P}_s$ is not orthogonal, $\mathcal{R}\mathsf{an}(\mathcal{P}_s)\cap\mathcal{N}\mathsf{ul}(\mathcal{P}_s)=\emptyset$ holds, and we have the nonorthogonal direct sum decomposition $\mathscr{H}=\mathcal{R}\mathsf{an}(\mathcal{P}_s)\oplus\mathcal{N}\mathsf{ul}(\mathcal{P}_s)$. Thus, by setting $z=\langle \boldsymbol{y},\boldsymbol{\phi}\rangle$ and $\bar z=\langle \bar{\boldsymbol{y}},\boldsymbol{\phi}\rangle$, we may decompose any vector $\boldsymbol{\phi}\in\mathscr{H}$ uniquely as

$$\boldsymbol{\phi}(t) \;=\; \boldsymbol{s}(t) \;+\; z(t)\,\boldsymbol{v} + \bar z(t)\,\bar{\boldsymbol{v}}, \qquad \begin{aligned}\mathcal{P}_s\,\boldsymbol{\phi} &= \boldsymbol{s}(t) &&\in\ \mathcal{T}_s\\ \mathcal{P}_c\boldsymbol{\phi} &= z(t)\,\boldsymbol{v} + \bar z(t)\,\bar{\boldsymbol{v}} &&\in\ \mathcal{T}_c.\end{aligned}$$

Projecting (3.26) onto these subspaces, the dynamical variables z and $\boldsymbol{s}$ evolve according to

$$\begin{aligned}\frac{dz}{dt} &= i\omega_\circ z \;+\; \Big\langle \boldsymbol{y},\tfrac{1}{2!}\mathrm{B}_{\mathcal{H}}\big(\boldsymbol{\phi},\boldsymbol{\phi}\big)\Big\rangle \;+\; \Big\langle \boldsymbol{y},\tfrac{1}{3!}\mathrm{C}_{\mathcal{H}}\big(\boldsymbol{\phi},\boldsymbol{\phi},\boldsymbol{\phi}\big)\Big\rangle \;+\; \mathcal{O}\big(\|\boldsymbol{\phi}\|^4\big),\\ \frac{d\boldsymbol{s}}{dt} &= \mathcal{M}_{\mathcal{H}}\boldsymbol{s} \;+\; \tfrac{1}{2!}\mathrm{B}_{\mathcal{H}}\big(\boldsymbol{\phi},\boldsymbol{\phi}\big) - \Big\langle \boldsymbol{y},\tfrac{1}{2!}\mathrm{B}_{\mathcal{H}}\big(\boldsymbol{\phi},\boldsymbol{\phi}\big)\Big\rangle\,\boldsymbol{v} - \Big\langle \bar{\boldsymbol{y}},\tfrac{1}{2!}\mathrm{B}_{\mathcal{H}}\big(\boldsymbol{\phi},\boldsymbol{\phi}\big)\Big\rangle\,\bar{\boldsymbol{v}} + \mathcal{O}\big(\|\boldsymbol{\phi}\|^3\big).\end{aligned} \tag{3.28}$$

We then rewrite system (3.28) in terms of the coordinates $z,\bar z$ on $\mathcal{T}_c$ and $\boldsymbol{s}\in\mathcal{T}_s$ as

$$\begin{aligned}\frac{dz}{dt} &= i\omega_\circ z \;+\; \tfrac{1}{2!}R_{20}z^2 \;+\; R_{11}z\bar z \;+\; \tfrac{1}{2!}R_{02}\bar z^2\\ &\qquad + \Big[\tfrac{1}{2!}R_{21}z^2\bar z \;+\; R_{10}(\boldsymbol{s})\,z \;+\; R_{01}(\boldsymbol{s})\,\bar z\Big] \;+\; \cdots,\end{aligned} \tag{3.29}$$

$$\frac{d\boldsymbol{s}}{dt} \;=\; \mathcal{M}_{\mathcal{H}}\boldsymbol{s} \;+\; \Big[\tfrac{1}{2!}\mathrm{H}_{20}z^2 + \mathrm{H}_{11}z\bar z + \tfrac{1}{2!}\mathrm{H}_{02}\bar z^2\Big] \;+\; \mathcal{O}\big(|z|^3\big) + \mathcal{O}\big(|z|\|s\|\big), \tag{3.30}$$

where the coefficients of the equation in z are given by the inner products

$$\begin{aligned} R_{20} &= \big\langle \boldsymbol{y},\mathrm{B}_{\mathcal{H}}(\boldsymbol{v},\boldsymbol{v})\big\rangle, & R_{21} &= \big\langle \boldsymbol{y},\mathrm{C}_{\mathcal{H}}(\boldsymbol{v},\boldsymbol{v},\bar{\boldsymbol{v}})\big\rangle, & R_{10}(\boldsymbol{s}) &= \big\langle \boldsymbol{y},\mathrm{B}_{\mathcal{H}}(\boldsymbol{v},\boldsymbol{s})\big\rangle,\\ R_{02} &= \big\langle \boldsymbol{y},\mathrm{B}_{\mathcal{H}}(\bar{\boldsymbol{v}},\bar{\boldsymbol{v}})\big\rangle, & R_{11} &= \big\langle \boldsymbol{y},\mathrm{B}_{\mathcal{H}}(\boldsymbol{v},\bar{\boldsymbol{v}})\big\rangle, & R_{01}(\boldsymbol{s}) &= \big\langle \boldsymbol{y},\mathrm{B}_{\mathcal{H}}(\bar{\boldsymbol{v}},\boldsymbol{s})\big\rangle,\end{aligned}$$

and those for the equation in $\boldsymbol{s}$ are given by

$$\begin{aligned}\bar{\mathrm{H}}_{02}(x) = \mathrm{H}_{20}(x) &= \mathrm{B}_{\mathcal{H}}(\boldsymbol{v},\boldsymbol{v})(x) \;-\; \big\langle \boldsymbol{y},\mathrm{B}_{\mathcal{H}}\big(\boldsymbol{v},\boldsymbol{v}\big)\big\rangle\,\boldsymbol{v}(x) \;-\; \big\langle \bar{\boldsymbol{y}},\mathrm{B}_{\mathcal{H}}\big(\boldsymbol{v},\boldsymbol{v}\big)\big\rangle\,\bar{\boldsymbol{v}}(x),\\ \mathrm{H}_{11}(x) &= \mathrm{B}_{\mathcal{H}}(\boldsymbol{v},\bar{\boldsymbol{v}})(x) \;-\; \big\langle \boldsymbol{y},\mathrm{B}_{\mathcal{H}}\big(\boldsymbol{v},\bar{\boldsymbol{v}}\big)\big\rangle\,\boldsymbol{v}(x) \;-\; \big\langle \bar{\boldsymbol{y}},\mathrm{B}_{\mathcal{H}}\big(\boldsymbol{v},\bar{\boldsymbol{v}}\big)\big\rangle\,\bar{\boldsymbol{v}}(x),\end{aligned}$$

all of which involve lengthy calculations that are collected in Appendices B and C. Note that in (3.29) we explicitly list only the terms that generate the resonant term $z^2\bar z$ at order $\mathcal{O}(|z|^3)$ since other terms at this order will be annihilated in a near-identity transformation to obtain the normal form.

To restrict the dynamics (3.29)–(3.30) to the center manifold (3.27), we first take

$$\boldsymbol{s} \;=\; \boldsymbol{m}\big(z,\bar z\big) = \tfrac{1}{2}\boldsymbol{w}_{20}z^2 \;+\; \boldsymbol{w}_{11}z\bar z + \tfrac{1}{2}\boldsymbol{w}_{02}\bar z^2 \;+\; \mathcal{O}\big(|z|^3\big). \tag{3.31}$$

We differentiate $\boldsymbol{s}$ in (3.31) and use (3.29) for dz/dt to find

$$\begin{aligned}\frac{d\boldsymbol{s}}{dt} \;=\; \frac{\partial \boldsymbol{m}}{\partial z}\frac{dz}{dt} \;+\; \frac{\partial \boldsymbol{m}}{\partial \bar{z}}\frac{d\bar{z}}{dt} \;&=\; \Big(\boldsymbol{w}_{20}z + \boldsymbol{w}_{11}\bar{z} + \cdots\Big)\Big(+ i\omega_\circ z \;+\; \cdots\Big) \\ &\quad +\; \Big(\boldsymbol{w}_{11}z + \boldsymbol{w}_{02}\bar{z} + \cdots\Big)\Big(- i\omega_\circ \bar{z} \;+\; \cdots\Big) \\ &= i2\omega_\circ\, \boldsymbol{w}_{20}z^2 - i2\omega_\circ\, \boldsymbol{w}_{02}\bar{z}^2 \;+\; \cdots .\end{aligned}$$

Next, we substitute (3.31) for $\boldsymbol{s}$ into the right-hand side of (3.30) to obtain

$$\frac{d\boldsymbol{s}}{dt} \;=\; \mathcal{M}_{\mathcal{H}}\Big(\tfrac{1}{2}\boldsymbol{w}_{20}z^2 \;+ \boldsymbol{w}_{11}z\bar{z} + \tfrac{1}{2}\boldsymbol{w}_{02}\bar{z}^2\Big) \;+\; \tfrac{1}{2}\mathrm{H}_{20}z^2 + \mathrm{H}_{11}z\bar{z} + \tfrac{1}{2}\mathrm{H}_{02}\bar{z}^2 \;+\; \cdots .$$

These two expressions for $\mathrm{d}\boldsymbol{s}/dt$ are equal, and the linear independence of the $z^2, z\bar{z}, \bar{z}^2$ terms yields the following equations determining the center manifold coefficients $\boldsymbol{w}_{ij}(x)$:

$$\begin{aligned}\Big(2\omega_\circ i\mathrm{I} - \mathcal{M}_{\mathcal{H}}\Big)\,\boldsymbol{w}_{20}(x) &= \mathrm{H}_{20}(x), \\ -\mathcal{M}_{\mathcal{H}}\;\boldsymbol{w}_{11}(x) &= \mathrm{H}_{11}(x), \\ \Big(-2\omega_\circ i\mathrm{I} - \mathcal{M}_{\mathcal{H}}\Big)\,\boldsymbol{w}_{02}(x) &= \mathrm{H}_{02}(x).\end{aligned} \tag{3.32}$$

Since 0 and $\pm i2\omega_\circ$ are not elements of the spectrum of $\mathcal{M}_{\mathcal{H}}$, (3.32) can be solved to calculate the second order coefficients $\boldsymbol{w}_{20}$, $\boldsymbol{w}_{11}$, $\boldsymbol{w}_{02} \in \mathcal{T}_s$ for the center manifold. The solution is given for $\boldsymbol{h}_{ij}$ in Appendix C.2 and completed for $\boldsymbol{w}_{ij}$ in Appendix C.3.

Substituting the results of (3.32) with (3.31) into $R_{10}(\boldsymbol{s})$ and $R_{01}(\boldsymbol{s})$, the following three terms in (3.29) can be expressed, listing only the resonant term $z|z|^2$, as

$$\Big[\tfrac{1}{2}R_{21}z^2\bar{z} \;+\; R_{10}(\boldsymbol{s})\,z \;+\; \tfrac{1}{2}R_{01}(\boldsymbol{s})\,\bar{z}\Big] \;=\; \tfrac{1}{2}R_{21}^{\circledast}\,z|z|^2 \;+\; \cdots ,$$

where the coefficient $R_{21}^{\circledast}$ of the *resonant term* $z|z|^2$ is given by

$$R_{21}^{\circledast} \;=\; \Big\langle \boldsymbol{y}, \mathrm{C}_{\mathcal{H}}(\boldsymbol{v},\boldsymbol{v},\bar{\boldsymbol{v}})\Big\rangle \;+\; 2\Big\langle \boldsymbol{y}, \mathrm{B}_{\mathcal{H}}\big(\boldsymbol{v},\boldsymbol{w}_{11}\big)\Big\rangle \;+\; \Big\langle \boldsymbol{y}, \mathrm{B}_{\mathcal{H}}\big(\bar{\boldsymbol{v}},\boldsymbol{w}_{20}\big)\Big\rangle. \tag{3.33}$$

Subsequently, (3.29) for z becomes

$$\frac{dz}{dt} \;=\; i\omega_\circ z \;+\; \Big[\tfrac{1}{2}R_{20}z^2 \;+\; R_{11}z\bar{z} \;+\; \tfrac{1}{2}R_{02}\bar{z}^2\Big] \;+\; \tfrac{1}{2}R_{21}^{\circledast}\,\bar{z}|\bar{z}|^2 \;+\; \cdots \tag{3.34}$$

and describes the evolution of the system on the center manifold in terms of the coordinates z and $\bar{z}$ in $\mathcal{T}_c$. Finally, it can be shown that (3.34) can be transformed into the Poincaré normal form (at criticality $\bar{a} = \bar{a}_{\mathcal{H}}$)

$$\frac{d\xi}{dt} \;=\; i\omega_\circ\,\xi \;+\; c_1(0)\,\xi|\xi|^2 \;+\; \mathcal{O}\big(|\xi|^4\big)$$

using a near-identity transformation $z = \xi + \mathcal{O}(|\xi|^2)$ that eliminates all second and third order terms, save the resonant term $\xi|\xi|^2$ [43, 44]. The coefficient $c_1(0)$ of the resonant term is expressed accordingly as

$$c_1(0) \;=\; \tfrac{1}{2}\,R_{21}^{\circledast} \;+\; \frac{i}{2\omega_\circ}\Big(R_{20}R_{11} - 2\big|R_{11}\big|^2 - \tfrac{1}{3}\big|R_{20}\big|^2\Big). \tag{3.35}$$

In Appendix C.3, we show in (C.13) that the expression for $c_1(0)$ given above in (3.35) may be further reduced to

$$\begin{aligned} c_1(0) \;&=\; \tfrac{1}{2}\Big[\,\Big\langle \boldsymbol{y},\, \mathrm{C}_{\mathcal{H}}\big(\boldsymbol{v},\boldsymbol{v},\bar{\boldsymbol{v}}\big)\Big\rangle + 2\Big\langle \boldsymbol{y},\, \mathrm{B}_{\mathcal{H}}\big(\boldsymbol{v},\boldsymbol{h}_{11}\big)\Big\rangle + \Big\langle \boldsymbol{y},\, \mathrm{B}_{\mathcal{H}}\big(\bar{\boldsymbol{v}},\boldsymbol{h}_{20}\big)\Big\rangle\Big] \\ &=\; \zeta\Big[\;\Lambda_{\pm}(\bar{a}_{\mathcal{H}}) \,+ 2\,\Xi^{c}_{\pm}(\bar{a}_{\mathcal{H}}) \,+\, \Xi^{d}_{\pm}(\bar{a}_{\mathcal{H}})\;\Big]. \end{aligned} \tag{3.36}$$

Now, $c_1(0)$ is identical to the coefficient $\mathcal{X}$ in the *complex amplitude equation* (3.23). The bifurcation is *supercritical* and *stable* periodic orbits bifurcate when $\mathcal{R}\mathrm{e}\, c_1(0) < 0$, whereas the bifurcation is *subcritical* with *unstable* periodic orbits bifurcating when $\mathcal{R}\mathrm{e}\, c_1(0) > 0$. Since $\mathcal{R}\mathrm{e}\,\zeta = (4\Omega_{\pm}(\bar{a}_{\mathcal{H}}))^{-1}$ and $\Lambda_{\pm}(\bar{a}_{\mathcal{H}})$,$\Xi^{c}_{\pm}(\bar{a}_{\mathcal{H}})$ are real, it follows that

$$\mathcal{R}\mathrm{e}\, c_1(0) \;=\; \frac{\Lambda_{\pm}(\bar{a}_{\mathcal{H}}) + 2\Xi^{c}_{\pm}(\bar{a}_{\mathcal{H}}) + \mathcal{R}\mathrm{e}\,\Big\{\big(1-\sqrt{\frac{\nu}{\rho-\nu}}\,i\big)\,\Xi^{d}_{\pm}(\bar{a}_{\mathcal{H}})\Big\}}{4\,\Omega_{\pm}(\bar{a}_{\mathcal{H}})},$$

where $\Lambda_{\pm}(\bar{a}_{\mathcal{H}})$ is calculated in Appendix B and $\Xi^{c}_{\pm}(\bar{a}_{\mathcal{H}}), \Xi^{d}_{\pm}(\bar{a}_{\mathcal{H}})$ in Appendix C.2. The first Lyapunov coefficient $\ell_1(0)$, in an associated normal form [62, 46], relates to $c_1(0)$ by

$$\ell_1(0) \;=\; \tfrac{1}{\omega_\circ}\,\mathcal{R}\mathrm{e}\, c_1(0).$$

$\mathcal{R}\mathrm{e}\, c_1(0)$ and $\ell_1(0)$ are of the same sign and track the direction of bifurcation similarly.

Until now we have concentrated on the dynamical system at the critical point $\bar{a} = \bar{a}_{\mathcal{H}}$ which is sufficient to calculate $c_1(0)$. However, it remains to calculate how the bifurcating periodic orbit and its period depend upon the bifurcation parameter $\bar{a}$ in a neighborhood of the critical point. The Poincaré normal form can be expressed as

$$\frac{d\xi}{dt} \;=\; \lambda(\bar{a}-\bar{a}_{\mathcal{H}})\,\xi \;+\; c_1(\bar{a}-\bar{a}_{\mathcal{H}})\,\xi|\xi|^2 \;+\; \mathcal{O}\big(|\xi|^4\big) \tag{3.37}$$

and leads to the following general bifurcation formulae [43]. Following Hopf's convention [45], the amplitude of the periodic orbit is treated as the small parameter ε, e.g., by setting $\xi = \varepsilon\hat{\xi}$ and taking $\hat{\xi} = \mathcal{O}(1)$. The bifurcation parameter $\bar{a}$, the critical eigenvalue λ, and the period T of the oscillation can be expanded in orders of ε, and from (3.37) it is straightforward to show for $0 < \varepsilon \ll 1$ that

$$\begin{aligned} \bar{a}(\varepsilon) &= \bar{a}_{\mathcal{H}} + a_2\,\varepsilon^2 + \cdots, & a_2 &= -\frac{\mathcal{R}\mathrm{e}\, c_1(0)}{\mathring{\alpha}(0)}, \\ T(\varepsilon) &= \frac{2\pi}{\omega_\circ}\Big(1+\tau_2\,\varepsilon^2+\cdots\Big), & \tau_2 &= -\frac{1}{\omega_\circ}\Big(\mathrm{Im}\, c_1(0) - \tfrac{\mathring{\omega}(0)}{\mathring{\alpha}(0)}\mathcal{R}\mathrm{e}\, c_1(0)\Big), \\ \lambda(\bar{a}-\bar{a}_{\mathcal{H}}) &= i\omega_\circ \,+\, \lambda'(0)\,a_2\,\varepsilon^2 + \cdots, & \lambda'(0) &= \mathring{\alpha}(0) + i\mathring{\omega}(0), \end{aligned} \tag{3.38}$$

where $\mathring{\alpha}(0) = \varrho_1$ and $\mathring{\omega}(0) = \omega_1$, which are calculated in (A.3) in Appendix A. The formula for $\bar{a}(\varepsilon)$ determines on which side of the bifurcation point $\bar{a} = \bar{a}_{\mathcal{H}}$ the periodic orbit appears as well as how $\bar{a}$ varies with respect to the amplitude ε of the periodic orbit. Note that these

expansions may be related directly to those in the approach in section 3.3 by making the transformation $\varepsilon^2 \longmapsto \epsilon^2/|a_2|$. The difference is that ϵ in section 3.3 is defined as the deviation of the parameter $\bar{a}$ from the bifurcation point $\bar{a} = \bar{a}_{\mathcal{H}}$, whereas the small parameter ε presently defines the amplitude of the oscillation. Additionally, the largest Lyapunov exponent (real part of a Floquet exponent) is given by

$$\beta(\varepsilon) \;=\; 2\mathcal{R}\mathsf{e}\; c_1(0)\,\varepsilon^2 \;+\; \mathcal{O}(\varepsilon^4).$$

The limit cycle is orbitally asymptotically stable with asymptotic phase if $\mathcal{R}\mathsf{e}\; c_1(0) < 0$. This means that the *limit cycle* $\boldsymbol{x}(t)$ is locally asymptotically stable, and, in some neighborhood $\mathcal{O} \subset \mathscr{H}$ of the limit cycle, each orbit $\boldsymbol{\phi} \subset \mathcal{O}$ has an associated phase ϕ along the limit cycle such that $\|\boldsymbol{\phi}(t) - \boldsymbol{x}(t-\phi)\| \longrightarrow 0$ as $t \to \infty$.

3.5. Direction of bifurcation calculation and numerical simulations. The sign of the real part of the critical coefficient ($\mathcal{X}$ or $c_1(0)$) determines whether the Hopf bifurcation is supercritical or subcritical, and the analytically determined expressions in (3.25) and (3.36) were used to determine the codimension 2 point along a curve of Hopf bifurcations at which the direction of bifurcation switches from supercritical to subcritical (or vice versa). This predicted codimension 2 point was then studied in numerical simulations to check for agreement. The numerics were solved using either an Euler or an improved Euler scheme for the temporal dynamics with the spatial integral computed using the antiderivative $W(x)$ according to

$$\int_{a_n}^{b_n} w(x-y)H\big(u(y,t_n)-\kappa\big)dy = W(x-a_n) - W(x-b_n),$$

where a_n and b_n track the left and right endpoints of the pulse of activity at $t = t_n$. On each iteration n, the points a_n and b_n are determined by using linear interpolation to identify the precise threshold crossings x^* where $u(x^*, t_n) = \kappa$ based upon the two neighboring gridpoints. This scheme is limited to the case of a single pulse of activity above threshold over the interval (a_n, b_n), but, as a consequence, it is fast and suitable to study the slow dynamics near the Hopf bifurcation point. Simulations were performed with 1001–2001 spatial gridpoints and time step $\Delta t \approx 10^{-2}$ to 10^{-4}. When the activity is no longer a *single* bump that is continually above threshold, the assumptions on the treatment of the integral in the numerical scheme break down, in which case we instead approximate the integral term by a Riemann sum.

With regard to the analysis in section 3, the input amplitude $I_\circ$ is the parameter used to control the Hopf bifurcation, and throughout our investigations the equilibrium generally was found to be unstable for $I_\circ < I_\circ^{\mathcal{H}}$. Varying a second parameter can unfold a generalized Hopf bifurcation with its codimension 2 point marking the point, along a curve of Hopf bifurcations, where $\mathcal{R}\mathsf{e}\;\mathcal{X} = \mathcal{R}\mathsf{e}\; c_1(0)$ passes through 0 causing the bifurcation to switch from sub- to supercritical. The curve of Hopf bifurcations can be determined by simultaneously solving (2.3) and $|I'(\bar{a})| = D_{\mathcal{H}}(\bar{a})$ in (2.15) for the critical point $(\bar{a}, I_\circ) = (\bar{a}_{\mathcal{H}}, I_\circ^{\mathcal{H}})$. An additional parameter ς, which we call the *switching parameter*, can be used to search for points where $\mathcal{R}\mathsf{e}\;\mathcal{X} = \mathcal{R}\mathsf{e}\; c_1(0) = 0$, and we denote such points by $(I_\circ^{\curlyvee}, \varsigma^{\curlyvee}, \bar{a}_{\mathcal{H}}^{\curlyvee})$. This additional parameter may subsequently be varied in numerical simulations to study the system in a neighborhood of the codimension 2 point to see if the appearance of the periodic orbit in the numerical simulations matches the prediction according to the coefficient. Specifically, on the

supercritical side, we expect the system to be locally attracted to a stable periodic orbit that grows from zero amplitude at the Hopf bifurcation point, whereas, on the subcritical side, an unstable limit cycle should be detected in the flow.

We investigated the neighborhood of points where $\mathcal{R}\mathsf{e}\,\mathcal{X} = \mathcal{R}\mathsf{e}\,c_1(0) = 0$ vanishes in three different regions in parameter space. Two cases involved the Hopf bifurcation of the sum mode using two different parameters to control the switch from sub- to supercritical, and, in the third case, the difference mode was examined using yet a different parameter. As noted above, we shall refer to the *switching parameter* ς as the additional parameter controlling the direction of bifurcation, whereas $I_\circ$ is always used to control the Hopf bifurcation. The predicted Hopf bifurcation point was checked in numerical simulations by taking the initial condition to be a small perturbation of the exact stationary pulse solution and determining the point $(I_\circ, \bar{a})$ at which the flow switches from inward (toward the equilibrium) to outward. This may be confounded by an unstable limit cycle surrounding the equilibrium, so various sizes of perturbation were tested. The oscillations are generally coherent across the domain, and orbits can be plotted for a fixed spatial point $x = x_\circ$ in the $(u(x_\circ, t), q(x_\circ, t))$-phase plane to study the structure of the oscillatory solutions. Although the slosher has a different orbit structure due to the spatial asymmetry [36], it is nevertheless straightforward to identify periodic orbits. In all cases, it was determined that the numerical simulations were in strong agreement with the prediction by the analysis, and in all cases in the supercritical regime it was possible to demonstrate the existence of a stable limit cycle growing from near zero amplitude from the predicted Hopf bifurcation point with the amplitude of the periodic orbit decreasing rapidly near the bifurcation point, as would be expected for $\mathcal{R}\mathsf{e}\,\mathcal{X} = \mathcal{R}\mathsf{e}\,c_1(0) < 0$ near 0. However, since the subcritical side is more varied, we shall describe each case separately. The descriptions are kept simple for exposition; however, many values of $I_\circ$ and a myriad of initial conditions were explored in all cases and simulated for a long time. When the bifurcation is subcritical, it is possible to detect the repelling flow of an unstable limit cycle for $I_\circ > I_\circ^{\mathcal{H}}$ (where the equilibrium is stable). This can be accomplished by a mix of using various initial conditions and solution continuation accompanied by a decrease in the input amplitude $I_\circ$, incrementally, toward the Hopf bifurcation.

Case 1. The switching parameter was taken to be the input space constant σ. The fixed parameters are $\rho = 2, \nu = 0.01, \kappa = 0.375, \bar{w}_e = 1, \sigma_e = 1, \bar{w}_i = 0, \sigma_i = 0$. The codimension 2 point was predicted to be $(I_\circ^\curlyvee, \sigma^\curlyvee, \bar{a}_{\mathcal{H}}^\curlyvee) \approx (1.5195, 1.0055, 0.9445)$. Taking the system a short distance in the subcritical region ($\sigma < \sigma^\curlyvee$), a small perturbation to the stationary pulse oscillates with an exponentially growing envelope until $u(x,t)$ drops below threshold κ across the domain, which is suggestive of a *type* II subcritical bifurcation, as illustrated in Figure 4. After this point, large amplitude relaxation oscillations ensue in a local region about the input in which the neural field oscillates between super- and subthreshold activity, with the periphery subthreshold. In this case, the sum mode destabilizes in the bifurcation.

Case 2. The switching parameter was taken to be the strength of adaptation ρ. The fixed parameters are $\sigma = 2, \nu = 0.01, \kappa = 0.375, \bar{w}_e = 1, \sigma_e = 1, \bar{w}_i = 0, \sigma_i = 0$. The codimension 2 point was predicted to occur at $(I_\circ^\curlyvee, \rho^\curlyvee, \bar{a}_{\mathcal{H}}^\curlyvee) \approx (2.724, 2.856, 1.193)$. Taking the system a short distance in the subcritical region ($\rho < \rho^\curlyvee$), with $I_\circ < I_\circ^{\mathcal{H}}$ so the equilibrium is unstable, a small perturbation of the stationary pulse leads to a large amplitude breathing

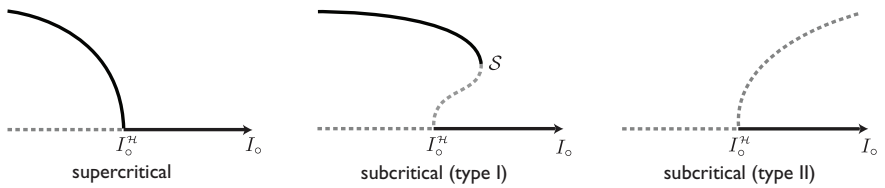

Figure 4. *Illustrative bifurcation diagrams for a Hopf bifurcation to aid the description of the numerical simulations in section 3.5. Solid black curves indicate stable solutions while dotted gray lines indicate unstable solutions. Solutions along the horizontal represent equilibria (stationary pulses), while solutions along the curves represent periodic orbits (breathers/sloshers) which emerge at the Hopf bifurcation point $I_\circ^{\mathcal{H}}$. The point $\mathcal{S}$ denotes a saddle-node bifurcation of limit cycles where a stable and unstable pair of periodic orbits emerges/vanishes. Supercritical is taken to mean that stability is transferred from the equilibrium to the periodic orbit.*

pulse localized about the input, and, in contrast to the periodic orbit in Case 1, the *breather* here is always superthreshold. It is possible to continue the periodic orbit back across the Hopf bifurcation point where $I_\circ > I_\circ^{\mathcal{H}}$, in which case there is bistability with the breather and the stationary pulse. The breather extends only a short distance above the bifurcation point before it vanishes, presumably in a saddle-node bifurcation of limit cycles which is consistent with a generalized Hopf bifurcation. This is suggestive of a *type* I subcritical bifurcation as illustrated in Figure 4, and, in this case, the sum mode destabilizes in the bifurcation.

Case 3. The switching parameter was taken to be the threshold for firing κ, and the fixed parameters are $\sigma = 1.2, \rho = 1, \nu = 0.025, \bar{w}_e = 1, \sigma_e = 1, \bar{w}_i = 0.4, \sigma_i = 2$. The codimension 2 point was found to occur at $(I_\circ^\curlyvee, \kappa^\curlyvee, \bar{a}_{\mathcal{H}}^\curlyvee) \approx (2.9312, 0.2253, 2.0691)$. Taking the system a short distance in the subcritical region ($\kappa < \kappa^\curlyvee$), with $I_\circ < I_\circ^{\mathcal{H}}$ so the equilibrium is unstable, a small perturbation of the stationary pulse with a lateral bias to trigger the difference-mode leads to a large amplitude breather with a local region about the input that remained entirely above threshold. This case is similar to Case 2, i.e., suggestive of a *type* I subcritical bifurcation (see Figure 4); however, destabilization of the difference mode leads to a side-to-side sloshing pulse rather than the symmetric breather. The slosher similarly may be continued a short distance over the bifurcation point where $I_\circ > I_\circ^{\mathcal{H}}$ with a similar region of bistability and vanishing in a purported saddle-node bifurcation of limit cycles.

4. Discussion. In this paper, we have extended the results of [33, 11] in a variety of ways regarding breathing pulses in the neural field model (1.1). First, we extended the existence and linear stability of the stationary pulse to the case of a Mexican hat weight function which changes sign so it is locally excitatory (positive) and laterally inhibitory (negative). In both cases, the input inhomogeneity precludes the 0 eigenvalue corresponding to the spatial eigenmode (*difference mode*) that is associated with the translation invariance of the stationary pulse in the homogeneous system. Consequently, this permits complex conjugate eigenvalues if parameters of the system are varied appropriately. Interestingly, the Mexican hat weight function is capable of destabilizing either of the 2 spatial eigenmodes (*sum* and *difference modes*) of the linearization in a Hopf bifurcation of a stationary pulse in (1.1); an excitatory weight function, conversely, always destabilizes the the sum mode [33]. Although the change of sign of the Mexican hat weight function was used in (1.1) to induce the Hopf bifurcation with respect to the difference mode, we have found that destabilization of the difference mode occurs

more commonly in other neural field models wherein the weight functions do not change sign, and we shall report these results elsewhere [36]. This lends support to the notion that (1.1) serves as a simplest neural field model for developing the nonlinear analysis of a stationary pulse undergoing a Hopf bifurcation. Moreover, our analysis can be extended to other neural fields that similarly use the Heaviside firing rate and analogous spatial integrals. The Heaviside firing rate function is enormously useful for making analytic calculations for special patterns in neural field models, and, moreover, it can be used in conjunction with a variety of different neuronal processes, e.g., synaptic excitation and inhibition, synaptic depression, nonlinear adaptation, etc., to explore different effects on the behavior of the network, which, in turn, can be composed of populations of different neuronal type.

We have extended the results of [33, 11] further by calculating explicit expressions for the higher order operators in the Taylor expansion of the dynamical system about the stationary pulse which exhibit intricate structure from higher order derivatives of the δ-function (see Appendix E). Although the linear stability analysis correctly determines the stability of the stationary pulse, higher order analysis is necessary to describe the dynamics and stability of the bifurcating periodic orbit. The nonlinear analysis for the Hopf bifurcation was developed using the two methods of amplitude equations and center manifold reduction; both were in agreement and gave rise to various spatial terms involving convolution of the synaptic weight function w with higher order derivatives of the δ-function composed with the stationary pulse $\mathcal{U}_{\bar{a}}$. These integrals produce a profusion of terms which are critical to the normal form coefficients, indicating why neglecting spatial terms in the Amari ODE-formulation could lead to a discrepancy. The critical coefficients $c_1(0)$ and $\mathfrak{X}$ were used to identify points at which the bifurcation switches from supercritical to subcritical, and the results of the analytic calculations were found to be in strong agreement with numerical simulations of (1.1) taken a small distance on either side of these switching points.

The motivation of this nonlinear analysis is to establish the basic framework for a perturbative analysis of the dynamics of the periodic solutions as it provides a representation for the breather/slosher in a vicinity of the bifurcation. Since the third order terms determine changes in dynamics of the breather for small deviations from the bifurcation point, additional terms that influence the dynamics of the oscillations may be introduced at this order to study their effects on the breather. To investigate interacting breathers, we consider a pair of breathers positioned a sufficient distance apart so that the strength of the interactions between the breathers is sufficiently weak to be introduced at third order. Thus, a pair of normal forms representing the two different breathers can be coupled through weak interaction terms to provide a framework for studying weakly interacting breathers. As we shall report elsewhere, we use this formalism to investigate the effects of weak modulatory interactions mediated by the reciprocal, long-range *patchy connections* in primary visual cortex which are found to occur between populations of neurons with similar feature preference [3].

Appendix A. Equations, approximations, $\mathcal{M}_1$, and λ_1. Here we collect a series of calculations regarding stationary pulses and the operator $\mathcal{M}_1$ and λ_1. Recall that $\bar{a}$ represents any stationary pulse half-width for a given set of parameter values. Fixing all other parameters and taking the input amplitude $I_\circ$ as the bifurcation parameter, $\bar{a}_{\mathcal{H}}$ is the stationary pulse half-width at the Hopf bifurcation point $I_\circ = I_\circ^{\mathcal{H}}$.

Higher order derivatives of the stationary pulse $\mathcal{U}_{\bar{a}}$. Differentiating (2.2) or (3.4) yields the following derivatives at criticality $\bar{a} = \bar{a}_{\mathcal{H}}$:

$$\mathcal{U}''_{\mathcal{H}} = \frac{d^2}{dx^2}\mathcal{U}_{\bar{a}_{\mathcal{H}}}(x)\Big|_{x=\bar{a}_{\mathcal{H}}} = \frac{d^2}{dx^2}\mathcal{U}_{\bar{a}_{\mathcal{H}}}(x)\Big|_{x=-\bar{a}_{\mathcal{H}}} = \frac{w'(2\bar{a}_{\mathcal{H}}) + I_\circ^{\mathcal{H}}\, G''(\bar{a}_{\mathcal{H}})}{1+\rho},$$
$$\mathcal{U}'''_{\mathcal{H}} = \frac{d^3}{dx^3}\mathcal{U}_{\bar{a}_{\mathcal{H}}}(x)\Big|_{x=\bar{a}_{\mathcal{H}}} = -\frac{d^3}{dx^3}\mathcal{U}_{\bar{a}_{\mathcal{H}}}(x)\Big|_{x=-\bar{a}_{\mathcal{H}}} = \frac{w''(2\bar{a}_{\mathcal{H}}) - w''(0) + I_\circ^{\mathcal{H}}\, G'''(\bar{a}_{\mathcal{H}})}{1+\rho}.$$

Approximation of $I(\bar{a})$. From (2.3), the dependence of $I_\circ$ on $\bar{a}$ is

$$\kappa(1+\rho) = W(2\bar{a}) + I_\circ\, G(\bar{a}) \qquad \Longrightarrow \qquad I_\circ(\bar{a}) = \frac{\kappa(1+\rho) - W(2\bar{a})}{G(\bar{a})}.$$

Setting $\bar{a} = \bar{a}_{\mathcal{H}} + \tilde{a}$, where $\tilde{a}$ is small, we expand $I_\circ(\bar{a}) = I_\circ^{\mathcal{H}} + \tilde{a}\, I'_\circ(\bar{a}_{\mathcal{H}}) + \mathcal{O}(\tilde{a}^2)$, where, from (2.4), the derivative $I'_\circ(\bar{a})$ can be expressed in two ways:

$$I'_\circ(\bar{a}) \equiv \frac{d}{d\bar{a}} I_\circ(\bar{a}) = -\frac{N'(\bar{a})}{G(\bar{a})} \overset{\text{OR}}{=} \frac{-2w(2\bar{a})}{G(\bar{a})} - \Big[\kappa(1+\rho) - W(2\bar{a})\Big]\frac{G'(\bar{a})}{\big(G(\bar{a})\big)^2}.$$

The expression following $\overset{\text{OR}}{=}$ differs in that, by reusing (2.3), it is independent of $I_\circ$.

Useful relationships for various functions. In the following equations, it is assumed that $\bar{a} > 0$ and that $I_\circ$ and $\bar{a}$ are related according to (2.3). Note, however, that the relation $\Omega_\pm(\bar{a}_{\mathcal{H}}) = (1+\nu)\big|\mathcal{U}'_{\mathcal{H}}\big|$ applies *only* to the critical mode.

$$\begin{aligned}
&\Omega_\pm(-x) = \pm\Omega_\pm(x), && \mathcal{U}_{\bar{a}}(-\bar{a}) = \mathcal{U}_{\bar{a}}(\bar{a}) = \kappa,\\
&\Omega'_\pm(-x) = -\big[\pm\Omega'_\pm(x)\big], && \mathcal{U}'_{\bar{a}}(-\bar{a}) = -\mathcal{U}'_{\bar{a}}(\bar{a}) = \big|\mathcal{U}'_{\bar{a}}(\bar{a})\big|,\\
&\Omega''_\pm(-x) = \pm\Omega''_\pm(x), && \mathcal{U}''_{\bar{a}}(-\bar{a}) = \mathcal{U}''_{\bar{a}}(\bar{a}),\\
&\Omega_\pm(\bar{a}_{\mathcal{H}}) = w(0) \pm w(2\bar{a}_{\mathcal{H}}) && \mathcal{U}'''_{\bar{a}}(-\bar{a}) = -\mathcal{U}'''_{\bar{a}}(\bar{a}),\\
&\Omega'_\pm(\bar{a}_{\mathcal{H}}) = \pm w'(2\bar{a}_{\mathcal{H}}), && (1+\rho)|\mathcal{U}'_{\mathcal{H}}| = w(0) - w(2\bar{a}_{\mathcal{H}}) - I_\circ^{\mathcal{H}} G'(\bar{a}_{\mathcal{H}}).
\end{aligned}$$

Calculation of operator $\mathcal{M}_1$. We calculate expansions for the operator $\mathcal{M}_{\bar{a}}$ and its eigenvalue $\lambda(\bar{a})$ that is becoming critical. Let $\tilde{a}$ be a small perturbation of the critical half-width $\bar{a}_{\mathcal{H}}$ so that $\bar{a} = \bar{a}_{\mathcal{H}} + \tilde{a}$; then we expand as follows:

$$\mathcal{M}_{\bar{a}} = \mathcal{M}_{\mathcal{H}} + \tilde{a}\,\mathcal{M}_1 + \mathcal{O}\big(\tilde{a}^2\big), \qquad \lambda(\bar{a}) = \lambda_\circ + \tilde{a}\,\lambda_1 + \mathcal{O}\big(\tilde{a}^2\big).$$

From section 3.2, it was shown that $\mathcal{M}_{\mathcal{H}}\boldsymbol{v} = \lambda_\circ \boldsymbol{v}$, where $\lambda_\circ = i\omega_\circ$, and we have

$$\Big\langle \boldsymbol{y},\, \mathcal{M}_{\mathcal{H}}\boldsymbol{v}\Big\rangle = \lambda_\circ \equiv i\,\omega_\circ, \qquad \Big\langle \boldsymbol{y},\, \mathcal{M}_1\boldsymbol{v}\Big\rangle = \lambda_1 \equiv \varrho_1 + i\,\omega_1$$

with $\mathcal{M}_1, \varrho_1, \omega_1$ calculated below. Note that $\tilde{a} = \alpha\,\epsilon^2$ in section 3.3, whereas $\tilde{a} = a_2\,\varepsilon^2$ in section 3.4.

The operator $\mathcal{M}_1$ is given by

$$\begin{aligned}
\mathcal{M}_1\boldsymbol{\phi}\,(x) \;&=\; \frac{d}{d\bar{a}}\,\mathcal{M}_{\bar{a}}\boldsymbol{\phi}\,(x)\,\Big|_{\bar{a}\,=\,\bar{a}_{\mathcal{H}}} \\
&=\; \begin{pmatrix}1\\0\end{pmatrix}\,\frac{d}{d\bar{a}}\,\left[\frac{1}{|\mathcal{U}'_{\bar{a}}(\bar{a})|}\,\int_{\mathbb{R}}\Big[\,\delta(y-\bar{a})+\delta(y+\bar{a})\Big]\,w(x-y)\,\varphi(y)\,dy\right]\Big|_{\bar{a}\,=\,\bar{a}_{\mathcal{H}}} \\
&=\; \mathcal{N}_1\,\boldsymbol{\phi}(x)\,\cdot\,\left[\frac{d}{d\bar{a}}\,\frac{1}{|\mathcal{U}'_{\bar{a}}(\bar{a})|}\right]\Big|_{\bar{a}\,=\,\bar{a}_{\mathcal{H}}}\;+\;\mathcal{N}_2\,\boldsymbol{\phi}(x)\,\cdot\,\frac{1}{|\mathcal{U}'_{\bar{a}}(\bar{a})|}\,\Big|_{\bar{a}\,=\,\bar{a}_{\mathcal{H}}} \\
&=\; \frac{\Psi(\bar{a}_{\mathcal{H}})}{|\mathcal{U}'_{\mathcal{H}}|^2}\,\cdot\,\mathcal{N}_1\,\boldsymbol{\phi}(x)\;+\;\frac{1}{|\mathcal{U}'_{\mathcal{H}}|}\,\cdot\,\mathcal{N}_2\,\boldsymbol{\phi}(x), \qquad \text{(A.1)}
\end{aligned}$$

where $\Psi(\bar{a})=-\frac{d}{d\bar{a}}\,\big|\mathcal{U}'_{\bar{a}}(\bar{a})\big|$ is given below in (A.2) and $\mathcal{N}_1$ and $\mathcal{N}_2$ are computed as

$$\begin{aligned}
\mathcal{N}_1\,\boldsymbol{\phi}(x) &\equiv \begin{pmatrix}1\\0\end{pmatrix}\;\;\int_{\mathbb{R}}\Big[\;\delta(y-\bar{a})+\delta(y+\bar{a})\;\Big]\,w(x-y)\,\varphi(y)\,dy\;\;\Big|_{\bar{a}\,=\,\bar{a}_{\mathcal{H}}}, \\
\mathcal{N}_2\,\boldsymbol{\phi}(x) &\equiv \begin{pmatrix}1\\0\end{pmatrix}\,\frac{d}{d\bar{a}}\int_{\mathbb{R}}\Big[\,\delta(y-\bar{a})+\delta(y+\bar{a})\Big]\,w(x-y)\,\varphi(y)\,dy\;\Big|_{\bar{a}\,=\,\bar{a}_{\mathcal{H}}} \\
&=\; \begin{pmatrix}1\\0\end{pmatrix}\;\;\int_{\mathbb{R}}\Big[\,\delta'(y+\bar{a})-\delta'(y-\bar{a})\Big]\,w(x-y)\,\varphi(y)\,dy\;\Big|_{\bar{a}\,=\,\bar{a}_{\mathcal{H}}} \\
&=\; \begin{pmatrix}1\\0\end{pmatrix}\;\;\int_{\mathbb{R}}\Big[\;\delta(y-\bar{a})\;-\;\delta(y+\bar{a})\;\Big]\,\cdot\,\frac{\partial}{\partial y}\Big[w(x-y)\,\varphi(y)\Big]\,dy\,\Big|_{\bar{a}\,=\,\bar{a}_{\mathcal{H}}}.
\end{aligned}$$

The relevant inner products for calculating λ_1 are given by

$$\Big\langle \boldsymbol{y},\,\mathcal{N}_1\boldsymbol{v}\Big\rangle = \zeta\int_{\mathbb{R}}\Delta_{\pm}(x)\,\mathcal{N}_1\Omega_{\pm}(x)\,dx \;=\; 2\zeta\Big(\Omega_{\pm}(\bar{a}_{\mathcal{H}})\Big)\;=\;\tfrac{1}{2}\Big(1-i\tfrac{\omega_\circ}{\rho-\nu}\Big),$$

$$\Big\langle \boldsymbol{y},\,\mathcal{N}_2\boldsymbol{v}\Big\rangle = \zeta\int_{\mathbb{R}}\Delta_{\pm}(x)\,\mathcal{N}_2\Omega_{\pm}(x)\,dx \;=\; 4\zeta\Big(\Omega_{\pm}(\bar{a}_{\mathcal{H}})\,\Omega'_{\pm}(\bar{a}_{\mathcal{H}})\Big)\;=\;\Big(1-i\tfrac{\omega_\circ}{\rho-\nu}\Big)\,\Omega'_{\pm}(\bar{a}_{\mathcal{H}}).$$

Next, (2.8) implies that $\big|\mathcal{U}'_{\bar{a}}(\bar{a})\big| = \frac{1}{1+\rho}\big(w(0)-w(2\bar{a})-I_\circ(\bar{a})\,G'(\bar{a})\big)$. Subsequently, by differentiating this expression with respect to $\bar{a}$ and substituting for $I'_\circ(\bar{a})$ using (2.4), $\Psi(\bar{a}_{\mathcal{H}})$ can be expressed as

$$\begin{aligned}
\Psi(\bar{a}_{\mathcal{H}}) \equiv -\frac{d}{d\bar{a}}\,\big|\mathcal{U}'_{\bar{a}}(\bar{a})\big|\,\Big|_{\bar{a}\,=\,\bar{a}_{\mathcal{H}}} &= \frac{1}{1+\rho}\Big(\underbrace{2w'(2\bar{a})+I_\circ(\bar{a})\,G''(\bar{a})}_{N''(\bar{a})}+I'_\circ(\bar{a})\,G'(\bar{a})\Big)\Big|_{\bar{a}\,=\,\bar{a}_{\mathcal{H}}} \\
&= \frac{1}{1+\rho}\left(\,N''_{\mathcal{H}}(\bar{a}_{\mathcal{H}})-N'_{\mathcal{H}}(\bar{a}_{\mathcal{H}})\,\frac{G'(\bar{a}_{\mathcal{H}})}{G(\bar{a}_{\mathcal{H}})}\right), \qquad \text{(A.2)}
\end{aligned}$$

where

$$N'_{\mathcal{H}}(\bar{a}_{\mathcal{H}}) = 2w(2\bar{a}_{\mathcal{H}})+I^{\mathcal{H}}_\circ G'(\bar{a}_{\mathcal{H}}), \qquad N''_{\mathcal{H}}(\bar{a}_{\mathcal{H}}) = 4w'(2\bar{a}_{\mathcal{H}})+I^{\mathcal{H}}_\circ G''(\bar{a}_{\mathcal{H}}).$$

The subscript $\mathcal{H}$ indicates simultaneous evaluation at $\bar{a} = \bar{a}_{\mathcal{H}}$ and $I_\circ(\bar{a}_{\mathcal{H}}) \equiv I_\circ^{\mathcal{H}}$ at the Hopf bifurcation point. This completes the calculation of $\mathcal{M}_1$; now we calculate λ_1.

Calculation of λ_1. From (A.1) and the above calculations, it follows that

$$\begin{aligned}\lambda_1 \;&=\; \big\langle \boldsymbol{y},\, \mathcal{M}_1 \boldsymbol{v} \big\rangle \;=\; \frac{\Psi(\bar{a}_{\mathcal{H}})}{|\mathcal{U}'_{\mathcal{H}}|^2} \Big\langle \boldsymbol{y},\, \mathcal{N}_1 \boldsymbol{v} \Big\rangle \;+\; \frac{1}{|\mathcal{U}'_{\mathcal{H}}|} \Big\langle \boldsymbol{y},\, \mathcal{N}_2 \boldsymbol{v} \Big\rangle \\ &=\; \Big(1 - i\frac{\omega_\circ}{\rho - \nu}\Big) \Big[\frac{1}{2}\frac{\Psi(\bar{a}_{\mathcal{H}})}{|\mathcal{U}'_{\mathcal{H}}|^2} + \frac{\Omega'_\pm(\bar{a}_{\mathcal{H}})}{|\mathcal{U}'_{\mathcal{H}}|}\Big].\end{aligned}$$

Finally, λ_1 may be expressed as

$$\text{(A.3)} \qquad \lambda_1 \;=\; \varrho_1 \;+\; i\,\omega_1, \qquad \begin{aligned} \varrho_1 \;&=\; \Phi(\bar{a}_{\mathcal{H}}), \qquad & \omega_1 \;&=\; -\big(\tfrac{\omega_\circ}{\rho-\nu}\big)\,\Phi(\bar{a}_{\mathcal{H}}), \\ \Phi(\bar{a}_{\mathcal{H}}) \;&=\; \frac{(1+\nu)^2}{2}\,\frac{\Psi(\bar{a}_{\mathcal{H}})}{\Omega_\pm^2(\bar{a}_{\mathcal{H}})} \;+\; (1+\nu)\,\frac{\Omega'_\pm(\bar{a}_{\mathcal{H}})}{\Omega_\pm(\bar{a}_{\mathcal{H}})} \end{aligned}$$

since ζ is the only complex quantity in the expression for λ_1 and $|\mathcal{U}'_{\mathcal{H}}| = \Omega\big(\bar{a}_{\mathcal{H}}\big)/(1+\nu)$. Note that this result agrees with the result obtained by calculating $\lambda'(\bar{a})$ directly from the expression for the critical eigenvalue $\lambda_+^{\pm}(a)$ in (2.10) or (2.12). Additionally, for clarity we mention that in section 3.4 we use the symbol $\lambda(\bar{a} - \bar{a}_{\mathcal{H}})$ so that $\lambda(0) = i\omega_\circ$, while elsewhere we use $\lambda(\bar{a})$ with $\lambda(\bar{a}_{\mathcal{H}}) = i\omega_\circ$. This was merely to preserve the use of the symbols $c_1(0)$ and $\ell_1(0)$ in section 3.4.

Appendix B. Calculation of $B(\boldsymbol{v},\boldsymbol{v})$, $B(\boldsymbol{v},\bar{\boldsymbol{v}})$, and $C(\boldsymbol{v},\boldsymbol{v},\bar{\boldsymbol{v}})$. In section 3.1 we express $B(\boldsymbol{v},\boldsymbol{v}), B(\boldsymbol{v},\bar{\boldsymbol{v}})$, and $C(\boldsymbol{v},\boldsymbol{v},\bar{\boldsymbol{v}})$ in terms of the functions $\Sigma(x)$ and $\Lambda(x)$, respectively. These functions depend on which of the two spatial modes goes critical in the bifurcation, and the two cases are distinguished by the appearance of $\pm$, which corresponds to spatial modes $\Omega = \Omega_\pm$. Furthermore, these complicated expressions reduce considerably by the *useful relations* listed in Appendix A and symmetries of w.

Calculation of $\mathrm{B}_{\mathcal{H}}(\boldsymbol{v},\boldsymbol{v})$ and $\mathrm{B}_{\mathcal{H}}(\boldsymbol{v},\bar{\boldsymbol{v}})$. From (3.5) the eigenvectors $\boldsymbol{v}, \bar{\boldsymbol{v}}$, where $\boldsymbol{v} = (v_1, v_2)^{\mathrm{T}}$,
satisfy $v_1(x) = \bar{v}_1(x) = \Omega(x)$. Hence, from (3.15), for all $\mathbf{v}_1, \mathbf{v}_2 \in \{\boldsymbol{v}, \bar{\boldsymbol{v}}\}$,

$$\mathrm{B}_{\mathcal{H}}\big(\mathbf{v}_1, \mathbf{v}_2\big)(x) = \begin{pmatrix} 1 \\ 0 \end{pmatrix} \Sigma(x),$$

where we have used (3.15) and (E.1) to obtain the following expression for $\Sigma(x)$:

$$\begin{aligned}\Sigma(x) \;&=\; \int_{\mathbb{R}} \left[\frac{\delta(y-\bar{a}_{\mathcal{H}})}{|\mathcal{U}'_{\mathcal{H}}|} + \frac{\delta(y+\bar{a}_{\mathcal{H}})}{|-\mathcal{U}'_{\mathcal{H}}|}\right] \cdot \frac{\partial}{\partial y}\left[-\frac{w(x-y)}{\mathcal{U}'_{\mathcal{H}}(y)}\,\Omega^2(y)\right] dy \\ &=\; \frac{h(x,\bar{a}_{\mathcal{H}})\,\mathcal{U}''_{\mathcal{H}}(\bar{a}_{\mathcal{H}}) - \dot{h}(x,\bar{a}_{\mathcal{H}})\,\mathcal{U}'_{\mathcal{H}}(\bar{a}_{\mathcal{H}})}{\big|\mathcal{U}'_{\mathcal{H}}(\bar{a}_{\mathcal{H}})\big|^3} + \frac{h(x,-\bar{a}_{\mathcal{H}})\,\mathcal{U}''_{\mathcal{H}}(-\bar{a}_{\mathcal{H}}) - \dot{h}(x,-\bar{a}_{\mathcal{H}})\,\mathcal{U}'_{\mathcal{H}}(-\bar{a}_{\mathcal{H}})}{\big|\mathcal{U}'_{\mathcal{H}}(-\bar{a}_{\mathcal{H}})\big|^3},\end{aligned}$$

where

$$h(x,y) \;=\; w(x-y)\,\Omega^2(y), \qquad \dot{h}(x,\bar{a}_{\mathcal{H}}) = \frac{\partial}{\partial y} h(x,y)\Big|_{y=\bar{a}_{\mathcal{H}}}.$$

After a lengthy calculation, the explosion of terms reduces significantly by the *useful relationships* listed in Appendix A, including $\Omega(\bar{a}_{\mathcal{H}}) = (1+\nu)|\mathcal{U}'_{\mathcal{H}}|$. Accordingly, for the two spatial modes $\Omega = \Omega_{\pm}$, we find

$$\Sigma_{\pm}(x) \;=\; \sigma^{\pm}_{\circ}(\bar{a}_{\mathcal{H}})\Big[w(x-\bar{a}_{\mathcal{H}}) + w(x+\bar{a}_{\mathcal{H}})\Big] + (1+\nu)^2\Big[-w'(x-\bar{a}_{\mathcal{H}}) + w'(x+\bar{a}_{\mathcal{H}})\Big], \tag{B.1}$$

where the $\pm$ indicates the dependency on the bifurcating mode $\Omega_{\pm}$ and $\sigma^{\pm}_{\circ}(\bar{a}_{\mathcal{H}})$ is

$$\sigma^{\pm}_{\circ}(\bar{a}_{\mathcal{H}}) \;=\; \frac{(1+\nu)^2}{\Omega_{\pm}(\bar{a}_{\mathcal{H}})}\Big[(1+\nu)\,\mathcal{U}''_{\mathcal{H}} \pm 2w'(2\bar{a}_{\mathcal{H}})\Big].$$

$\Sigma_{\pm}(x)$ are even in x, and we use the relationship $\Sigma_{\pm}(\bar{a}_{\mathcal{H}}) = \Sigma_{\pm}(-\bar{a}_{\mathcal{H}})$, where

$$\Sigma_{\pm}(\bar{a}_{\mathcal{H}}) = \sigma^{\pm}_{\circ}(\bar{a}_{\mathcal{H}})\left[w\big(0\big) + w\big(2\bar{a}_{\mathcal{H}}\big)\right] \;+\; (1+\nu)^2\, w'(2\bar{a}_{\mathcal{H}}), \tag{B.2}$$

$$\Sigma'_{\pm}(\bar{a}_{\mathcal{H}}) = \sigma^{\pm}_{\circ}(\bar{a}_{\mathcal{H}})\, w'(2\bar{a}_{\mathcal{H}}) - (1+\nu)^2\big(w''(0) - w''(2\bar{a}_{\mathcal{H}})\big). \tag{B.3}$$

The even symmetry of $\Sigma_{\pm}$ simplifies this integral with $\Delta_{\pm}(x) = \delta(x-\bar{a}_{\mathcal{H}}) \pm \delta(x+\bar{a}_{\mathcal{H}})$:

$$\int_{\mathbb{R}} \Delta_{\pm}(x)\,\Sigma_{\pm}(x)\,dx \;=\; \begin{cases} 2\,\Sigma_{+}(\bar{a}_{\mathcal{H}}), & \text{(SUM MODE)} \\ 0, & \text{(DIFFERENCE MODE)} \end{cases}$$

where $\Sigma_{+}(\bar{a}_{\mathcal{H}})$ can be further reduced to

$$\Sigma_{+}(\bar{a}_{\mathcal{H}}) \;=\; (1+\nu)^2\Big\{(1+\nu)\,\mathcal{U}''_{\mathcal{H}} + \,3w'(2\bar{a}_{\mathcal{H}})\Big\}. \tag{B.4}$$

Note that $\Sigma'_{\pm}(\bar{a}_{\mathcal{H}})$ appears in the calculations of $\Xi^{c}_{\pm}(\bar{a}_{\mathcal{H}})$ and $\Xi^{d}_{\pm}(\bar{a}_{\mathcal{H}})$.

Calculation of $\mathrm{C}_{\mathcal{H}}(\boldsymbol{v},\boldsymbol{v},\bar{\boldsymbol{v}})$. As above, for all permutations $\mathbf{v}_1,\mathbf{v}_2,\mathbf{v}_3 \in \{\boldsymbol{v},\bar{\boldsymbol{v}}\}$,

$$\mathrm{C}_{\mathcal{H}}\big(\mathbf{v}_1,\mathbf{v}_2,\mathbf{v}_3\big)(x) = \binom{1}{0}\Lambda(x).$$

From (3.16), we use (E.2) to obtain the following expression for $\Lambda(x)$:

$$\Lambda(x) = \int_{\mathbb{R}}\left[\frac{\delta(y-\bar{a}_{\mathcal{H}})}{|\mathcal{U}'_{\mathcal{H}}|} + \frac{\delta(y+\bar{a}_{\mathcal{H}})}{|-\mathcal{U}'_{\mathcal{H}}|}\right]\cdot\frac{d}{dy}\left[\frac{1}{\mathcal{U}'_{\mathcal{H}}(y)}\frac{d}{dy}\left[\frac{w(x-y)}{\mathcal{U}'_{\mathcal{H}}(y)}\,\Omega^3(y)\right]\right]dy$$

$$\begin{aligned}
= &+\frac{3\mathcal{U}''_{\mathcal{H}}(\bar{a}_{\mathcal{H}})}{\big|\,\mathcal{U}'_{\mathcal{H}}(\bar{a}_{\mathcal{H}})\,\big|^5}\;\Big[f(x,\bar{a}_{\mathcal{H}})\mathcal{U}''_{\mathcal{H}}(\bar{a}_{\mathcal{H}}) - \dot{f}(x,\bar{a}_{\mathcal{H}})\mathcal{U}'_{\mathcal{H}}(\bar{a}_{\mathcal{H}})\Big] \\
&+\frac{\mathcal{U}'_{\mathcal{H}}(\bar{a}_{\mathcal{H}})}{\big|\,\mathcal{U}'_{\mathcal{H}}(\bar{a}_{\mathcal{H}})\,\big|^5}\;\Big[\ddot{f}(x,\bar{a}_{\mathcal{H}})\mathcal{U}'_{\mathcal{H}}(\bar{a}_{\mathcal{H}}) - f(x,\bar{a}_{\mathcal{H}})\mathcal{U}'''_{\mathcal{H}}(\bar{a}_{\mathcal{H}})\Big] \\
&+\frac{3\mathcal{U}''_{\mathcal{H}}(-\bar{a}_{\mathcal{H}})}{\big|\mathcal{U}'_{\mathcal{H}}(-\bar{a}_{\mathcal{H}})\big|^5}\;\Big[f(x,-\bar{a}_{\mathcal{H}})\mathcal{U}''_{\mathcal{H}}(\bar{a}_{\mathcal{H}}) - \dot{f}(x,-\bar{a}_{\mathcal{H}})\mathcal{U}'_{\mathcal{H}}(-\bar{a}_{\mathcal{H}})\Big] \\
&+\frac{\mathcal{U}'_{\mathcal{H}}(-\bar{a}_{\mathcal{H}})}{\big|\mathcal{U}'_{\mathcal{H}}(-\bar{a}_{\mathcal{H}})\big|^5}\;\Big[\ddot{f}(x,-\bar{a}_{\mathcal{H}})\mathcal{U}'_{\mathcal{H}}(-\bar{a}_{\mathcal{H}}) - f(x,-\bar{a}_{\mathcal{H}})\mathcal{U}'''_{\mathcal{H}}(-\bar{a}_{\mathcal{H}})\Big]
\end{aligned}$$

where $f(x,y) = w(x-y)\,\Omega^3(y)$,

$$\dot{f}(x,\pm\bar{a}_{\mathcal{H}}) = \frac{\partial}{\partial y} f(x,y)\Big|_{y=\pm\bar{a}_{\mathcal{H}}}, \qquad \ddot{f}(x,\pm\bar{a}_{\mathcal{H}}) = \frac{\partial^2}{\partial y^2} f(x,y)\Big|_{y=\pm\bar{a}_{\mathcal{H}}}.$$

After a doubly lengthy calculation and using $w^{(n)}(x-\bar{a}_{\mathcal{H}}) \pm w^{(n)}(x+\bar{a}_{\mathcal{H}}) = \Omega_{\pm}^{(n)}(x)$ and $w'(0) = 0$, we apply symmetry conditions to reduce $\Lambda_{\pm}(x)$ to

$$\begin{aligned}\Lambda_{\pm}(x) = (1+\nu)^3\,\Omega_{\pm}''(x) \;+\; \breve{B}_{\pm}\,\Big[-w'(x-\bar{a}_{\mathcal{H}}) \pm w'(x+\bar{a}_{\mathcal{H}})\Big] \\ +\; \breve{C}_{\pm}\,\Omega_{\pm}(x) \;+\; \breve{D}_{\pm}\,\Big[\;w\,(x-\bar{a}_{\mathcal{H}}) + w\,(x+\bar{a}_{\mathcal{H}})\Big],\end{aligned} \tag{B.5}$$

where

$$\breve{B}_{\pm} = 3\,(1+\nu)^4\,\frac{\mathcal{U}_{\mathcal{H}}''}{\Omega_{\pm}(\bar{a}_{\mathcal{H}})} + 6\,(1+\nu)^3\,\frac{\Omega_{\pm}'(\bar{a}_{\mathcal{H}})}{\Omega_{\pm}(\bar{a}_{\mathcal{H}})}, \qquad \breve{D}_{\pm} = \;3\,(1+\nu)^3\,\frac{\Omega_{\pm}''(\bar{a}_{\mathcal{H}})}{\Omega_{\pm}(\bar{a}_{\mathcal{H}})},$$

$$\breve{C}_{\pm} = 3\,(1+\nu)^5\left(\frac{\mathcal{U}_{\mathcal{H}}''}{\Omega_{\pm}(\bar{a}_{\mathcal{H}})}\right)^2 + (1+\nu)^4\left(\frac{\mathcal{U}_{\mathcal{H}}'''}{\Omega_{\pm}(\bar{a}_{\mathcal{H}})} + 9\,\frac{\mathcal{U}_{\mathcal{H}}''\,\Omega_{\pm}'(\bar{a}_{\mathcal{H}})}{\Omega_{\pm}^2(\bar{a}_{\mathcal{H}})}\right) + 6\,(1+\nu)^3\left(\frac{\Omega_{\pm}'(\bar{a}_{\mathcal{H}})}{\Omega_{\pm}(\bar{a}_{\mathcal{H}})}\right)^2.$$

These expressions have two forms according to the relationship $\Omega_{\pm}(\bar{a}_{\mathcal{H}}) = (1+\nu)|\mathcal{U}_{\mathcal{H}}'|$; however, the expression for $\Omega_{\pm}(\bar{a}_{\mathcal{H}}) = w(0) \pm w(2\bar{a}_{\mathcal{H}})$ is simpler than that of $|\mathcal{U}_{\mathcal{H}}'|$.

In the case of the *sum mode* Ω_+, the function $\Lambda_+(x)$ is an *even* function, whereas in the case of the *difference mode* Ω_-, the function $\Lambda_-(x) = \Lambda_-^{\mathrm{e}}(x) + \Lambda_-^{\mathrm{o}}(x)$ is composed of *even* $\Lambda_-^{\mathrm{e}}(x)$ and *odd* $\Lambda_-^{\mathrm{o}}(x)$ parts where

$$\Lambda_-^{\mathrm{e}}(x) \;=\; \breve{D}_{\pm}\,\Big[w(x-\bar{a}_{\mathcal{H}}) + w(x+\bar{a}_{\mathcal{H}})\Big], \qquad \Lambda_-^{\mathrm{o}}(x) \;=\; \Lambda_{\pm}(x) - \Lambda_{\pm}^{\mathrm{e}}(x).$$

The following integral also simplifies in the two cases $\Delta_{\pm}(x) = \delta(x-\bar{a}_{\mathcal{H}}) \pm \delta(x+\bar{a}_{\mathcal{H}})$:

$$\int_{\mathbb{R}} \Delta_{\pm}(x)\,\Lambda_{\pm}(x)\,dx \;=\; \begin{cases} 2\Lambda_+(\bar{a}_{\mathcal{H}}), & \text{(SUM MODE)} \\ 2\Lambda_-^{\mathrm{o}}(\bar{a}_{\mathcal{H}}), & \text{(DIFFERENCE MODE)} \end{cases}$$

where

$$\begin{aligned}\Lambda_+(\bar{a}_{\mathcal{H}}) &= (1+\nu)^3\,\Omega_+''(\bar{a}_{\mathcal{H}}) \;+\; \breve{B}_+\,\Omega_+'(\bar{a}_{\mathcal{H}}) \;+\; \big(\breve{C}_+ + \breve{D}_+\big)\,\Omega_+(\bar{a}_{\mathcal{H}}), \\ \Lambda_-^{\mathrm{o}}(\bar{a}_{\mathcal{H}}) &= (1+\nu)^3\,\Omega_-''(\bar{a}_{\mathcal{H}}) \;+\; \breve{B}_-\,\Omega_-'(\bar{a}_{\mathcal{H}}) \;+\; \breve{C}_-\,\Omega_-(\bar{a}_{\mathcal{H}})\end{aligned}$$

as a result of the symmetries of $\Lambda_{\pm}(x)$.

Appendix C.

C.1. Solving the second order equations. We first derive the solution for the class of equations arising from the second order equations with a *general* right-hand side $\mathbf{H}(x)$. Subsequently, we use this to express the solutions $\boldsymbol{h}_{20}(x)$ and $\boldsymbol{h}_{11}(x)$ of (3.21), where $\mathbf{H}(x) = \mathrm{H}_{20} \equiv \mathrm{B}_{\mathcal{H}}(\boldsymbol{v},\boldsymbol{v})$ and $\mathbf{H}(x) = \mathrm{H}_{11} \equiv \mathrm{B}_{\mathcal{H}}(\boldsymbol{v},\bar{\boldsymbol{v}})$, respectively. The even symmetry of $\Sigma(x)$ simplifies the expression for each solution. The related solutions $\boldsymbol{w}_{20}(x)$ and $\boldsymbol{w}_{11}(x)$ of (3.32), arising in the center manifold reduction in section 3.4, are given explicitly in Appendix C.3. In particular, we show in Appendix C.3 that the solution $\boldsymbol{w}_{11}$ is related to $\boldsymbol{h}_{11}$ (similarly, $\boldsymbol{w}_{20}$ is related to $\boldsymbol{h}_{20}$); however, we also show that the differences between $\boldsymbol{w}_{11}$ and $\boldsymbol{h}_{11}$ (and between $\boldsymbol{w}_{20}$ and $\boldsymbol{h}_{20}$) do not contribute to $\mathcal{X}$ and $c_1(0)$ (the critical normal form coefficients at third order in sections 3.3 and 3.4, respectively). In particular, $\mathcal{X}$ and $c_1(0)$ are shown in (C.13) to be identical.

Solution of the general equation. The general integral equation that arises at second order in $\boldsymbol{\phi}$ is given by

$$\Big(\eta \mathrm{I} - \mathcal{M}_{\mathcal{H}}\Big)\,\boldsymbol{w}(x) \;=\; \mathbf{H}(x), \tag{C.1}$$

where $\boldsymbol{w}, \mathbf{H} \in \mathscr{H}$ and η is not an eigenvalue of $\mathcal{M}_{\mathcal{H}}$. In sections 3.3 and 3.4, the critical eigenvalues of $\mathcal{M}_{\mathcal{H}}$ are $\pm i\omega_\circ$ and η is $\pm i2\omega_\circ$ or 0. Assume $\boldsymbol{w}(x) = (s_1(x), s_2(x))^{\mathrm{T}}$ and $\mathbf{H}(x) = (\mathrm{H}_1(x), \mathrm{H}_2(x))^{\mathrm{T}}$; then (C.1) can be expressed as the integral equation

$$\begin{bmatrix} \eta+1 & \rho \\ -\nu & \eta+\nu \end{bmatrix} \begin{pmatrix} s_1(x) \\ s_2(x) \end{pmatrix} - \begin{pmatrix} \big(w * \big[\delta'\big(\mathcal{U}_{\mathcal{H}} - \kappa\big)\, s_1\big]\big)(x) \\ 0 \end{pmatrix} \;=\; \begin{pmatrix} \mathrm{H}_1(x) \\ \mathrm{H}_2(x) \end{pmatrix}. \tag{C.2}$$

Since the nonlocal operator is present only in the first component of this equation, we can immediately solve for $s_2(x)$ to obtain

$$s_2(x) \;=\; \Big(\tfrac{\nu}{\nu+\eta}\Big)\, s_1(x) \;+\; \Big(\tfrac{1}{\nu+\eta}\Big)\, \mathrm{H}_2(x). \tag{C.3}$$

Substituting for $s_2(x)$ in the first component of (C.2), we obtain the equation

$$\mu(\eta)\, s_1(x) \;-\; \int_{\mathbb{R}} w(x-y)\Big(\delta'\big(\mathcal{U}_{\mathcal{H}}(y) - \kappa\big)\, s_1(y)\Big)\, dy \;=\; \mathrm{H}_1^{\circledcirc}(x), \tag{C.4}$$

where

$$\mu(\eta) \;=\; 1 + \eta \;+\; \frac{\nu\rho}{\nu+\eta}, \qquad\qquad \mathrm{H}_1^{\circledcirc}(x) \;=\; \mathrm{H}_1(x) - \Big(\tfrac{\rho}{\nu+\eta}\Big)\, \mathrm{H}_2(x).$$

Evaluating the convolution subsequently results in the equation

$$\mu(\eta)\, s_1(x) \;-\; \left(\frac{s_1(\bar{a}_{\mathcal{H}})}{|\mathcal{U}'_{\mathcal{H}}|} w(x-\bar{a}_{\mathcal{H}}) + \frac{s_1(-\bar{a}_{\mathcal{H}})}{|-\mathcal{U}'_{\mathcal{H}}|} w(x+\bar{a}_{\mathcal{H}})\right) \;=\; \mathrm{H}_1^{\circledcirc}(x). \tag{C.5}$$

Substituting $x = \bar{a}_{\mathcal{H}}$ and $x = -\bar{a}_{\mathcal{H}}$ yields the following matrix equation as a compatibility condition determining the values of $s_1(\bar{a}_{\mathcal{H}})$ and $s_1(-\bar{a}_{\mathcal{H}})$ that satisfy (C.5):

$$\begin{bmatrix} \mu(\eta) - \hat{w}(0) & \hat{w}(2\bar{a}_{\mathcal{H}}) \\ \hat{w}(2\bar{a}_{\mathcal{H}}) & \mu(\eta) - \hat{w}(0) \end{bmatrix} \begin{pmatrix} s_1(\bar{a}_{\mathcal{H}}) \\ s_1(-\bar{a}_{\mathcal{H}}) \end{pmatrix} = \begin{pmatrix} \mathrm{H}_1^{\circledcirc}(\bar{a}_{\mathcal{H}}) \\ \mathrm{H}_1^{\circledcirc}(-\bar{a}_{\mathcal{H}}) \end{pmatrix}, \tag{C.6}$$

where $\hat{w}(x) = \frac{w(x)}{|\mathcal{U}'_{\mathcal{H}}|}$. The matrix is invertible, and $s_1(\bar{a}_{\mathcal{H}})$ and $s_1(-\bar{a}_{\mathcal{H}})$ are given by

$$\begin{pmatrix} s_1(\bar{a}_{\mathcal{H}}) \\ s_1(-\bar{a}_{\mathcal{H}}) \end{pmatrix} = \frac{1}{\big(\mu(\eta) - \hat{w}(0)\big)^2 - \big(\hat{w}(2\bar{a}_{\mathcal{H}})\big)^2} \begin{bmatrix} \mu(\eta) - \hat{w}(0) & \hat{w}(2\bar{a}_{\mathcal{H}}) \\ \hat{w}(2\bar{a}_{\mathcal{H}}) & \mu(\eta) - \hat{w}(0) \end{bmatrix} \begin{pmatrix} \mathrm{H}_1^{\circledcirc}(\bar{a}_{\mathcal{H}}) \\ \mathrm{H}_1^{\circledcirc}(-\bar{a}_{\mathcal{H}}) \end{pmatrix}.$$

Finally, using (C.5) and (C.3), the solution $\boldsymbol{w}(x)$ of (C.2) is then expressed as

$$\boldsymbol{w}(x) = \begin{pmatrix} s_1(x) \\ s_2(x) \end{pmatrix}, \qquad \begin{aligned} s_1(x) &= \frac{1}{\mu(\eta)} \Big[\mathcal{S}^{+} w(x - \bar{a}_{\mathcal{H}}) + \mathcal{S}^{-} w(x + \bar{a}_{\mathcal{H}}) + \mathrm{H}_1^{\circledcirc}(x) \Big], \\ s_2(x) &= \frac{1}{\nu + \eta} \Big[\nu\, s_1(x) - \mathrm{H}_2(x) \Big], \end{aligned}$$

where

$$\mathcal{S}^{+} \equiv \frac{s_1(\bar{a}_{\mathcal{H}})}{|\mathcal{U}'_{\mathcal{H}}|} = \frac{\Big(\mu(\eta)|\mathcal{U}'_{\mathcal{H}}| - w(0)\Big)\, \mathrm{H}_1^{\circledcirc}(\bar{a}_{\mathcal{H}}) + w(\bar{a}_{\mathcal{H}})\, \mathrm{H}_1^{\circledcirc}(-\bar{a}_{\mathcal{H}})}{\Big(\mu(\eta)|\mathcal{U}'_{\mathcal{H}}| - w(0)\Big)^2 - \Big(w(2\bar{a}_{\mathcal{H}})\Big)^2},$$

$$\mathcal{S}^{-} \equiv \frac{s_1(-\bar{a}_{\mathcal{H}})}{|\mathcal{U}'_{\mathcal{H}}|} = \frac{w(\bar{a}_{\mathcal{H}})\, \mathrm{H}_1^{\circledcirc}(\bar{a}_{\mathcal{H}}) + \Big(\mu(\eta)|\mathcal{U}'_{\mathcal{H}}| - w(0)\Big)\, \mathrm{H}_1^{\circledcirc}(-\bar{a}_{\mathcal{H}})}{\Big(\mu(\eta)|\mathcal{U}'_{\mathcal{H}}| - w(0)\Big)^2 - \Big(w(2\bar{a}_{\mathcal{H}})\Big)^2}. \qquad \blacksquare$$

Using this solution for the general equation (C.2), we now solve (3.21) as special cases.

Solution of $-\mathcal{M}_{\mathcal{H}} \boldsymbol{h}_{11} = \mathrm{B}_{\mathcal{H}}(\boldsymbol{v}, \bar{\boldsymbol{v}})$. In this case, $\eta = 0$ implying $\mu(0) = (1 + \rho)$, and we must solve

$$-\mathcal{M}_{\mathcal{H}} \boldsymbol{h}_{11} = \mathrm{B}_{\mathcal{H}}(\boldsymbol{v}, \bar{\boldsymbol{v}}) = \begin{pmatrix} \Sigma(x) \\ 0 \end{pmatrix}.$$

Let $\boldsymbol{h}_{11}(x) = \big(c_1(x), c_2(x)\big)^{\mathrm{T}}$. Since $\mathrm{H}_2(x) = 0$, it follows that $\mathrm{H}_1^{\circledcirc}(x) = \mathrm{H}_1(x) = \Sigma(x)$, and, since $\Sigma(x)$ is an even function, $\mathrm{H}_1^{\circledcirc}(-\bar{a}_{\mathcal{H}}) = \mathrm{H}_1^{\circledcirc}(\bar{a}_{\mathcal{H}}) = \Sigma(\bar{a}_{\mathcal{H}})$ implies that $\mathcal{S}^{-} = \mathcal{S}^{+} = \mathcal{C}$, where the coefficient $\mathcal{C}\,(\bar{a}_{\mathcal{H}})$ is

$$\mathcal{C}\,(\bar{a}_{\mathcal{H}}) = \frac{\Sigma(\bar{a}_{\mathcal{H}})}{\frac{(1+\rho)}{(1+\nu)}\Omega(\bar{a}_{\mathcal{H}}) - \big(w(0) + w(2\bar{a}_{\mathcal{H}})\big)}$$

since $(1 + \nu)|\mathcal{U}'_{\mathcal{H}}| = \Omega(\bar{a}_{\mathcal{H}})$. Then, since $c_2(x) = c_1(x)$, we arrive at the solution

$$\boldsymbol{h}_{11}(x) = \begin{pmatrix} c\,(x) \\ c\,(x) \end{pmatrix}, \qquad c\,(x) = \frac{1}{1+\rho} \Big(\mathcal{C}\,(\bar{a}_{\mathcal{H}}) \Big[w(x - \bar{a}_{\mathcal{H}}) + w(x + \bar{a}_{\mathcal{H}}) \Big] + \Sigma(x) \Big).$$

Moreover, it can be shown that $c\,(x)$ is even-symmetric in x, providing the useful results $c\,(-\bar{a}_{\mathcal{H}}) = c\,(\bar{a}_{\mathcal{H}})$ and $c'(-\bar{a}_{\mathcal{H}}) = -c'(\bar{a}_{\mathcal{H}})$, where

$$c\,(\bar{a}_{\mathcal{H}}) = \frac{\Sigma(\bar{a}_{\mathcal{H}})\,\Omega(\bar{a}_{\mathcal{H}})}{{}_{(1+\rho)}\,\Omega(\bar{a}_{\mathcal{H}}) - {}_{(1+\nu)}\Big(w(0) + w(2\bar{a}_{\mathcal{H}})\Big)}, \tag{C.7}$$

$$c'(\bar{a}_{\mathcal{H}}) = \frac{1}{1+\rho}\left[\frac{\Sigma(\bar{a}_{\mathcal{H}})w'(2\bar{a}_{\mathcal{H}})}{\frac{(1+\rho)}{(1+\nu)}\,\Omega(\bar{a}_{\mathcal{H}}) - \big(w(0) + w(2\bar{a}_{\mathcal{H}})\big)} + \Sigma'(\bar{a}_{\mathcal{H}})\right]. \tag{C.8}$$

In the case $\Omega = \Omega_{+}$, we have the additional simplifications

$$c_{+}(\bar{a}_{\mathcal{H}}) = \left(\frac{\Sigma_{+}(\bar{a}_{\mathcal{H}})}{\rho-\nu}\right), \qquad c'_{+}(\bar{a}_{\mathcal{H}}) = \frac{1}{1+\rho}\left(\frac{1+\nu}{\rho-\nu}\frac{\Sigma_{+}(\bar{a}_{\mathcal{H}})w'(2\bar{a}_{\mathcal{H}})}{\Omega_{+}(\bar{a}_{\mathcal{H}})} + \Sigma'_{+}(\bar{a}_{\mathcal{H}})\right). \qquad \blacksquare$$

Solution of $(2\omega_{\circ}i\mathbf{I} - \mathcal{M}_{\mathcal{H}})\boldsymbol{h}_{20} = \mathrm{B}_{\mathcal{H}}(\boldsymbol{v},\boldsymbol{v})$. In this case, $\eta = 2\omega_{\circ}i$, and we have

$$\mu(2\omega_{\circ}i) \;=\; \left(1 + 2\omega_{\circ}i + \frac{\rho\nu}{\nu + 2\omega_{\circ}i}\right) \;=\; \left[1 + \frac{\rho\nu}{4\rho - 3\nu}\right] + i6\omega_{\circ}\left[\frac{\rho-\nu}{4\rho-3\nu}\right].$$

As before, $\mathrm{H}_2(x) = 0$ and $\mathrm{H}_1^{\circledcirc}(x) = \mathrm{H}_1(x) = \Sigma(x)$, and the even symmetry of $\Sigma(x)$ implies that $\mathcal{S}^{-} = \mathcal{S}^{+} = \mathcal{D}$, where the coefficient $\mathcal{D}\,(\bar{a}_{\mathcal{H}})$ is

$$\mathcal{D}(\bar{a}_{\mathcal{H}}) = \frac{\Sigma(\bar{a}_{\mathcal{H}})}{\frac{\mu(2\omega_{\circ}i)}{(1+\nu)}\Omega(\bar{a}_{\mathcal{H}}) - \big(w(0) + w(2\bar{a}_{\mathcal{H}})\big)}$$

and we have used $(1+\nu)|u'_{\mathcal{H}}| = \Omega(\bar{a}_{\mathcal{H}})$. Hence, we arrive at the solution

$$\boldsymbol{h}_{20}(x) = \begin{pmatrix} d(x) \\ \frac{\nu\, d(x)}{\nu + 2\omega_{\circ}i} \end{pmatrix}, \qquad d(x) = \frac{1}{\mu(2\omega_{\circ}i)}\Big(\mathcal{D}(\bar{a}_{\mathcal{H}})\Big[w(x-\bar{a}_{\mathcal{H}}) + w(x+\bar{a}_{\mathcal{H}})\Big] + \Sigma(x)\Big).$$

Similarly, it can be shown that $d(x)$ is even-symmetric in x and

$$d(\bar{a}_{\mathcal{H}}) = \frac{\Sigma(\bar{a}_{\mathcal{H}})\,\Omega(\bar{a}_{\mathcal{H}})}{\mu(2\omega_{\circ}i)\,\Omega(\bar{a}_{\mathcal{H}}) - {}_{(1+\nu)}\Big(w(0) + w(2\bar{a}_{\mathcal{H}})\Big)}, \tag{C.9}$$

$$d'(\bar{a}_{\mathcal{H}}) = \frac{1}{\mu(2\omega_{\circ}i)}\left[\frac{\Sigma(\bar{a}_{\mathcal{H}})\,w'(2\bar{a}_{\mathcal{H}})}{\frac{\mu(2\omega_{\circ}i)}{(1+\nu)}\Omega(\bar{a}_{\mathcal{H}}) - \big(w(0) + w(2\bar{a}_{\mathcal{H}})\big)} + \Sigma'(\bar{a}_{\mathcal{H}})\right] \tag{C.10}$$

and, in the case $\Omega = \Omega_{+}$, simplifies to

$$d_{+}(\bar{a}_{\mathcal{H}}) = \left[\frac{\Sigma_{+}(\bar{a}_{\mathcal{H}})}{\mu(2\omega_{\circ}i) - (1+\nu)}\right]. \qquad \blacksquare$$

C.2. Inner products involving the solutions $\boldsymbol{h}_{11}$ and $\boldsymbol{h}_{20}$. In this appendix, we calculate first the functions $\Xi^{c}(x)$ and $\Xi^{d}(x)$ and subsequently the inner products $\big\langle \boldsymbol{y}, \mathrm{B}_{\mathcal{H}}(\bar{\boldsymbol{v}}, \boldsymbol{h}_{11})\big\rangle$ and $\big\langle \boldsymbol{y}, \mathrm{B}_{\mathcal{H}}(\bar{\boldsymbol{v}}, \boldsymbol{h}_{20})\big\rangle$. The superscripts ^{c} and ^{d} correspond to the functions $c(x)$ and $d(x)$, which form the solutions $\boldsymbol{h}_{11}(x)$ and $\boldsymbol{h}_{20}(x)$ respectively, in Appendix C.1.

Calculation of $\Xi^c(x)$ and $\langle \boldsymbol{y}, \mathrm{B}_{\mathcal{H}}(\bar{\boldsymbol{v}}, \boldsymbol{h}_{11})\rangle$. A third order term in (3.36) involves

$$\mathrm{B}_{\mathcal{H}}\big(\boldsymbol{v}, \boldsymbol{h}_{11}\big)(x) = \begin{pmatrix} 1 \\ 0 \end{pmatrix} \Xi^c(x),$$

where $\boldsymbol{h}_{11}(x) = \big(c(x), c(x)\big)^{\mathrm{T}}$. We can express $\Xi^c(x)$ from (3.15) as follows using symmetry conditions and the relation $[w(x-\bar{a}_{\mathcal{H}}) \pm w(x+\bar{a}_{\mathcal{H}})] = \Omega_{\pm}(x)$:

$$\begin{aligned}\Xi^c(x) &= \int_{\mathbb{R}} \left[\frac{\delta(y-\bar{a}_{\mathcal{H}})}{|\mathcal{U}'_{\mathcal{H}}|} + \frac{\delta(y+\bar{a}_{\mathcal{H}})}{|-\mathcal{U}'_{\mathcal{H}}|}\right] \cdot \frac{\partial}{\partial y}\left[-\frac{w(x-y)}{\mathcal{U}'_{\mathcal{H}}(y)}\,\Omega(y)\,c(y)\right] dy \\ &= \frac{c(\bar{a}_{\mathcal{H}})\,\Omega(\bar{a}_{\mathcal{H}})}{|\mathcal{U}'_{\mathcal{H}}|^2}\,\Pi(x) + \left[\frac{c(\bar{a}_{\mathcal{H}})\Omega'(\bar{a}_{\mathcal{H}}) + c'(\bar{a}_{\mathcal{H}})\Omega(\bar{a}_{\mathcal{H}})}{|\mathcal{U}'_{\mathcal{H}}|^2} + \frac{c(\bar{a}_{\mathcal{H}})\,\Omega(\bar{a}_{\mathcal{H}})\,\mathcal{U}''_{\mathcal{H}}}{|\mathcal{U}'_{\mathcal{H}}|^3}\right]\Omega(x),\end{aligned}$$

where $\Pi_{\pm}(x) = -w'(x-\bar{a}_{\mathcal{H}}) \pm w'(x+\bar{a}_{\mathcal{H}})$.

In the *sum mode* case $\Omega = \Omega_+$, the function $\Xi^c_+(x)$ is even-symmetric and

$$\Xi^c_+(\bar{a}_{\mathcal{H}}) \;=\; \Big[+2\,(1{+}\nu)^2\,w'(2\bar{a}_{\mathcal{H}}) + (1{+}\nu)^3\,\mathcal{U}''_{\mathcal{H}}\Big]\frac{c_+(\bar{a}_{\mathcal{H}})}{\Omega_+(\bar{a}_{\mathcal{H}})} + (1{+}\nu)^2\,c'_+(\bar{a}_{\mathcal{H}}).$$

In the *difference mode* case $\Omega = \Omega_-$, the function $\Xi^c_-(x)$ is odd-symmetric and

$$\Xi^c_-(\bar{a}_{\mathcal{H}}) = \Big[-2\,(1{+}\nu)^2\,w'(2\bar{a}_{\mathcal{H}}) + (1{+}\nu)^3\,\mathcal{U}''_{\mathcal{H}}\Big]\frac{c_-(\bar{a}_{\mathcal{H}})}{\Omega_-(\bar{a}_{\mathcal{H}})} + (1{+}\nu)^2\,c'_-(\bar{a}_{\mathcal{H}}),$$

and we have the inner product

$$\Big\langle \boldsymbol{y}, \mathrm{B}_{\mathcal{H}}\big(\boldsymbol{v}, \boldsymbol{h}_{11}\big)\Big\rangle = \int_{\mathbb{R}} \Delta_{\pm}(x)\,\Xi^c_{\pm}(x)\,dx \;=\; 2\,\Xi^c_{\pm}(\bar{a}_{\mathcal{H}}).$$

The quantities $c\,(\bar{a}_{\mathcal{H}})$ and $c'(\bar{a}_{\mathcal{H}})$ are given in (C.7) and (C.8). ■

Calculation of $\Xi^d(x)$ and $\langle \boldsymbol{y}, \mathrm{B}_{\mathcal{H}}(\bar{\boldsymbol{v}}, \boldsymbol{h}_{20})\rangle$. A third order term in (3.36) involves

$$\mathrm{B}_{\mathcal{H}}\big(\bar{\boldsymbol{v}}, \boldsymbol{h}_{20}\big)(x) = \begin{pmatrix} 1 \\ 0 \end{pmatrix} \Xi^d(x),$$

where $\boldsymbol{h}_{20}(x) = \big(d(x), \frac{\nu\,d(x)}{\nu + 2\omega_o i}\big)^{\mathrm{T}}$. Analogously, from (3.15) using symmetry conditions

$$\begin{aligned}\Xi^d(x) &= \int_{\mathbb{R}} \left[\frac{\delta(y-\bar{a}_{\mathcal{H}})}{|\mathcal{U}'_{\mathcal{H}}|} + \frac{\delta(y+\bar{a}_{\mathcal{H}})}{|-\mathcal{U}'_{\mathcal{H}}|}\right] \cdot \frac{\partial}{\partial y}\left[-\frac{w(x-y)}{\mathcal{U}'_{\mathcal{H}}(y)}\,\Omega(y)\,d(y)\right] dy \\ &= \frac{d(\bar{a}_{\mathcal{H}})\,\Omega(\bar{a}_{\mathcal{H}})}{|\mathcal{U}'_{\mathcal{H}}|^2}\,\Pi(x) + \left[\frac{d(\bar{a}_{\mathcal{H}})\,\Omega'(\bar{a}_{\mathcal{H}}) + d'(\bar{a}_{\mathcal{H}})\,\Omega(\bar{a}_{\mathcal{H}})}{|\mathcal{U}'_{\mathcal{H}}|^2} + \frac{d(\bar{a}_{\mathcal{H}})\,\Omega(\bar{a}_{\mathcal{H}})\,\mathcal{U}''_{\mathcal{H}}}{|\mathcal{U}'_{\mathcal{H}}|^3}\right]\Omega(x),\end{aligned}$$

where $\Pi_{\pm}(x) = -w'(x-\bar{a}_{\mathcal{H}}) \pm w'(x+\bar{a}_{\mathcal{H}})$.

In the *sum mode* case $\Omega = \Omega_+$, the function $\Xi^d_+(\bar{a}_{\mathcal{H}})$ is even-symmetric and

$$\Xi^d_+(\bar{a}_{\mathcal{H}}) \;=\; \Big[+2\,(1{+}\nu)^2\,w'(2\bar{a}_{\mathcal{H}}) + (1{+}\nu)^3\,\mathcal{U}''_{\mathcal{H}}\Big]\frac{d_+(\bar{a}_{\mathcal{H}})}{\Omega_+(\bar{a}_{\mathcal{H}})} + (1{+}\nu)^2\,d'_+(\bar{a}_{\mathcal{H}}).$$

In the *difference mode* case $\Omega = \Omega_-$, the function $\Xi^d_-(\bar a_{\mathcal{H}})$ is odd-symmetric and

$$\Xi^d_-(\bar a_{\mathcal{H}}) = \Big[-2\,(1{+}\nu)^2\, w'(2\bar a_{\mathcal{H}}) + (1{+}\nu)^3\, \mathfrak{U}''_{\mathcal{H}} \Big] \frac{d_-(\bar a_{\mathcal{H}})}{\Omega_-(\bar a_{\mathcal{H}})} + (1{+}\nu)^2\, d'_-(\bar a_{\mathcal{H}}),$$

and we have the inner product

$$\Big\langle \boldsymbol{y}, \mathrm{B}_{\mathcal{H}}\big(\bar{\boldsymbol{v}}, \boldsymbol{h}_{20}\big) \Big\rangle = \int_{\mathbb{R}} \Delta_\pm(x)\, \Xi^d_\pm(x)\, dx \;=\; 2\, \Xi^d_\pm(\bar a_{\mathcal{H}}).$$

The quantities $d(\bar a_{\mathcal{H}})$ and $d'(\bar a_{\mathcal{H}})$ are given in (C.9) and (C.10). ■

C.3. Reduction of the coefficient $c_1(0)$. This final section serves (i) to show how the coefficient $c_1(0)$ in section 3.4 reduces to $\mathfrak{X}$ in section 3.3 and (ii) to provide the solutions $\boldsymbol{w}_{20}(x)$ and $\boldsymbol{w}_{11}(x)$ of the center manifold equations (3.32):

$$-\mathcal{M}_{\mathcal{H}} \boldsymbol{w}_{11} = \mathrm{H}_{11}, \qquad\qquad \big(2\omega_\circ i\mathrm{I} - \mathcal{M}_{\mathcal{H}}\big)\boldsymbol{w}_{20} = \mathrm{H}_{20},$$

where H_{11} and H_{20} are given by

$$\begin{aligned} \mathrm{H}_{11}(x) &= \mathrm{B}_{\mathcal{H}}(\boldsymbol{v}, \bar{\boldsymbol{v}})(x) \;-\; \big\langle \boldsymbol{y}, \mathrm{B}_{\mathcal{H}}\big(\boldsymbol{v}, \bar{\boldsymbol{v}}\big)\big\rangle\, \boldsymbol{v}(x) \;-\; \big\langle \bar{\boldsymbol{y}}, \mathrm{B}_{\mathcal{H}}\big(\boldsymbol{v}, \bar{\boldsymbol{v}}\big)\big\rangle\, \bar{\boldsymbol{v}}(x), \\ \mathrm{H}_{20}(x) &= \mathrm{B}_{\mathcal{H}}(\boldsymbol{v}, \boldsymbol{v})(x) \;-\; \big\langle \boldsymbol{y}, \mathrm{B}_{\mathcal{H}}\big(\boldsymbol{v}, \boldsymbol{v}\big)\big\rangle\, \boldsymbol{v}(x) \;-\; \big\langle \bar{\boldsymbol{y}}, \mathrm{B}_{\mathcal{H}}\big(\boldsymbol{v}, \boldsymbol{v}\big)\big\rangle\, \bar{\boldsymbol{v}}(x). \end{aligned}$$

Since $\boldsymbol{h}_{11}(x)$ solves $-\mathcal{M}_{\mathcal{H}}\boldsymbol{h}_{11} = \mathrm{B}_{\mathcal{H}}(\boldsymbol{v}, \bar{\boldsymbol{v}})$ (see Appendix C.2) and since $\boldsymbol{v}$ and $\bar{\boldsymbol{v}}$ are eigenvectors of $\mathcal{M}_{\mathcal{H}}$, it can be shown that the solution $\boldsymbol{w}_{11}(x)$ is given by

$$\boldsymbol{w}_{11}(x) = \boldsymbol{h}_{11}(x) \;-\; \frac{i}{\omega_\circ}\Big(\big\langle \boldsymbol{y}, \mathrm{B}_{\mathcal{H}}(\boldsymbol{v}, \bar{\boldsymbol{v}})\big\rangle\, \boldsymbol{v}(x) - \big\langle \bar{\boldsymbol{y}}, \mathrm{B}_{\mathcal{H}}(\boldsymbol{v}, \bar{\boldsymbol{v}})\big\rangle\, \bar{\boldsymbol{v}}(x) \Big).$$

Analogously, $\boldsymbol{h}_{20}(x)$ solves $\big(2\omega_\circ i\mathrm{I} - \mathcal{M}_{\mathcal{H}}\big)\boldsymbol{h}_{20} = \mathrm{B}_{\mathcal{H}}(\boldsymbol{v}, \boldsymbol{v})$, and it can also be shown that

$$\boldsymbol{w}_{20}(x) = \boldsymbol{h}_{20}(x) \;+\; \frac{i}{\omega_\circ}\Big(\big\langle \boldsymbol{y}, \mathrm{B}_{\mathcal{H}}\big(\boldsymbol{v}, \boldsymbol{v}\big)\big\rangle\, \boldsymbol{v}(x) + \tfrac{1}{3}\big\langle \bar{\boldsymbol{y}}, \mathrm{B}_{\mathcal{H}}\big(\boldsymbol{v}, \boldsymbol{v}\big)\big\rangle\, \bar{\boldsymbol{v}}(x) \Big).$$

The inner products involving $\boldsymbol{w}_{11}(x)$ and $\boldsymbol{w}_{20}(x)$ are subsequently expressed as

$$\begin{aligned} \Big\langle \boldsymbol{y}, \mathrm{B}_{\mathcal{H}}\big(\boldsymbol{v}, \boldsymbol{w}_{11}\big)\Big\rangle &= \Big\langle \boldsymbol{y}, \mathrm{B}_{\mathcal{H}}\big(\boldsymbol{v}, \boldsymbol{h}_{11}\big)\Big\rangle - \frac{i}{\omega_\circ}\Big[\big\langle \boldsymbol{y}, \mathrm{B}_{\mathcal{H}}(\boldsymbol{v}, \bar{\boldsymbol{v}})\big\rangle \big\langle \boldsymbol{y}, \mathrm{B}_{\mathcal{H}}(\boldsymbol{v}, \boldsymbol{v})\big\rangle - \big\langle \bar{\boldsymbol{y}}, \mathrm{B}_{\mathcal{H}}(\boldsymbol{v}, \bar{\boldsymbol{v}})\big\rangle \big\langle \boldsymbol{y}, \mathrm{B}_{\mathcal{H}}(\boldsymbol{v}, \bar{\boldsymbol{v}})\big\rangle \Big] \\ &= \Big\langle \boldsymbol{y}, \mathrm{B}_{\mathcal{H}}\big(\boldsymbol{v}, \boldsymbol{h}_{11}\big)\Big\rangle - \frac{i}{\omega_\circ}\Big[R_{11}\, R_{20} - \big|R_{11}\big|^2 \Big], \end{aligned} \tag{C.11}$$

$$\begin{aligned} \Big\langle \boldsymbol{y}, \mathrm{B}_{\mathcal{H}}\big(\bar{\boldsymbol{v}}, \boldsymbol{w}_{20}\big)\Big\rangle &= \Big\langle \boldsymbol{y}, \mathrm{B}_{\mathcal{H}}\big(\bar{\boldsymbol{v}}, \boldsymbol{h}_{20}\big)\Big\rangle + \frac{i}{\omega_\circ}\Big[\big\langle \boldsymbol{y}, \mathrm{B}_{\mathcal{H}}(\boldsymbol{v}, \boldsymbol{v})\big\rangle \big\langle \boldsymbol{y}, \mathrm{B}_{\mathcal{H}}(\bar{\boldsymbol{v}}, \boldsymbol{v})\big\rangle + \tfrac{1}{3}\big\langle \bar{\boldsymbol{y}}, \mathrm{B}_{\mathcal{H}}(\boldsymbol{v}, \boldsymbol{v})\big\rangle \big\langle \boldsymbol{y}, \mathrm{B}_{\mathcal{H}}(\bar{\boldsymbol{v}}, \bar{\boldsymbol{v}})\big\rangle \Big] \\ &= \Big\langle \boldsymbol{y}, \mathrm{B}_{\mathcal{H}}\big(\bar{\boldsymbol{v}}, \boldsymbol{h}_{20}\big)\Big\rangle - \frac{i}{\omega_\circ}\Big[-R_{20}\, R_{11} - \tfrac{1}{3}\big|R_{20}\big|^2 \Big], \end{aligned} \tag{C.12}$$

where $R_{20} = \langle \boldsymbol{y}, \mathrm{B}_{\mathcal{H}}(\boldsymbol{v},\boldsymbol{v})\rangle$ and $R_{11} = \langle \boldsymbol{y}, \mathrm{B}_{\mathcal{H}}(\boldsymbol{v},\bar{\boldsymbol{v}})\rangle$ were defined in (3.29). Then substituting (C.12) and (C.11) into (3.33), we can then express $R_{21}^{\circledast}$ as

$$\begin{aligned} R_{21}^{\circledast} &= \Big\langle \boldsymbol{y}, \mathrm{C}_{\mathcal{H}}(\boldsymbol{v},\boldsymbol{v},\bar{\boldsymbol{v}})\Big\rangle + 2\Big\langle \boldsymbol{y}, \mathrm{B}_{\mathcal{H}}\big(\boldsymbol{v},\boldsymbol{w}_{11}\big)\Big\rangle + \Big\langle \boldsymbol{y}, \mathrm{B}_{\mathcal{H}}\big(\bar{\boldsymbol{v}},\boldsymbol{w}_{20}\big)\Big\rangle \\ &= \Big\langle \boldsymbol{y}, \mathrm{C}_{\mathcal{H}}(\boldsymbol{v},\boldsymbol{v},\bar{\boldsymbol{v}})\Big\rangle + 2\Big\langle \boldsymbol{y}, \mathrm{B}_{\mathcal{H}}\big(\boldsymbol{v},\boldsymbol{h}_{11}\big)\Big\rangle + \Big\langle \boldsymbol{y}, \mathrm{B}_{\mathcal{H}}\big(\bar{\boldsymbol{v}},\boldsymbol{h}_{20}\big)\Big\rangle \\ &\quad - \frac{i}{\omega_\circ}\Big[R_{20}\,R_{11} - 2\big|R_{11}\big|^2 - \tfrac{1}{3}\big|R_{20}\big|^2\Big]. \end{aligned}$$

It follows immediately that

$$\begin{aligned} c_1(0) &= \tfrac{1}{2}\,R_{21}^{\circledast} + \frac{i}{2\omega_\circ}\Big(R_{20}R_{11} - 2\big|R_{11}\big|^2 - \tfrac{1}{3}\big|R_{20}\big|^2\Big) \\ &= \tfrac{1}{2}\Big[\Big\langle \boldsymbol{y}, \mathrm{C}_{\mathcal{H}}(\boldsymbol{v},\boldsymbol{v},\bar{\boldsymbol{v}})\Big\rangle + 2\Big\langle \boldsymbol{y}, \mathrm{B}_{\mathcal{H}}\big(\boldsymbol{v},\boldsymbol{h}_{11}\big)\Big\rangle + \Big\langle \boldsymbol{y}, \mathrm{B}_{\mathcal{H}}\big(\bar{\boldsymbol{v}},\boldsymbol{h}_{20}\big)\Big\rangle\Big] = \mathfrak{X}. \end{aligned} \tag{C.13}$$

This shows that the coefficients $c_1(0)$ in section 3.4 and $\mathfrak{X}$ in section 3.3 are identical. ∎

Appendix D. Nullspace of $\big(\mathcal{N}_{\mathcal{H}}^{*} - (1+\nu)\mathbf{I}\big)$. We now demonstrate how to use the method of Fourier transforms to solve (3.14), which we repeat here:

$$(1+\nu)\Delta(x) = \mathcal{N}_{\mathcal{H}}^{*}\Delta(x). \tag{D.1}$$

Recall that the operator $\mathcal{N}_{\mathcal{H}}^{*}$ is defined in the sense of distributions:

$$\mathcal{N}_{\mathcal{H}}^{*}\varphi(x) = \left(\frac{\delta(x-\bar{a}_{\mathcal{H}})}{|u_{\mathcal{H}}'|} + \frac{\delta(x+\bar{a}_{\mathcal{H}})}{|-u_{\mathcal{H}}'|}\right)\int_{\mathbb{R}} w(x-y)\,\varphi(y)\,dy.$$

For simplicity, define

$$f(x) = \delta(x-\bar{a}_{\mathcal{H}}) + \delta(x+\bar{a}_{\mathcal{H}}), \qquad g(x) = \big(w*\varphi\big)(x) = \int_{\mathbb{R}} w(x-y)\,\varphi(y)\,dy,$$

and define the following notation for the Fourier transform of $u(x)$ in the variable ξ:

$$\hat{u}(\xi) \equiv \mathcal{F}\big[u(x)\big](\xi).$$

Since the Fourier transforms of f and g are

$$\begin{aligned} \hat{f}(\xi) &\equiv \mathcal{F}\big[\delta(x-\bar{a}_{\mathcal{H}}) + \delta(x+\bar{a}_{\mathcal{H}})\big](\xi) = \tfrac{1}{\sqrt{2\pi}}\big(e^{i\xi\bar{a}_{\mathcal{H}}} + e^{-i\xi\bar{a}_{\mathcal{H}}}\big), \\ \hat{g}(\xi) &\equiv \mathcal{F}\big[(w*\Delta)(x)\big](\xi) = \hat{w}(\xi)\,\hat{\Delta}(\xi), \end{aligned}$$

respectively, applying the Fourier transform to both sides of (D.1) yields

$$(1+\nu)|u_{\mathcal{H}}'|\hat{\Delta}(\xi) = \mathcal{F}\big[f(x)\,g(x)\big](\xi) = \frac{1}{\sqrt{2\pi}}\int_{\mathbb{R}}\Big(e^{i(\xi-\eta)\bar{a}_{\mathcal{H}}} + e^{-i(\xi-\eta)\bar{a}_{\mathcal{H}}}\Big)\hat{w}(\eta)\hat{\Delta}(\eta)d\eta.$$

Defining $\gamma = (1+\nu)\,|u'_{\mathcal{H}}|$, this reduces to the following equation for $\hat{\Delta}(\xi)$:

$$\gamma\,\hat{\Delta}(\xi) \;=\; \sqrt{\frac{2}{\pi}}\int_{\mathbb{R}} \cos\big(\bar{a}_{\mathcal{H}}(\xi-\eta)\big)\,\hat{w}(\eta)\,\hat{\Delta}(\eta)\,d\eta.$$

Expanding the cosine results in

$$\begin{aligned}\gamma\sqrt{\frac{\pi}{2}}\,\hat{\Delta}(\xi) =& \left[\int_{\mathbb{R}} \sin\big(\bar{a}_{\mathcal{H}}\eta\big)\,\hat{w}(\eta)\,\hat{\Delta}(\eta)\,d\eta\right]\sin\big(\bar{a}_{\mathcal{H}}\xi\big)\\ &+\left[\int_{\mathbb{R}} \cos\big(\bar{a}_{\mathcal{H}}\eta\big)\,\hat{w}(\eta)\,\hat{\Delta}(\eta)\,d\eta\right]\cos\big(\bar{a}_{\mathcal{H}}\xi\big),\end{aligned} \tag{D.2}$$

which suggests that solutions may be expressed as

$$\hat{\Delta}(\xi) \;=\; C_1\sin\big(\bar{a}_{\mathcal{H}}\xi\big) + C_2\cos\big(\bar{a}_{\mathcal{H}}\xi\big).$$

Case: $\hat{\Delta}(\xi) = \sin\big(\bar{a}_{\mathcal{H}}\xi\big)$. Substituting $\hat{\Delta}(x) = \sin\big(\bar{a}_{\mathcal{H}}\xi\big)$ into (D.2) and using the fact that the Fourier transform $\hat{w}(\xi)$ is even (since $w(x)$ is even), we find that

$$\left(\int_{\mathbb{R}} \sin\big(\bar{a}_{\mathcal{H}}\eta\big)\,\sin\big(\bar{a}_{\mathcal{H}}\eta\big)\,\hat{w}(\eta)\,d\eta\right)\sin\big(\bar{a}_{\mathcal{H}}\xi\big) \;=\; \gamma\sqrt{\frac{\pi}{2}}\,\sin\big(\bar{a}_{\mathcal{H}}\xi\big),$$

assuming the integrals converge. The above equation is satisfied when

$$\sqrt{\frac{2}{\pi}}\int_{\mathbb{R}} \sin^2\big(\bar{a}_{\mathcal{H}}\eta\big)\,\hat{w}(\eta)\,d\eta \;=\; \gamma \;\equiv\; (1+\nu)\,|u'_{\mathcal{H}}|. \tag{D.3}$$

To determine which mode this solution corresponds to, we compute

$$\begin{aligned}\sqrt{\frac{2}{\pi}}\int_{\mathbb{R}}\sin^2\big(\bar{a}_{\mathcal{H}}\eta\big)\hat{w}(\eta)\,d\eta \;&=\; \sqrt{\frac{2}{\pi}}\int_{-\infty}^{\infty}\sin^2\big(\bar{a}_{\mathcal{H}}\eta\big)\left(\frac{1}{\sqrt{2\pi}}\int_{-\infty}^{\infty}e^{i\eta x}w(x)\,dx\right)d\eta\\ &=\; \sqrt{\frac{2}{\pi}}\int_{-\infty}^{\infty}w(x)\left(\frac{1}{\sqrt{2\pi}}\int_{-\infty}^{\infty}e^{i\eta x}\sin^2\big(\bar{a}_{\mathcal{H}}\eta\big)\,d\eta\right)dx\\ &=\; \sqrt{\frac{2}{\pi}}\int_{-\infty}^{\infty}w(x)\,\mathcal{F}^{-1}\Big[\sin^2(\bar{a}_{\mathcal{H}}\eta)\Big](x)\,dx\\ &=\; \sqrt{\frac{2}{\pi}}\int_{-\infty}^{\infty}w(x)\,\mathcal{F}^{-1}\left[\frac{1-\cos(2\bar{a}_{\mathcal{H}}\eta)}{2}\right](x)\,dx\\ &=\; \sqrt{\frac{1}{2\pi}}\int_{-\infty}^{\infty}w(x)\left(\sqrt{2\pi}\,\delta(x)-\sqrt{\frac{\pi}{2}}\Big(\delta(x-2\bar{a}_{\mathcal{H}})+\delta(x+2\bar{a}_{\mathcal{H}})\Big)\right)dx\\ &=\; \sqrt{\frac{1}{2\pi}}\left(\sqrt{2\pi}w(0)-\sqrt{\frac{\pi}{2}}\Big(w(2\bar{a}_{\mathcal{H}})+w(-2\bar{a}_{\mathcal{H}})\Big)\right)\\ &=\; w(0)-w(2\bar{a}_{\mathcal{H}}) \;\equiv\; \Omega_-(\bar{a}_{\mathcal{H}}) \qquad \big(\text{DIFFERENCE MODE } \Omega_-\big)\end{aligned}$$

since w is even. Condition (D.3) is therefore satisfied when the *difference mode* $\Omega_-(x)$ becomes critical, since (3.7) and (3.8) imply that

$$(1+\nu)|\mathfrak{u}'_{\mathcal{H}}| = \Omega_-(\bar{a}_{\mathcal{H}}) = w(0) - w(2\bar{a}_{\mathcal{H}}).$$

Case: $\hat{\Delta}(x) = \cos\big(\bar{a}_{\mathcal{H}}\xi\big)$. Substituting $\hat{\Delta}(\xi) = \cos\big(\bar{a}_{\mathcal{H}}\xi\big)$ into (D.2) results in

$$\sqrt{\frac{2}{\pi}}\int_{\mathbb{R}} \cos^2\big(\bar{a}_{\mathcal{H}}\eta\big)\,\hat{w}(\eta)\,d\eta \;=\; \gamma \;\equiv\; (1+\nu)\,|\mathfrak{u}'_{\mathcal{H}}|. \tag{D.4}$$

Following a similar calculation, it can be shown that

$$\sqrt{\frac{2}{\pi}}\int_{\mathbb{R}} \cos^2\big(\bar{a}_{\mathcal{H}}\eta\big)\,\hat{w}(\eta)\,d\eta \;=\; w(0) + w(2\bar{a}_{\mathcal{H}}) \;\equiv\; \Omega_+(\bar{a}_{\mathcal{H}}), \qquad \big(\text{SUM MODE } \Omega_+\big)$$

indicating that condition (D.4) is satisfied when the *sum mode* goes critical, since (3.6) and (3.8) imply that

$$(1+\nu)|\mathfrak{u}'_{\mathcal{H}}| = \Omega_+(\bar{a}_{\mathcal{H}}) = w(0) + w(2\bar{a}_{\mathcal{H}}).$$

Summary. $\hat{\Delta}(\xi) = \cos(\bar{a}_{\mathcal{H}}\xi)$ is the only solution of (D.1) when the *sum mode* $\Omega_+(x) = w(x-\bar{a}_{\mathcal{H}}) + w(x-\bar{a}_{\mathcal{H}})$ goes critical. The inverse Fourier transform reveals

$$\Delta(x) \;= \Delta_+(x) \;=\; C_2\,\mathcal{F}^{-1}\big[\cos(\bar{a}_{\mathcal{H}}\xi)\big](x) \;=\; C_2\sqrt{\frac{\pi}{2}}\Big(\delta(x-\bar{a}_{\mathcal{H}}) + \delta(x+\bar{a}_{\mathcal{H}})\Big).$$

Conversely, $\hat{\Delta}(\xi) = \sin(\bar{a}_{\mathcal{H}}\xi)$ is the only solution of (D.1) when the *difference mode* $\Omega_-(x) = w(x-\bar{a}_{\mathcal{H}}) - w(x-\bar{a}_{\mathcal{H}})$ goes critical, and similarly

$$\Delta(x) \;= \Delta_-(x) \;=\; C_1\,\mathcal{F}^{-1}\big[\sin(\bar{a}_{\mathcal{H}}\xi)\big](x) \;=\; C_1\sqrt{\frac{\pi}{2}}\Big(\delta(x-\bar{a}_{\mathcal{H}}) - \delta(x+\bar{a}_{\mathcal{H}})\Big).$$

Since only the nullspace of the operator $\mathcal{N}^*_{\mathcal{H}}$ is of interest, we ignore the coefficients.

Appendix E. Higher order derivatives of $\delta\big(h(x)\big)$. For the cases $n = 1, 2$, we evaluate the following integral in a formal manner using integration-by-parts:

$$\int_{\mathbb{R}} \delta^{(n)}\big(h(x)\big)\,f(x)\,dx \qquad \text{for } n = 1, 2.$$

Suppose f, h are sufficiently smooth functions on $\mathbb{R}$, note that h here differs from h in

Appendix B) and suppose that h has N isolated simple zeros ($h(a_k) = 0$) ordered as a_k, $k = 1, \ldots, N$, at which $h'(a_k) \neq 0$.

$$\begin{aligned}
\int_{-\infty}^{\infty} \delta'\big(h(x)\big)\, f(x)\, dx &= \int_{-\infty}^{\infty} \delta'\big(h(x)\big)\, \frac{h'(x)}{h'(x)}\, f(x)\, dx = \int_{-\infty}^{\infty} \frac{d}{dx}\Big(\delta\big(h(x)\big)\Big)\, \frac{f(x)}{h'(x)}\, dx \\
&= -\int_{-\infty}^{\infty} \delta\big(h(x)\big)\, \frac{d}{dx}\left[\frac{f(x)}{h'(x)}\right] dx \\
&= \boxed{-\sum_{k=1}^{N} \frac{1}{\big|h'(\alpha_k)\big|} \cdot \frac{d}{dx}\left[\frac{f(x)}{h'(x)}\right]\Bigg|_{x=\alpha_k}} \qquad \text{(compact form)} \\
&= -\sum_{k=1}^{N} \frac{f'(\alpha_k)h'(\alpha_k) - f(\alpha_k)h''(\alpha_k)}{\big|h'(\alpha_k)\big|^3}, \qquad \text{(E.1)}
\end{aligned}$$

$$\begin{aligned}
\int_{-\infty}^{\infty} \delta''\big(h(x)\big)\, f(x)\, dx &= \int_{-\infty}^{\infty} \delta''\big(h(x)\big) \frac{h'(x)}{h'(x)}\, f(x)\, dx = \int_{-\infty}^{\infty} \frac{d}{dx}\Big(\delta'\big(h(x)\big)\Big) \cdot \frac{f(x)}{h'(x)}\, dx \\
&= -\int_{-\infty}^{\infty} \delta'\big(h(x)\big) \cdot \frac{d}{dx}\left[\frac{f(x)}{h'(x)}\right] dx \\
&= -\int_{-\infty}^{\infty} \frac{d}{dx}\Big(\delta\big(h(x)\big)\Big) \cdot \frac{1}{h'(x)} \frac{d}{dx}\left[\frac{f(x)}{h'(x)}\right] dx \\
&= \int_{-\infty}^{\infty} \delta\big(h(x)\big) \cdot \frac{d}{dx}\left[\frac{1}{h'(x)} \frac{d}{dx}\left[\frac{f(x)}{h'(x)}\right]\right] dx \\
&= \boxed{\sum_{k=1}^{N} \frac{1}{\big|h'(\alpha_k)\big|} \cdot \frac{d}{dx}\left[\frac{1}{h'(x)} \frac{d}{dx}\left[\frac{f(x)}{h'(x)}\right]\right]\Bigg|_{x=\alpha_k}} \\
&= \sum_{k=1}^{N} \frac{1}{\big|h'(\alpha_k)\big|^5} \Bigg\{ 3h''(\alpha_k)\Big[f(\alpha_k)h''(\alpha_k) - f'(\alpha_k)h'(\alpha_k)\Big] \\
&\qquad + h'(\alpha_k)\Big[f''(\alpha_k)h'(\alpha_k) - f(\alpha_k)h'''(\alpha_k)\Big] \Bigg\}. \qquad \text{(E.2)}
\end{aligned}$$

The proof of the above result (which has been omitted for simplicity) uses the implicit function theorem and $x = h^{-1}(y)$ to reexpress the integral in terms of y. The absolute value in the denominator in (E.1) and (E.2) is due to the change in sign of the integral depending on whether h is increasing or decreasing in a neighborhood of each α_k.

Acknowledgments. The author would like to thank P. C. Bressloff, T. Kaper, and C. E. Wayne for many valuable discussions. The author would also like to thank the referees for providing helpful comments and suggestions.

REFERENCES

[1] S. Amari, *Dynamics of pattern formation in lateral inhibition type neural fields*, Biol. Cybernet., 27 (1977), pp. 77–87.

[2] A. Andronov, *Sur les cycles limites de Poincaré et la théorie des oscillations autoentretenues*, Note in the Comptes Rendues de l'Acad. des Sci.. presented by J. Hadamard, Oct. 14, 1929.

[3] A. Angelucci, J. B. Levitt, E. J. S. Walton, J-M. Hupé, J. Bullier, and J. S. Lund, *Circuits for local and global signal integration in primary visual cortex*, J. Neurosci., 22 (2002), pp. 8633–8646.

[4] F. M. Atay and A. Hutt, *Stability and bifurcations in neural fields with finite propagation speed and general connectivity*, SIAM J. Appl. Math., 65 (2005), pp. 644–666.

[5] F. M. Atay and A. Hutt, *Neural fields with distributed transmission speeds and long-range feedback delays*, SIAM J. Appl. Dyn. Syst., 5 (2006), pp. 670–698.

[6] P. W. Bates and C. K. R. T. Jones, *Invariant manifolds for semilinear partial differential equations*, Dynamics Reported, 2 (1989), pp. 1–39.

[7] P. Blomquist, J. Wyller, and G. T. Einevoll, *Localized activity patterns in two-population neuronal networks*, Phys. D, 206 (2005), pp. 180–212.

[8] P. C. Bressloff, *Pattern formation in visual cortex*, in Les Houches 2003: Methods and Models in Neurophysics, C. C. Chow, B. Gutkin, D. Hansel, C. Meunier, and J. Dalibard, eds., Elsevier, New York, 2005, pp. 477–574.

[9] P. C. Bressloff, *Weakly interacting pulses in synaptically coupled neural media*, SIAM J. Appl. Math., 66 (2005), pp. 57–81.

[10] P. C. Bressloff, *Spontaneous symmetry breaking in self-organizing neural fields*, Biol. Cybernet., 93 (2005), pp. 256–274.

[11] P. C. Bressloff, S. E. Folias, A. Pratt, and Y.-X. Li, *Oscillatory waves in inhomogeneous neural media*, Phys. Rev. Lett., 91 (2003), 178101.

[12] P. C. Bressloff and S. E. Folias, *Front bifurcations in an excitatory neural network*, SIAM J. Appl. Math., 65 (2004), pp. 131–151.

[13] P. C. Bressloff and Z. P. Kilpatrick, *Two-dimensional bumps in piecewise smooth neural fields with synaptic depression*, SIAM J. Appl. Math., 71 (2011), pp. 379–408.

[14] J. Carr, *Applications of Centre Manifold Theory*, Springer-Verlag, London, 1981.

[15] X. Chen, *Existence, uniqueness, and asymptotic stability of traveling waves in nonlocal evolution equations*, Adv. Differential Equations, 2 (1997), pp. 125–160.

[16] S. Coombes, *Waves, bumps, and patterns in neural field theories*, Biol. Cybernet., 93 (2005), pp. 91–108.

[17] S. Coombes and M. R. Owen, *Evans functions for integral neural field equations with Heaviside firing rate function*, SIAM J. Appl. Dyn. Syst., 3 (2004), pp. 574–600.

[18] S. Coombes and M. R. Owen, *Bumps, breathers, and waves in a neural network with spike frequency adaptation*, Phys. Rev. Lett., 94 (2005), 148102.

[19] S. Coombes and M. R. Owen, *Exotic dynamics in a firing rate model of neural tissue with threshold accommodation*, Fluids and Waves: Recent Trends in Applied Analysis, 440 (2007), pp. 123–144.

[20] S. Coombes, N. A. Venkov, L. Shiau, I. Bojak, D. T. J. Liley, and C. R. Laing, *Modeling electrocortical activity through improved local approximations of integral neural field equations*, Phys. Rev. E, 76 (2007), 051901.

[21] M. G. Crandall and P. H. Rabinowitz, *Hopf bifurcation theorem in infinite dimensions*, Arch. Ration. Mech. Anal., 67 (1977), pp. 53–72.

[22] R. Curtu and G. B. Ermentrout, *Pattern formation in a network of excitatory and inhibitory cells with adaptation*, SIAM J. Appl. Dyn. Syst., 3 (2004), pp. 191–231.

[23] W. Eckhaus, *Studies in Non-linear Stability Theory*, Springer Tracts in Natural Philosophy 6, Springer-Verlag, New York, 1965.

[24] M. Enculescu and M. Bestehorn, *Activity dynamics in nonlocal interacting neural fields*, Phys. Rev. E, 67 (2003), 041904.

[25] G. B. Ermentrout, *Neural networks as spatial pattern forming systems*, Rep. Progr. Phys., 61 (1998), pp. 353–430.

[26] G. B. Ermentrout and J. D. Cowan, *A mathematical theory of visual hallucination patterns*, Biol. Cybernet., 34 (1979), pp. 137–150.

[27] G. B. Ermentrout and J. B. Mcleod, *Existence and uniqueness of travelling waves for a neural network*, Proc. Roy. Soc. Edinburgh Sect. A, 123 (1993), pp. 461–478.
[28] G. B. Ermentrout, J. Z. Jalics, and J. E. Rubin, *Stimulus-driven traveling solutions in continuum neuronal models with a general smooth firing rate function*, SIAM J. Appl. Math., 70 (2010), pp. 3039–3064.
[29] R. Estrada and R. P. Kanwal, *Asymptotic Analysis: A Distributional Approach*, Birkhäuser Boston, Boston, 1994.
[30] O. Faugeras, F. Grimbert, and J.-J. Slotine, *Absolute stability and complete synchronization in a class of neural fields models*, SIAM J. Appl. Math., 69 (2008), pp. 205–250.
[31] O. Faugeras, R. Veltz, and F. Grimbert, *Persistent neural states: Stationary localized activity patterns in nonlinear continuous n-population, q-dimensional neural networks*, Neural Comput., 21 (2009), pp. 147–187.
[32] G. Faye and O. Faugeras, *Some theoretical and numerical results for delayed neural field equations*, Phys. D, 239 (2010), pp. 561–578.
[33] S. E. Folias and P. C. Bressloff, *Breathing pulses in an excitatory neural network*, SIAM J. Appl. Dyn. Syst., 3 (2004), pp. 378–407.
[34] S. E. Folias and P. C. Bressloff, *Stimulus-locked traveling waves and breathers in an excitatory neural network*, SIAM J. Appl. Math., 65 (2005), pp. 2067–2092.
[35] S. E. Folias and P. C. Bressloff, *Breathers in two-dimensional excitable neural media*, Phys. Rev. Lett., 95 (2005), 208107.
[36] S. E. Folias, *Spatially coherent oscillations in neural fields with inhibition and adaptation*, in preparation.
[37] M. Golubitsky and W. F. Langford, *Classification and unfoldings of degenerate Hopf bifurcations*, J. Differential Equations, 41 (1981), pp. 375–415.
[38] O. Gurel, *Bifurcations in nerve membrane dynamics*, Internat. J. Neurosci., 5 (1973), pp. 281–286.
[39] Y. Guo and C. C. Chow, *Existence and stability of standing pulses in neural networks:* I. *Existence*, SIAM J. Appl. Dyn. Syst., 4 (2005), pp. 217–248.
[40] Y. Guo and C. C. Chow, *Existence and stability of standing pulses in neural networks:* II. *Stability*, SIAM J. Appl. Dyn. Syst., 4 (2005), pp. 249–281.
[41] D. Hansel and H. Sompolinsky, *Modeling feature selectivity in local cortical circuits,* in Methods in Neuronal Modeling: From Ions to Networks, 2nd ed., C. Koch and I. Segev, eds., MIT Press, Cambridge, MA, 1998.
[42] B. D. Hassard, *Bifurcation of periodic solutions of the Hodgkin-Huxley model for the squid giant axon*, J. Theoret. Biol., 71 (1978), pp. 401–442.
[43] B. D. Hassard, N. D. Kazarinoff, and Y.-H. Wan, *Theory and Applications of Hopf Bifurcation,* London Mathematical Society Lecture Note Series 41, Cambridge University Press, New York, 1981.
[44] B. D. Hassard and Y.-H. Wan, *Bifurcation formulae derived from center manifold theory*, J. Math. Anal. Appl., 63 (1978), pp. 297–312.
[45] E. Hopf, *Abzweigung einer periodischen Losung von einer stationaren Losung eines Differentialsystems*, Ber. Verh. Saechs. Akad. Wiss. Leipzig, Math. Naturwiss., 94 (1942), pp. 3–22.
[46] L. N. Howard and N. Kopell, *Translation, with editorial comments, of E. Hopf's Abzeigung einer periodischen Losung von einer stationaren Losungeines Differential systems*, in The Hopf Bifurcation and its Applications, Appl. Math. Sci. 19, J. Marsden and M. McCracken, eds., Springer-Verlag, New York, 1978, pp. 163–205.
[47] I.-D. Hsü and N. D. Kazarinoff, *An applicable Hopf bifurcation formula and instability of small periodic solutions of the Field-Noyes model*, J. Math. Anal. Appl., 55 (1976), pp. 61–89.
[48] X. Huang, W. C. Troy, Q. Yang, H. Ma, C. Laing, S. J. Schiff, and J-Y. Wu, *Spiral waves in disinhibited mammalian cortex*, J. Neurosci., 24 (2004), pp. 9897–9902.
[49] A. Hutt, M. Bestehorn, and T. Wennekers, *Pattern formation in intracortical neuronal fields*, Network, 14 (2003), pp. 351–368.
[50] A. Hutt, *Local excitation-lateral inhibition interaction yields oscillatory instabilities in nonlocally interacting systems involving finite propagation delay*, Phys. Lett. A, 372 (2008), pp. 541–546.
[51] A. Hutt and N. Rougier, *Activity spread and breathers induced by finite transmission speeds in two-dimensional neural fields*, Phys. Rev. E, 82 (2010), 055701.

[52] M. A. P. Idiart and L. F. Abbott, *Propagation of excitation in neural network models*, Network, 4 (1993), pp. 285–294.
[53] D. D. Joseph and D. H. Sattinger, *Bifurcating time periodic solutions and their stability*, Arch. Ration. Mech. Anal., 45 (1972), pp. 79–109.
[54] T. Kato, *Perturbation Theory for Linear Operators*, Springer-Verlag, New York, 1966.
[55] Z. P. Kilpatrick and P. C. Bressloff, *Stability of bumps in piecewise smooth neural fields with nonlinear adaptation*, Phys. D, 239 (2010), pp. 1048–1060.
[56] Z. P. Kilpatrick and P. C. Bressloff, *Effects of synaptic depression and adaptation on spatio-temporal dynamics of an excitatory neuronal network*, Phys. D, 239 (2010), pp. 547–560.
[57] Z. P. Kilpatrick and P. C. Bressloff, *Spatially structured oscillations in a two-dimensional excitatory neuronal network with synaptic depression*, J. Comput. Neurosci., 28 (2010), pp. 193–209.
[58] Z. P. Kilpatrick, S. E. Folias, and P. C. Bressloff, *Traveling pulses and wave propagation failure in inhomogeneous neural media*, SIAM J. Appl. Dyn. Syst., 7 (2008), pp. 161–185.
[59] K. Kishimoto and S. Amari, *Existence and stability of local excitations in homogeneous neural fields*, J. Math. Biol., 7 (1979), pp. 303–318.
[60] S. Koga and Y. Kuramoto, *Localized patterns in reaction-diffusion systems*, Progr. Theoret. Phys., 63 (1980), pp. 106–121.
[61] Y. Kuramoto, *Chemical Oscillations, Waves, and Turbulence*, Dover, New York, 1984.
[62] Y. A. Kuznetsov, *Elements of Applied Bifurcation Theory*, 3rd ed., Springer-Verlag, Berlin, 2004.
[63] C. R. Laing, *Spiral waves in nonlocal equations*, SIAM J. Appl. Dyn. Syst., 4 (2005), pp. 588–606.
[64] C. R. Laing and S. Coombes, *The importance of different timings of excitatory and inhibitory pathways in neural field models*, Network, 17 (2006), pp. 151–172.
[65] C. R. Laing and W. C. Troy, *Two-bump solutions of Amari-type models of neuronal pattern formation*, Phys. D, 178 (2003), pp. 190–218.
[66] C. R. Laing and W. C. Troy, *PDE methods for nonlocal models*, SIAM J. Appl. Dyn. Syst., 2 (2003), pp. 487–516.
[67] C. R. Laing, W. C. Troy, B. Gutkin, and G. B. Ermentrout, *Multiple bumps in a neuronal model of working memory*, SIAM J. Appl. Math., 63 (2002), pp. 62–97.
[68] L. Landau, *On the problem of turbulence*, C. R. (Doklady) Acad. Sci. URSS (N.S.), 44 (1944), pp. 311–314.
[69] L. Landau, *Collected Papers of L.D. Landau*, D. Ter Haar, ed., Pergamon, New York, 1965.
[70] P. N. Loxley and P. A. Robinson, *Soliton model of competitive neural dynamics during binocular rivalry*, Phys. Rev. Lett., 102 (2009), 258701.
[71] Y. Lu, Y. Sato, and S. Amari, *Traveling bumps and their collision in a two-dimensional neural field*, Neural Comput., 23 (2011), pp. 1248–1260.
[72] J. E. Marsden and M. F. McCracken, *The Hopf Bifurcation and Its Applications*, Springer-Verlag, London, 1976.
[73] D. Mitrović and D. Zubrinić, *Fundamentals of Applied Functional Analysis*, Pitman Monographs and Surveys in Pure and Applied Mathematics 91, Longman Harlow, UK, 1998.
[74] J. A. Murdock, F. Botelho, and J. E. Jamison, *Persistence of spatial patterns produced by neural field equations*, Phys. D, 215 (2006), pp. 106–116.
[75] M. R. Owen, C. R. Laing, and S. Coombes, *Bumps and rings in a two-dimensional neural field: Splitting and rotational instabilities*, New J. Phys., 9 (2007), p. 378.
[76] D. E. Pelinovsky and V. G. Yakhno, *Generation of collective-activity structures in a homogeneous neuron-like medium.* I. *Bifurcation analysis of static structures*, Internat. J. Bifur. Chaos Appl. Sci. Engrg., 6 (1996), pp. 81–87.
[77] D. E. Pelinovsky and V. G. Yakhno, *Generation of collective-activity structures in a homogeneous neuron-like medium.* II: *Dynamics of propagating and pulsating structures*, Internat. J. Bifur. Chaos Appl. Sci. Engrg., 6 (1996), pp. 89–100.
[78] D. J. Pinto, *Computational, experimental, and analytical explorations of neuronal circuits in the cerebral cortex*, Ph.D. Thesis, Dept. of Mathematics, University of Pittsburgh, Pittsburgh, PA, 1997.
[79] D. J. Pinto and G. B. Ermentrout, *Spatially structured activity in synaptically coupled neuronal networks:* I. *Traveling fronts and pulses*, SIAM J. Appl. Math., 62 (2001), pp. 206–225.

[80] D. J. Pinto and G. B. Ermentrout, *Spatially structured activity in synaptically coupled neuronal networks:* II. *Lateral inhibition and standing pulses*, SIAM J. Appl. Math., 62 (2001), pp. 226–243.
[81] D. J. Pinto, R. K. Jackson, and C. E. Wayne, *Existence and stability of traveling pulses in a continuous neuronal network*, SIAM J. Appl. Dyn. Syst., 4 (2005), pp. 954–984.
[82] D. J. Pinto, S. L. Patrick, W. C. Huang, and B. W. Connors, *Initiation, propagation, and termination of epileptiform activity in rodent neocortex in vitro involve distinct mechanisms*, J. Neurosci., 25 (2005), pp. 8131–8140.
[83] H. Poincaré, *Les Méthods Nouvelles de la Méchanique Céleste* 3, Gauthier-Villars, Paris, 1892.
[84] M. R. Qubbaj and V. K. Jirsa, *Neural field dynamics under variation of local and global connectivity and finite transmission speed*, Phys. D, 238 (2009), pp. 2331–2346.
[85] K. A. Richardson, S. J. Schiff, and B. J. Gluckman, *Control of traveling waves in the mammalian cortex*, Phys. Rev. Lett., 94 (2005), 028103.
[86] J. Rinzel and J. P. Keener, *Hopf bifurcation to repetitive activity in nerve*, SIAM J. Appl. Math., 43 (1983), pp. 907–922.
[87] A. Roxin, N. Brunel, and D. Hansel, *Role of delays in shaping spatiotemporal dynamics of neuronal activity in large networks*, Phys. Rev. Lett., 94 (2005), 238103.
[88] J. E. Rubin, D. Terman, and C. Chow, *Localized bumps of activity sustained by inhibition in a two-layer thalamic network*, J. Comput. Neurosci., 10 (2001), pp. 313–331.
[89] J. E. Rubin and W. C. Troy, *Sustained spatial patterns of activity in neuronal populations without recurrent excitation*, SIAM J. Appl. Math., 64 (2004), pp. 1609–1635.
[90] B. Sandstede, *Evans functions and nonlinear stability of travelling waves in neuronal network models*, Internat. J. Bifur. Chaos Appl. Sci. Engrg., 17 (2007), pp. 2693–2704.
[91] D. H. Sattinger, *Topics in Stability and Bifurcation Theory*, Lecture Notes Math. 309, Springer-Verlag, Berlin, 1973.
[92] J. T. Stuart, *On the non-linear mechanics of wave disturbances in stable and unstable parallel flows. Part* I: *The basic behavior in plane Poiseuille flow*, J. Fluid Mech., 9 (1960), pp. 353–370.
[93] J. G. Taylor, *Neural "bubble" dynamics in two dimensions: Foundations*, Biol. Cybernet., 80 (1999), pp. 303–409.
[94] W. C. Troy, *Oscillation phenomena in nerve conduction equations*, Ph.D. thesis, Department of Mathematics, SUNY at Buffalo, Bufalo, NY, 1974.
[95] W. C. Troy and V. Shusterman, *Patterns and features of families of traveling waves in large-scale neuronal networks*, SIAM J. Appl. Dyn. Syst., 6 (2007), pp. 263–292.
[96] R. Veltz and O. Faugeras, *Local/global analysis of the stationary solutions of some neural field equations*, SIAM J. Appl. Dyn. Syst., 9 (2010), pp. 954–998.
[97] N. A. Venkov, S. Coombes, and P. C. Matthews, *Dynamic instabilities in scalar neural field equations with space-dependent delays*, Phys. D, 232 (2007), pp. 1–15.
[98] N. A. Venkov, *Dynamics of neural field models*, Ph.D. thesis, School of Mathematical Sciences, University of Nottingham, Nottingham, UK, 2009.
[99] J. Watson, *On the non-linear mechanics of wave disturbances in stable and unstable parallel flows. Part* II: *The development of a solution for plane Poiseuille flow and for plane Couette flow*, J. Fluid Mech., 9 (1960), pp. 371–389.
[100] H. Werner and T. Richter, *Circular stationary solutions in two-dimensional neural fields*, Biol. Cybernet., 85 (2001), pp. 211–217.
[101] H. R. Wilson and J. D. Cowan, *A mathematical theory of the functional dynamics of cortical and thalamic nervous tissue*, Kybernetik, 13 (1973), pp. 55–80.
[102] J. Wyller, P. Blomquist, and G. T. Einevoll, *Turing instability and pattern formation in a two-population neuronal network model*, Phys. D, 225 (2007), 051904.
[103] X. Xie and M. Giese, *Nonlinear dynamics of direction-selective recurrent neural media*, Phys. Rev. E, 65 (2002), pp. 75–93.
[104] L. Zhang, *On stability of traveling wave solutions in synaptically coupled neuronal networks*, Differential Integral Equations, 16 (2003), pp. 513–536.